ESMC-TR-88-03

A REVIEW OF ENERGY RELEASE PROCESSES FROM THE FAILURE OF PNEUMATIC PRESSURE VESSELS

August 1988

General Physics Corporation
Cape Canaveral Air Force Station
Florida

Eastern Space and Missile Center
Air Force Systems Command
Patrick Air Force Base, Florida

DISCLAIMER NOTICE

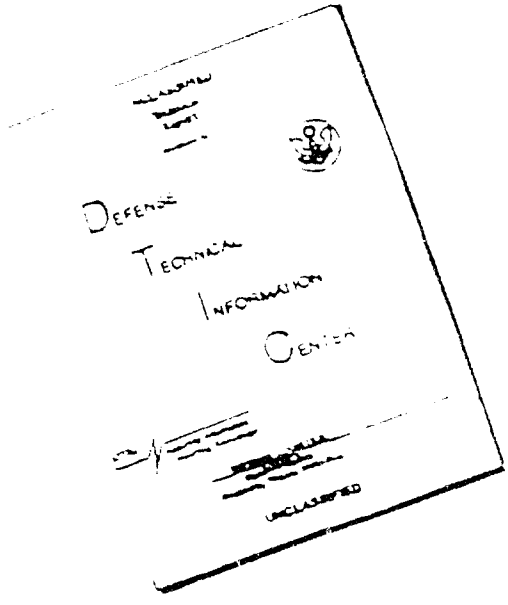

THIS DOCUMENT IS BEST QUALITY AVAILABLE. THE COPY FURNISHED TO DTIC CONTAINED A SIGNIFICANT NUMBER OF PAGES WHICH DO NOT REPRODUCE LEGIBLY.

NOTICE

When government specifications, or other data are used for any purpose other than in connection with a definitely related government procurement operation, the United States Government thereby incurs no responsibility nor any obligation whatsoever; and the fact that the government may have formulated, furnished, or in any way supplied the said specifications, or other data, is not to be regarded by implication or otherwise as in any manner licensing the holder or any other person or corporation, or conveying any right or permission to manufacture use, or sell any patented invention that may in any way be related thereto.

This report has been reviewed by the Office of Public Affairs (ESMC/PA) and is releasable to the National Technical Information Service (NTIS). At NTIS, it will be available to the general public, including foreign nations.

This technical report has been reviewed and is approved for publication.

BOBBY J. WEBB
Project Engineer

THOMAS L. WILSON, LTC, USAF
Chief, Missile Systems Safety Division

FOR THE DIRECTOR:

ROBERT F. SCHULTZ, COL, USAF
Director of Safety

UNCLASSIFIED
SECURITY CLASSIFICATION OF THIS PAGE

REPORT DOCUMENTATION PAGE

1a. REPORT SECURITY CLASSIFICATION: UNCLASSIFIED	1b. RESTRICTIVE MARKINGS: NONE
2a. SECURITY CLASSIFICATION AUTHORITY	3. DISTRIBUTION/AVAILABILITY OF REPORT: APPROVED FOR PUBLIC RELEASE: DISTRIBUTION UNLIMITED
2b. DECLASSIFICATION/DOWNGRADING SCHEDULE	
4. PERFORMING ORGANIZATION REPORT NUMBER(S): GP-R-213083	5. MONITORING ORGANIZATION REPORT NUMBER(S): ESMC-TR-88-03
6a. NAME OF PERFORMING ORGANIZATION: GENERAL PHYSICS CORP. SPACE COAST OFFICE; 6b. OFFICE SYMBOL (If applicable):	7a. NAME OF MONITORING ORGANIZATION: DIRECTORATE OF SAFETY
6c. ADDRESS (City, State and ZIP Code): P.O. BOX 21265 KENNEDY SPACE CENTER, FL 32815	7b. ADDRESS (City, State and ZIP Code): EASTERN SPACE AND MISSILE CENTER PATRICK AIR FORCE BASE, FL 32925
8a. NAME OF FUNDING/SPONSORING ORGANIZATION: ESMC; 8b. OFFICE SYMBOL (If applicable): SEM	9. PROCUREMENT INSTRUMENT IDENTIFICATION NUMBER: F08606-86-C-0030
8c. ADDRESS (City, State and ZIP Code):	10. SOURCE OF FUNDING NOS. — PROGRAM ELEMENT NO.: / PROJECT NO.: / TASK NO.: / WORK UNIT NO.:
11. TITLE (Include Security Classification): Review of Energy Release Processes from the	
12. PERSONAL AUTHOR(S): M.COLEMAN, M.CAIN, R.DANNA, C.HARLEY AND D.SHARP, GENERAL PHYSICS CORPORATION	
13a. TYPE OF REPORT: INITIAL RELEASE; 13b. TIME COVERED: FROM 861001 TO 880831; 14. DATE OF REPORT (Yr., Mo., Day): 880831; 15. PAGE COUNT: 125	
16. SUPPLEMENTARY NOTATION	
17. COSATI CODES — FIELD / GROUP / SUB. GR.:	18. SUBJECT TERMS (Continue on reverse if necessary and identify by block number): PRESSURE VESSELS, BLAST WAVE, FRAGMENTATION, VESSEL BURST, BURST TEST, AND FRAGMENTS

19. ABSTRACT (Continue on reverse if necessary and identify by block number)

This report presents the results of a review of the currently available methodologies for predicting the characteristics of the blast wave and fragments produced by the failure of a pneumatic pressure vessel. Methodologies are presented and evaluated for their usefulness in accurately predicting the hazards presented by a pressure vessel failure. Deficiencies in the current methodologies are identified as well as the areas which require additional testing for verification. Computer codes which predict blast wave overpressure and fragment initial velocity and range are described and their results are compared to experimental data. Finally, a preliminary test program is presented to provide guidance on setting up burst tests to obtain necessary additional data.

20. DISTRIBUTION/AVAILABILITY OF ABSTRACT: UNCLASSIFIED/UNLIMITED ☒ SAME AS RPT. ☐ DTIC USERS ☐	21. ABSTRACT SECURITY CLASSIFICATION: UNCLASSIFIED
22a. NAME OF RESPONSIBLE INDIVIDUAL: Bobby L. Webb	22b. TELEPHONE NUMBER (Include Area Code): 407-494-7077; 22c. OFFICE SYMBOL: SEM

DD FORM 1473, 83 APR EDITION OF 1 JAN 73 IS OBSOLETE.

UNCLASSIFIED
SECURITY CLASSIFICATION OF THIS PAGE

11. TITLE (Continued)

Failure of Pneumatic Pressure Vessels (UNCLASSIFIED).

ESMC-TR-88-03

A REVIEW OF ENERGY RELEASE PROCESSES FROM THE FAILURE OF PNEUMATIC PRESSURE VESSELS

August 1988

Prepared by

General Physics Corporation
Cape Canaveral Air Force Station
Florida

M. Coleman
M. Cain
R. Danna
C. Harley
D. Sharp

for
Eastern Space and Missile Center
Air Force Systems Command
Patrick Air Force Base, Florida

UNCLASSIFIED

SECURITY CLASSIFICATION OF THIS PAGE

REPORT DOCUMENTATION PAGE

1a. REPORT SECURITY CLASSIFICATION UNCLASSIFIED	1b. RESTRICTIVE MARKINGS NONE
2a. SECURITY CLASSIFICATION AUTHORITY	3. DISTRIBUTION/AVAILABILITY OF REPORT APPROVED FOR PUBLIC RELEASE: DISTRIBUTION UNLIMITED
2b. DECLASSIFICATION/DOWNGRADING SCHEDULE	
4. PERFORMING ORGANIZATION REPORT NUMBER(S) GP-R-213083	5. MONITORING ORGANIZATION REPORT NUMBER(S) ESMC-TR-88-03
6a. NAME OF PERFORMING ORGANIZATION GENERAL PHYSICS CORP. SPACE COAST OFFICE 6b. OFFICE SYMBOL (If applicable)	7a. NAME OF MONITORING ORGANIZATION DIRECTORATE OF SAFETY
6c. ADDRESS (City, State and ZIP Code) P.O. BOX 21265 KENNEDY SPACE CENTER, FL 32815	7b. ADDRESS (City, State and ZIP Code) EASTERN SPACE AND MISSILE CENTER PATRICK AIR FORCE BASE, FL 32925
8a. NAME OF FUNDING/SPONSORING ORGANIZATION ESMC 8b. OFFICE SYMBOL (If applicable) SEM	9. PROCUREMENT INSTRUMENT IDENTIFICATION NUMBER F08606-86-C-0030
8c. ADDRESS (City, State and ZIP Code) EASTERN SPACE AND MISSILE CENTER PATRICK AIR FORCE BASE, FL 32925	10. SOURCE OF FUNDING NOS. PROGRAM ELEMENT NO.: 78022F PROJECT NO.: TASK NO.: 5 WORK UNIT NO.:
11. TITLE (Include Security Classification) Review of Energy Release Processes from the	
12. PERSONAL AUTHOR(S) M.COLEMAN, M.CAIN, R. DANNA, C.HARLEY AND D. SHARP, GENERAL PHYSICS CORPORATION	
13a. TYPE OF REPORT INITIAL RELEASE	13b. TIME COVERED FROM 861001 TO 880831
14. DATE OF REPORT (Yr., Mo., Day) 880831	15. PAGE COUNT 125
16. SUPPLEMENTARY NOTATION	

17. COSATI CODES		
FIELD	GROUP	SUB. GR.

18. SUBJECT TERMS (Continue on reverse if necessary and identify by block number)
PRESSURE VESSELS, BLAST WAVE, FRAGMENTATION, VESSEL BURST, BURST TEST, AND FRAGMENTS.

19. ABSTRACT (Continue on reverse if necessary and identify by block number)

This report presents the results of a review of the currently available methodologies for predicting the characteristics of the blast wave and fragments produced by the failure of a pneumatic pressure vessel. Methodologies are presented and evaluated for their usefulness in accurately predicting the hazards presented by a pressure vessel failure. Deficiencies in the current methodologies are identified as well as the areas which require additional testing for verification. Computer codes which predict blast wave overpressure and fragment initial velocity and range are described and their results are compared to experimental data. Finally, a preliminary test program is presented to provide guidance on setting up burst tests to obtain necessary additional data.

20. DISTRIBUTION/AVAILABILITY OF ABSTRACT UNCLASSIFIED/UNLIMITED XX SAME AS RPT. ☐ DTIC USERS ☐	21. ABSTRACT SECURITY CLASSIFICATION UNCLASSIFIED
22a. NAME OF RESPONSIBLE INDIVIDUAL Bobby L. Webb	22b. TELEPHONE NUMBER (Include Area Code) 407-494-7077 22c. OFFICE SYMBOL SEM

DD FORM 1473, 83 APR EDITION OF 1 JAN 73 IS OBSOLETE.

SECURITY CLASSIFICATION OF THIS PAGE

11. TITLE (Continued)

Failure of Pneumatic Pressure vessels (UNCLASSIFIED)

COMMENT FORM

TITLE: **Review of Energy Release Processes from the Failure of Pneumatic Pressure Vessels**

Publication: **ESMC-TR-88-03** **Revision:** **0 (Initial Release)**

1. **USAF** solicits your comments concerning this report so that its usefulness may be improved in later editions. Send any comments to the following address:

   Directorate of Safety
   Attn: B.L. Webb
   Eastern Space and Missile Center (AFSC)
   Patrick Air Force Base, Florida 32925

2. Comments are solicited in the following areas:

   a. Is the report adequate to support the development of a test program to further research pressure vessel failures?

   b. What improvements would make the report more adequate?

   c. Are there any general comments concerning the report?

3. Please note any specific errors which have been discovered. Include the page number for reference.

PREFACE

Work on the study leading to this report began in order to identify whether any methodologies exist for determining the hazards associated with a pressure vessel failure and the safe location of pressure vessels with respect to nearby facilities. As more references were reviewed, it became clear that most of the test data on blast waves and fragments were specific to munitions blasts and did not model the failure of a pressure vessel very closely. Most of the theoretical work and computer codes developed specifically for vessel bursts have not been sufficiently verified due to a lack of experimental data. As a result, a major goal of this study became the identification of additional testing necessary to validate methodologies to predict blast wave overpressure and fragment initial velocity and range.

Program work continues with the development of a series of comprehensive test plans for vessel bursts, using the Preliminary Test Program contained herein as a starting point. Initial conduct of vessel bursts is planned for the summer of 1989 and continuing into subsequent years. Vessels and instrumentation are currently being sought for the tests. Interested parties are invited to contact the authors.

ACKNOWLEDGEMENTS

This report was developed by the Space Coast Office of the General Physics Corporation at the direction of the Directorate of Safety, Eastern Space and Missile Center (ESMC), Cape Canaveral Air Force Station and Patrick Air Force Base. We would like to thank the ESMC Directorate of Safety for their support, especially Mr. B. Webb and Mr. L. Ullian for their guidance and input to the research project and this report. Thanks also is given to Mr. Wayne Frazier of the National Aeronautics and Space Administration (NASA) Headquarters, Mr. P. Taddie, ESMC, Mr. J. Marshall and Mr. R. Grove of the Air Force Astronautics Laboratory and Dr. Louis Huang of Air Force Space Division for their consultation and support.

TABLE OF CONTENTS

Page

TABLE OF CONTENTS (CONT'D)

TABLE OF CONTENTS (CONT'D)

Page

LIST OF FIGURES

LIST OF TABLES

SECTION 1. INTRODUCTION

1.1 Report Summation

The hazards associated with the failure of pressure vessels are of considerable interest to those responsible for safeguarding against such failures. In general, much study has been afforded toward the identification of pressure vessel failure modes and has resulted in the development of methods for the design against failure: such as the development of the ASME Boiler and Pressure Vessel Code, Section VIII. In some applications, a prediction of the hazards of a failed pressure vessel, and the effects on its surroundings, is warranted. Methods for predicting hazards of pressure vessel failures, however, have received much less study and a consensus methodology is not to be found. Establishing the potential hazard is required for the effective mitigation of the consequences of failure through facility design and operation.

The objective of this study is to identify the current methods available to establish the hazard associated with the failure of a pneumatic pressure vessel (see Figure 1-1). It is desirable to safely locate the vessels with respect to nearby facilities, systems and equipment. This involves determining the range at which blast overpressure and fragments jeopardize the integrity of the facilities, systems and equipment.

The approach used in this study was to review the available literature on the theory, experimental data and computer codes for determining the effects of a blast wave and characteristics of the fragments generated as a result of the burst.

Methodologies are considered to predict the overpressure from a blast wave and the initial velocities and ranges of fragments produced from the vessel burst. The major limitation is that no methodology has been adequately validated by experimental data.

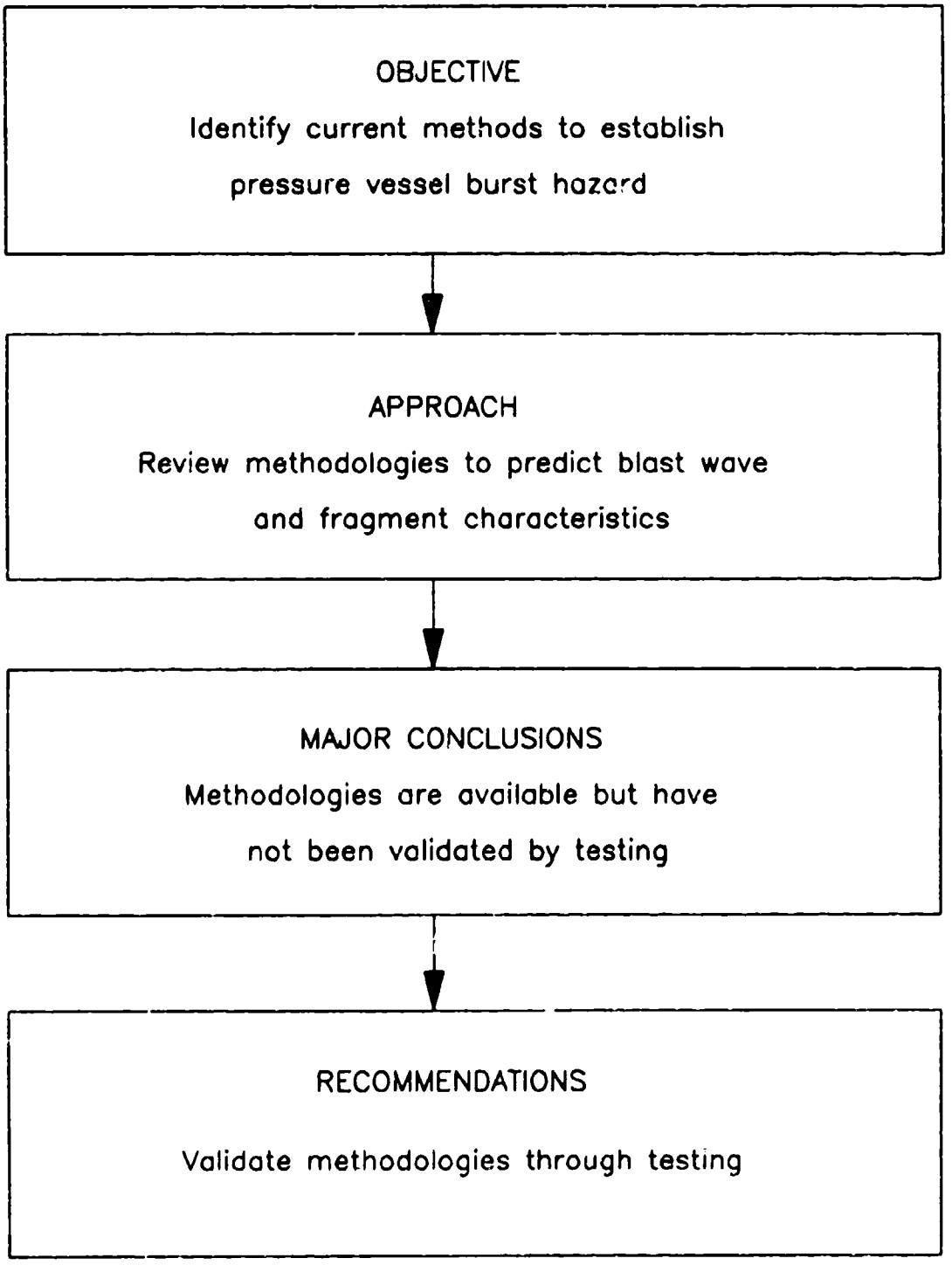

Figure 1-1. Report Summation

The report concludes with a recommendation for testing to generate the data necessary to verify methodologies for predicting pressure vessel burst hazards. A preliminary test program is presented to address this concern.

The scope of this report is limited to the determination of the blast wave and the determination of fragmentation; or specifically, the overpressure in air versus distance from the gas filled pressure vessel rupture, and the quantity of vessel material pieces following rupture and their respective velocities and masses. The studied rupture is without detonation, deflagration or other chemical reaction. The effects of the generated blast wave and fragmentation on the surroundings (e.g., facilities, personnel) and the generation of secondary fragmentation or debris is not discussed.

1.2 Current Blast Wave Determination

Although limited, there have been milestone studies developed and published on the prediction of blast waves generated by pressure vessel ruptures. These were found, however, to differ in methods and results and thereby led to the development of this study and report. These studies are discussed in Section 2 with specific emphasis given to those factors that can vary the determination of blast wave strength versus distance, such as expansion energy available in a compressed gas, and the comparison of a vessel rupture with TNT detonation. In addition, and perhaps more importantly, the results of a literature search for actual pressure vessel burst test data are discussed and compared to current blast wave prediction methods. A brief review of computer models developed for blast wave prediction is also presented.

1.2.1 Background

A pressure vessel rupture results in the uncontrolled release of the potential energy of the compressed gas to the surroundings. A rupture of small size (i.e., leak), with low tearing force, will dissipate the stored energy in the vessel but over a relatively long period of time [1] and may not generate a blast wave. An explosive rupture of a pressure vessel, where the stored energy is released

instantaneously, would create a blast wave (i.e., shockwave) in the surrounding air. For the purpose of analysis of available expansion energy and prediction of blast waves, the vessel material is assumed to completely disintegrate upon rupture with no work performed on the vessel fragments. However, 10% or more of the available energy is expended to deform the vessel structure and impart velocity to fragments.

Explosive disintegration will generate a blast wave resulting in overpressure (pressure above atmospheric) at the vessel surface equal to the pressure in the vessel [1]. As the blast wave advances, the energy is spread over the waves' spherical frontal area, this area increasing with the square of the distance from the point of rupture [2]. Overpressure, blast wave velocity and therefore, blast effect, decrease rapidly with distance. After passage of the shockwave, the pressure decreases progressively until a suction phase follows in which pressure drops below normal atmospheric pressure. The negative pressure is a result of the spherical outrush of gases from the center of the rupture causing an overexpansion [4]. The pressure above atmospheric at the shock wave front is the peak overpressure and is the blast wave characteristic most often used to establish the relative hazard (i.e., shock wave intensity) associated with ruptures and explosions at a given distance. (The potential hazard to personnel and structures for varying overpressures is very well documented.) Overpressure is related to other blast wave characteristics such as velocity and impulse, and is usually presented as "side-on" pressure, that is, the overpressure which would be observed when there is no interaction between blast and the structure. A blast wave incident with a structure, such as a wall, generates a reflected shockwave This initial reflected pressure may be several times as great as the side-on peak overpressure.

1.2.2 Peak Overpressure Determination

Determining the total amount of energy transferred from a pressure vessel rupture (or any explosion) to the resulting blastwave is required to assess explosive blast and peak overpressure. The explosive energy from the rapid expansion of compressed gas can be determined by application of basic thermodynamic relationships that are a function of

pressure, volume, and temperature. The expansion is most often assumed to be isentropic, defined as adiabatic (no heat transfer) and reversible (no losses due to friction, intermixing etc.). However, isothermal expansion is also considered applicable by some references (for example, the Air Force System Command Design Handbook) for the determination of expansion energy. Isothermal expansion implies heat is transferred into the expanding gas, maintaining constant temperature. Assuming this expansion process results in a calculated energy of approximately three times greater than for isentropic expansion. Section 2 derives relationships for both isentropic and isothermal expansion energy for ideal gas and discusses the applicability of each. The influence of expanding real versus ideal gas is also presented.

By assuming the expansion energy of the initially compressed gas develops a blastwave and that the blast generated from a pressure vessel rupture is the same as the blast generated by a TNT (symmetrical 2, 4, 6-trinitrotoluene) explosion, the peak overpressure versus distance for a pressure vessel rupture could then be taken as that of a TNT explosion of equivalent blast energy yield. This approach is frequently used, since significant data exists on TNT explosions and the resulting blast wave.

The data is usually presented as peak overpressure versus distance per unit weight of TNT. Discussion of converting expansion energy (e.g., ft-lbs) to equivalent weight of TNT is provided is Section 2.3.

1.3 Current Fragmentation Determination

There has been some study in the last 20 years on the prediction of characteristics of fragments generated from pressure vessel ruptures. These studies were found to be generally related to the same theory for establishing the energy imparted to the fragments and varied principally in the assumptions necessary to model a specific vessel rupture. Further, as with blast wave determination, limited testing has been accomplished toward predicting fragmentation characteristics. Published studies on fragments from bursting pressure vessels are discussed in Section 3.0 with specific purpose given to those factors that determine the fragment hazard, such as velocity and distance traveled. The

results of actual pressure vessel burst test fragmentation data are also discussed, as well as a brief review of computer codes developed from fragment characteristics.

1.3.1 Background

A pressure vessel rupture occurs with structural failure of the vessel material. Failure is due to an overstressed condition resulting in crack initiation and propagation caused by either defects, designed stress concentrations, missile impact or overloading. If crack propagation is stable such that the overstress is relieved following crack growth, a rupture of small size (i.e. leak) may occur and dissipate the stored energy in the vessel without the generation of fragments. When crack propagation is unstable, an explosive rupture of the vessel may occur with the vessel material separating into two or more fragments. The expanding gas will accelerate those fragments no longer integral with the vessel or otherwise fixed.

To estimate the hazard of fragments, regardless of source, complete knowledge of the fragment characteristics is required; this includes fragment mass, shape, drag coefficient and initial velocity (speed and direction). For ground-based vessels, this data can be used with ballistic type calculations to determine the impact range and terminal kinetic energy. However, determining these fragmentation characteristics is exceedingly difficult. The most difficult problem is the prediction of the total number of fragments and the mass of each individual fragment. The current state-of-the-art analysis of fragmentation does not provide any analytical theory to predict either the individual mass or the total number of fragments.

1.3.2 Fragment Velocity and Range Determination

Fragments produced upon vessel burst are accelerated away from the vessel by the gas remaining within the vessel. The pressure of the still contained gas decreases as gas escapes the confines of the vessel remains. As this gas pressure decreases, the fragment acceleration also

decreases. The gas pressure can be written in terms of an appropriate equation of state for either an ideal or real gas. Initial fragment velocity is determined when the acceleration becomes negligible.

Fragment range is a function of the fragment trajectory. The trajectory is dependent upon the fragment's initial speed and launch angle, mass and coefficient of drag (or lift) while in flight. The coefficient of drag or lift depends upon the speed, size, and shape of the fragment and can generally be found from tables or estimated. Fragment range would then be determined by a computer program using numerical integration of the basic ballistic equations.

1.4 Bibliography

An exhaustive bibliography of literature pertinent to blast waves and fragmentation is contained in Reference [6]. A number of these publications are applicable to the failure of pneumatic pressure vessels and were reviewed during the preparation of this report. Those which were finally used as sources for this report are listed in the References herein.

1.5 Summary of Conclusions and Recommendations

The two major methodologies for predicting blast wave overpressure involve isothermal and isentropic expansion of a gas which might be either real or ideal. Both models tend to be overconservative in the near field in that they predict greater overpressures than are actually observed Of the two methodologies, the isentropic model appears to be the more accurate and suitable for verification. The ideal gas approximation is also overconservative; either the ideal or real gas model might be suitable for further study. A lack of available blast data specific to pressure vessels makes impossible the verification of a methodology of either of two computer codes currently available.

There are several methodologies available to predict initial fragment velocity; these models differ principally in their assumptions and applications. Two limitations generally apply to all of these models: (1) input data is required that involves knowledge of how the

vessel fails or, at least, what fragments are generated, and (2) there is insufficient data to verify any of the methodologies. The available computer codes suffer from the same limitations.

It is much easier to predict the ranges of the fragments, given their initial velocities. Computer codes are also available.

It is strongly recommended that additional testing be conducted to obtain the necessary data to validate the blast wave and fragment methodologies. A preliminary test program is presented to provide guidance in setting up testing.

SECTION 2. BLAST WAVE THEORY AND EXPERIMENTAL APPROACHES

The purpose of this section is to describe current methodologies that analyze the effects of a blast wave generated by the burst of a pneumatic vessel. The section begins with an introductory description of the blast wave formed by a vessel burst. Four models are then developed to approximate the energy release in the blast wave; an ideal gas is assumed to expand isentropically, adiabatically and isothermally. The isentropic and isothermal models are chosen for further review and compared. Next, the differences between real and ideal gas are discussed and the isentropic and isothermal models are compared using ideal gases. The energy release from a bursting vessel is then equated to a TNT explosion, and the TNT equivalency is compared with experimental data. Finally, computer codes which have been generated to predict the blast waves from vessel bursts are reviewed.

2.1 Theory

The bursting of a high pressure vessel results in an instantaneous release of the energy stored within the vessel. The energy is dissipated through various means, including rupture of the vessel, propulsion of fragments, and a blast wave.

In general, for failures of vessels filled with a compressed gas, it may be assumed that the gas expands in an adiabatic manner. Up to an initial pressure of about 1500 psi (about 100 atmospheres) it can further be assumed that the gas expands in an ideal manner. Above 1500 psi, the ideal gas laws are not accurate and real gas effects become important, causing the actual energy release to be less than that predicted by ideal gas laws [3]. Therefore, the use of ideal, adiabatic expansion equations for vessel pressures above about 100 atmospheres will produce conservative results. Ideal gas and real gas energy releases are examined later in this section.

The mediums in pressure vessels can be put into three categories from the highest hazard potential from a blast wave to the least: (1) compressed gases, (2) compressed flash-evaporating liquids, and (3) compressed liquids. These hazard categories are based on the stored

energy per unit volume. Pressure vessel failure can occur for numerous reasons with the major ones being the following: overpressurization, material failure, and missile impact.

This report analyzes the energy stored in a compressed (ideal and real) gas pressure vessel based upon the thermodynamic relationships for isentropic, adiabatic, and isothermal expansions.

2.1.1 Introduction to Blast Wave Characteristics

A blast wave (shock) is formed when the atmosphere surrounding a vessel that fails is forced away by the expanding fluid from the vessel. Figures 2-1a & 1b illustrate theoretical pressure vessel blast waves in the form of a pressure-time curve at a fixed location from the vessel. Some experts say the blast wave is characterized by a sharp rise to a peak pressure and an exponential decay thereafter (Figure 2-1a) while others contend that there is a less rapid rise to a less distinct peak with a gradual decay to ambient pressure (Figure 2-1b). As more experimental pressure vessel burst data is generated, a better determination as to blast wave characteristics will be obtainable. Figure 2-2 shows a theoretical pressure-distance plot for a blast wave at several specific times. Once any blast wave has traveled several vessel diameters from the source, it tends to follow these configurations. Near the vessel, there can be differences in the curves depending on the source of the blast.

It can be seen from Figure 2-1a that there are both positive and negative pressure phases. In general, the positive pressure pulse is much stronger and has greater effects than the negative pulse [4]. An important point to notice from Figure 2-2 is that as the distance from the blast wave source increases, the peak overpressure decreases. Eventually, the peak overpressure will decrease to a point where no damage will be done to structures, equipment, or personnel. Methods will be described later to relate distance to overpressure.

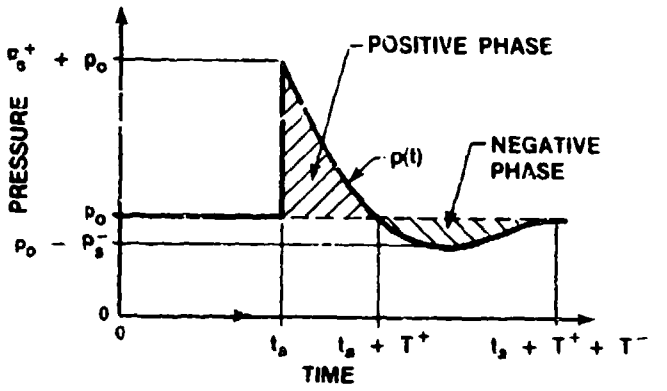

Figure 2-1a. Pressure — Time Curve at a Fixed Location

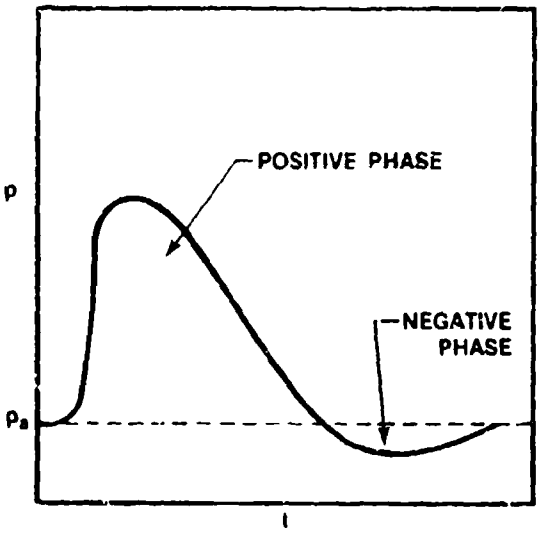

Figure 2-1b. Pressure — Time Curve at a Fixed Location

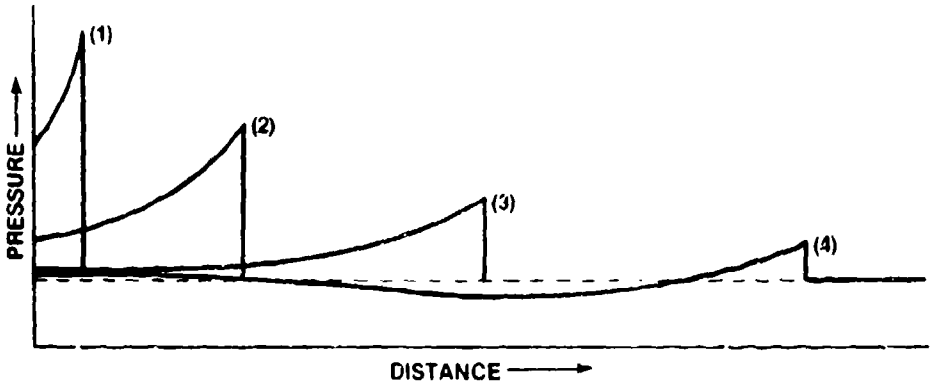

Figure 2-2. Pressure — Distance Curves at Specific Time Intervals [4]

Overpressure is an important factor in determining safe separation distances, because once the overpressure vs. distance is determined, it is possible to enter a table that identifies potential damage from overpressures. (Note that there are various such tables published, many of which give different data.)

Referring back to Figure 2-1a, it can be seen that at a specific distance from the blast, the blast wave arrives as an instantaneous pressure increase, which immediately begins to decay and eventually becomes negative. Prior to shock front arrival, the pressure is ambient pressure P_o. At arrival time t_a, the pressure rises abruptly to a peak value $P_s^+ + P_o$. The pressure then decays to ambient in total time $t_a + T^+$, drops to a partial vacuum of amplitude P_s^-, and eventually returns to P_o in total time $t_a + T^+ + T^-$. The quantity P_s^+ is usually termed the peak side-on overpressure, or merely the peak overpressure. The portion of the time history above initial ambient pressure is called the positive phase, of duration T^+. That portion below P_o, of amplitude P_s^- and duration T^- is called the negative phase [5].

Now that these basic concepts of a blast wave have been introduced, the theoretical approaches to determining the energy released by the failure of a gas-filled pressure vessel will be discussed. A critical problem has been to accurately assess the energy release as a result of the accident or incident. Current prediction methods determine the energy stored in the pressure vessel and equate it to an equivalent quantity of TNT (equivalency based on energy release). This method is used because a large amount of experimental data exists for blast waves generated from TNT explosions. Although the comparison with TNT is convenient, it will be shown in Section 2.3 that the correlation is at best a fair approximation.

2.1.2 Energy Released by Isentropic Expansion of an Ideal Gas

The blast energy is defined as the energy released by the pressurized gas following vessel failure. In this subsection, a relationship for the blast energy based upon isentropic expansion of an ideal gas will be derived, beginning with the first law of thermodynamics.

The system of concern in this study consists of gas under high pressure contained in a pressure vessel at a ground level. Initially, this system is at pressure P_1 and it contains a volume V_1 of gas. After vessel rupture, the gas in the vessel expands to $P_2 = P_{atm}$ and to an unknown volume V_2.

The first law of thermodynamics can be written as:

$$Q - W = \Delta E = \Delta U + \Delta KE + \Delta PE + \ldots \quad (1)$$

where :
- Q = heat transferred
- W = work done on surroundings
- ΔE = change in total energy
- ΔU = change in internal energy
- ΔKE = change in kinetic energy
- ΔPE = change in potential energy
- $\ldots$ = change in other energies (e.g., chemical, electrical)

Because the expansion is isentropic, (i.e., adiabatic and reversible), $Q = 0$ (Later sections will examine other processes.). Because the system is initially at rest, and is also at rest following the expansion process, ΔKE is negligible. Similarly, ΔPE is negligible because we shall assume the entire process takes place at ground level. Other energies such as chemical and electrical are not applicable to this process and are also negligible. These assumptions reduce Equation (1) to:

$$-W = \Delta E = \Delta U \quad (2)$$

The ideal gas law states that for the expansion of a gas:

$$W = -C_v \Delta T \quad (3)$$

where: C_v = constant volume specific heat
$\Delta T = T_2 - T_1$ (temperature change)

The constant volume specific heat is a property of a fluid and can be written as:

$$C_v = \frac{R}{K-1} \tag{4}$$

where: R = universal gas constant

K = specific heat ratio (for a particular ideal gas)

Inserting Equation (4) into Equation (3), the relationship for work becomes:

$$W = \frac{R}{K-1} (T_1 - T_2) \tag{5}$$

The basic ideal gas law is:

$$PV = RT \tag{6}$$

or

$$R = \frac{P\ V}{T} \tag{7}$$

Substituting Equation (7) into Equation (5) and reducing:

$$W = \frac{P_1\ V_1}{K-1} \left(1 - \frac{T_2}{T_1}\right) \tag{8}$$

An isentropic ideal gas relation is:

$$\frac{T_2}{T_1} = \frac{P_2}{P_1}^{\frac{K-1}{K}} \tag{9}$$

Substituting Equation (9) into Equation (8):

$$W = \frac{P_1\ V_1}{K-1} \left[1 - \left(\frac{P_2}{P_1}\right)^{\frac{K-1}{K}}\right] \tag{10}$$

Equation (10) gives the isentropic energy released by the failure of a vessel containing a volume of ideal gas, V_1, at a pressure of P_1. P_2 is the surrounding atmospheric pressure. From this equation, the energy available from a given vessel can be calculated. The isentropic formula is used often in gas dynamics because it is a simple formula, and the friction losses and dissipation losses are usually very minimal.

The specific heat ratio K is essentially independent of pressure and temperature for monatomic gases. For diatomic gases and other gases, specific heat ratio decreases somewhat with increasing temperature. Data are tabulated and readily available [24] if increased accuracy is desired.

As will be seen later in Section 2.3, this energy can be converted into an equivalent quantity of TNT. Then, the blast wave associated with the vessel failure can be assumed to be equivalent to the effects of that quantity of TNT.

In a real situation, the blast wave energy released by the vessel failure would be less than that of the theoretical value obtained through Equation (10). One reason for this has been discussed - at pressures above about 1500 psi and ambient temperature, real gas effects become significant and reduce the energy released as compared to an ideal gas. (Real gas effects are discussed later in this section.) Another reason that Equation (10) or the equations developed in the next two subsections would give a conservative result is that a portion of the energy contained in the pressurized gas would not go into the blast wave, but instead would be expended through vessel rupture and fragmentation. Estimates of the energy expended through a shock wave range from 20% to 80% of the total energy available [6]. In real situations, the energy expended through vessel rupture and fragmentation will vary based upon material characteristics (e.g., fracture toughness, material flaws, and mode of vessel failure).

2.1.3 Energy Released by Adiabatic Expansion of an Ideal Gas

This subsection develops the energy release equation based upon adiabatic expansion, whereas the previous subsection examined isentropic (i.e., adiabatic and reversible) expansion.

Again starting with the first law of thermodynamics:

$$Q-W = \Delta E = \Delta U + \Delta KE + \Delta PE + \ldots \tag{11}$$

As was the case for the previous section, $Q = 0$, and ΔKE and ΔPE are negligible.

The development of the adiabatic equation is identical to the development of the isentropic equation up through Equation (8):

$$W = \frac{P_1V_1}{K-1}\left(1 - \frac{T_2}{T_1}\right) \tag{12}$$

At this point, the temperatures can be replaced with the following relationship:

$$T = \frac{PV}{R} \tag{13}$$

Substituting Equation (13) into Equation (12), and reducing:

$$W = \frac{P_1V_1}{K-1}\left(1 - \frac{P_2V_2}{P_1V_1}\right) \tag{14}$$

Also, the total volume, V, equals the specific volume, v, multiplied by the mass, m:

$$V = mv \tag{15}$$

Also, $$v = \frac{1}{\rho} \tag{16}$$

where ρ = density

Substituting Equations (15) and (16), Equation (14) now becomes:

$$W = \frac{P_1 V_1}{K-1}\left(1 - \frac{P_2}{P_1}\frac{\rho_1}{\rho_2}\right) \tag{17}$$

Equation (17) gives the maximum work that gas undergoing an adiabatic expansion can perform on its surroundings.

Adiabatic means that no heat is transferred into or out of the system. This is the most likely situation during tank burst, because the gas expands so fast it does not have time to transfer significant heat and the adiabatic formula does not assume the expansion to be reversible. However, this formula is not widely used because it requires knowledge of the gas density at point 2.

2.1.4 Energy Released by Isothermal Expansion of an Ideal Gas

This subsection develops the energy release equation based upon isothermal expansion, whereas the previous two subsections examined isentropic and adiabatic expansion. The isothermal process can be modeled by adding a heat source to the isentropic process of subsection 2.1.2, so that heat would be available to the system during the expansion process making temperature constant.

For an isothermal process, $T_1 = T_2$. Starting with the first law of thermodynamics:

$$Q - W = \Delta E = \Delta U + \Delta KE + \Delta PE \tag{18}$$

In this case $Q \neq 0$ because of the heat source. Again, ΔKE, ΔPE and changes in other energies are negligible, so Equation (18) reduces to:

$$Q - W = \Delta U \tag{19}$$

But ΔU is defined as:

$$\Delta U = \int C_v dT \tag{20}$$

Because the process is isothermal, $dT = 0$; therefore, $\Delta U = 0$, so Equation (19) is further reduced to:

$$Q - W = 0 \text{ or } W = Q \tag{21}$$

Work can be defined in terms of pressure and volume as follows:

$$W = \int P dV \tag{22}$$

And since $PV = RT$, or $P = \frac{RT}{V}$:

$$W = \int \frac{RT}{V} \, dV \tag{23}$$

R is the universal gas constant. Because we are examining an isothermal process, T is also constant.

Equation (23) now becomes:

$$W = RT \int \frac{dV}{V}$$

$$W = RT \ln \frac{V_2}{V_1} \tag{24}$$

The ideal gas law of $PV = RT$ can be written for two separate points as:

$$\frac{P_1 V_1}{T_1} = \frac{P_2 V_2}{T_2} \quad \text{and since } T_1 = T_2$$

$$P_1 V_1 = P_2 V_2, \quad \text{or}$$

$$\frac{P_1}{P_2} = \frac{V_2}{V_1} \tag{25}$$

Substituting Equation (25) into Equation (24):

$$W = RT \ln \frac{P_1}{P_2} \tag{26}$$

Also, $P_1V_1 = RT$

So Equation (26) now becomes:

$$W = P_1V_1 \ln \frac{P_1}{P_2} \tag{27}$$

P_1, V_1, and P_2 are all determinable; therefore, the maximum work that an isothermal expansion can do to its surroundings can be calculated using Equation (27).

2.1.5 Comparison of Energy Releases Calculated by Isentropic, Adiabatic and Isothermal Expansion Equations for Ideal Gas

Equations (10), (17), and (27) present the isentropic, adiabatic and isothermal expansion formulas, respectively, for ideal gas. This section will compare the results of the isentropic and isothermal equations for vessel failure where initial pressures (P_1) range from 100 to 15,000 psi and P_2 is assumed to be atmospheric pressure (14.7 psia) in all cases.

The isothermal expansion formula is a single parameter (pressure) formula, easy to use. However, for the non-burning high pressure burst, isothermal expansion is not realistic, due to the fact that there is no heat generated to support constant temperature gas expansion. For this reason TNT equivalency based on isothermal expansion is over-conservative. The adiabatic expansion formula requires both tank pressure and density to determine the TNT equivalency. Adiabatic means no heat transfer in or out of the system. This is the most likely situation during tank bursts, because the gas expands so fast it does not have time to transfer significant heat into or out, and the adiabatic case does not assume the expansion to be reversible. This formula is not widely used because it requires knowledge of the gas density at point 2. The isentropic relationship reduces the two-parameter adiabatic formula to a one-parameter (pressure) formula. However, there is concern over the fact that isentropic implies reversible because the reversible process is an idealization [7]. It is a concept which can be approximated very closely at times, but never

matched. In many actual cases, effects such as friction, electrical resistance, and inelasticity can be substantially reduced, but their complete elimination is not found. These and similar effects are frequently called dissipative effects, since in all cases a portion of the energy originally in the system is converted or dissipated into a less useful form. Only in the absence of dissipativ effects can certain forms of energy be converted into other forms without any apparent loss in the capabilities of the system. Any system which is returned to its initial state after experiencing an irreversible process will leave a history in the surroundings due to irreversibilities. A partial list of these effects relating to pressure vessel bursts are: shock waves, unrestrained expansion of a fluid, mixing of dissimilar gases, and mixing of the same two fluids initially at different pressures and temperatures. Nevertheless, the reversible processes have been found to be an appropriate starting place on which to base engineering calculations. This is why the isentropic formula is the most often used formula in gas dynamics.

Table 2-1 shows calculated values for equations (10) and (27). Figure 2-3 shows plots of energy versus vessel pressure for a comparison of isentropic and isothermal expansion formulas. Energy was calculated per unit volume for purposes of comparison.

2.2 Real Gas Theory

The ideal gas assumption for high pressure (greater than 1500 psi) ruptures gives expansion energies that are unrealistically high. Accurate estimates of blast parameters from high pressure bursts require calculations based on real gas equations of state supported by empirical data. Ideal gas behavior is adequate for most low pressure situations (<1500 psi). The expansion energy from pneumatic pressure vessel rupture depends on fill gas temperature, ratio of specific heats, pressure, and volume. Pittman [8] found in his studies that for monatomic fill gas argon at ambient temperature, about 77 °F, increasing burst pressure above 15,000 psi results in less significant increases in expansion energy than at lower pressures.

Table 2-1
Comparison of Isentropic and Isothermal Expansion Energies for Ideal Gas (GN2)

Initial Vessel Pressure, P_i (psia)	Isentropic Expansion Energy, Eq (10) $\frac{ft\text{-}lb_f}{ft^3}$	Isothermal Expansion Energy, Eq (27) $\frac{ft\text{-}lb_f}{ft^3}$
0	0	0
50	8040	13807
100	18334	33933
300	66082	138840
500	118204	263540
750	186278	435142
1000	256347	618732
1500	400235	1010999
2500	696967	1862027
5000	1464214	4211588
7500	2249958	6748912
10000	3046281	9408315

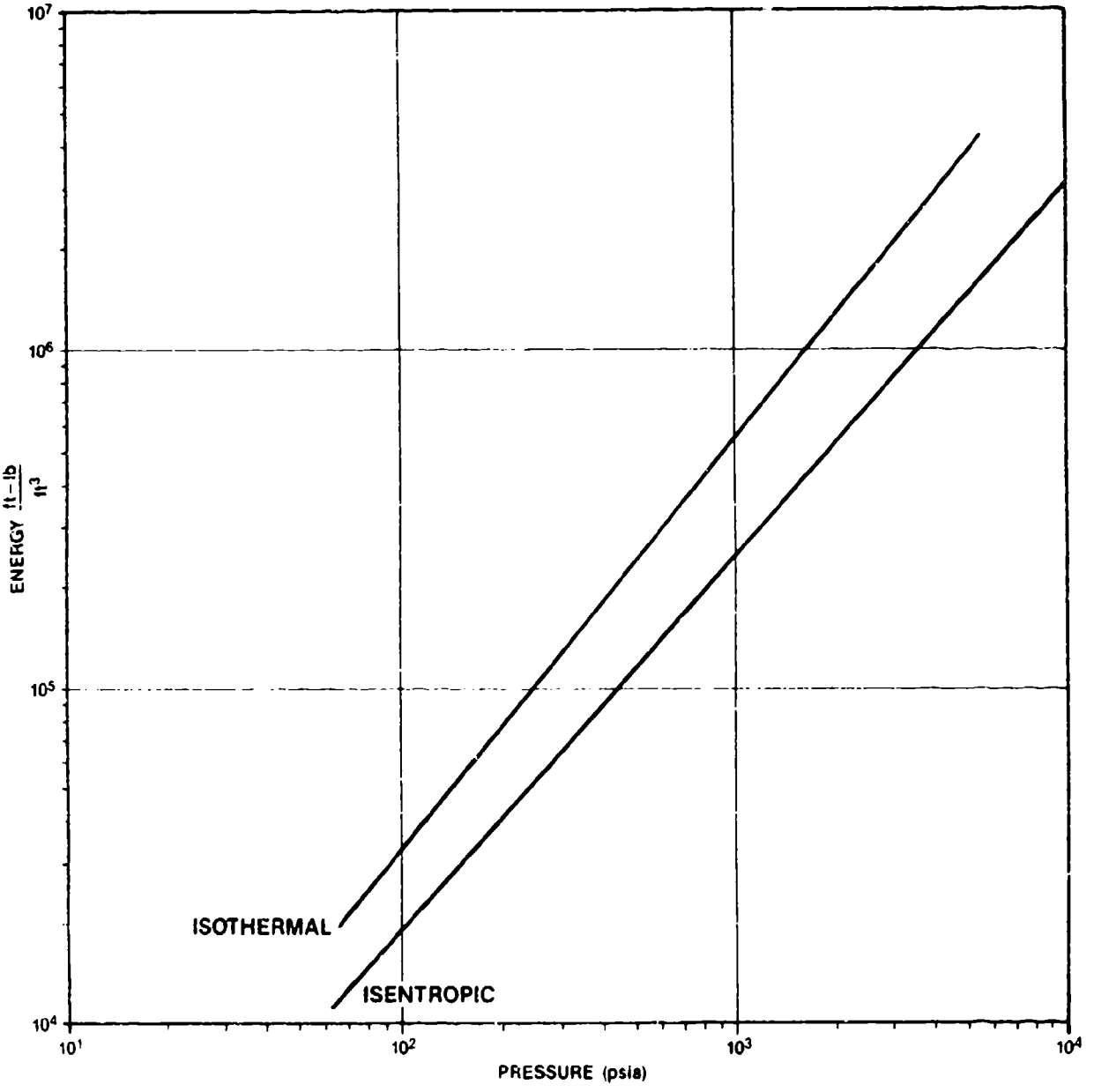

Figure 2-3. Comparison of Isentropic and Isothermal Expansion Energies for Ideal GN2

The effect of burst pressure on expansion energy is illustrated in Figure 2-4, a graph of pressure versus specific volume. A path is shown for argon, whereby it is isothermally compressed, beginning at 1 atmosphere and 290 K, to 15,000 psia; following vessel burst, it isentropically expands. The expansion energy is the work that is enclosed on the P-v curve by the path followed. If the argon had been isothermally compressed to 50,000 psia, however, the additional decrease in volume is very small. When the gas isentropically expands, the increase in work (enclosed area) is correspondingly small.

Pittman went on to determine that by increasing the gas temperature, for a given pressure, the expansion energy will increase until the limit is reached where the gas approaches ideal behavior, see Figure 2-5. For an ideal gas, expansion energy is independent of temperature and molecular weight; and the ideal gas internal energy represents an upper limit to the blast energy available from an argon vessel rupture. Pittman determined this occurred for argon at a pressure of 15,000 psi as the temperature approached 1970 F. Higher gas pressures require increasingly higher temperatures to approach ideal behavior. For this study, vessel temperature will be ambient (70 F) and vessel pressures will range from 50 to 15,000 psi. So for vessel pressures <1500 psi (100 atm), an ideal gas approximation will be used and for vessel pressures >1500 psi, a real gas approximation will be used. However, a problem arises for vessel pressures >10,000 psi in that compressibility (Z) data is very limited for GAr and GN2 in this region. Yet, for GAr at ambient temperature, increasing pressure above 15,000 psi only slightly increases expansion energy. So the problem of limited (Z) data above 10,000 psi may not be a significant problem. Further vessel burst testing may resolve this.

For real gases, especially at high pressures and very low temperatures, the ideal gas equation of state (PV = RT) is not a good approximation. There are several equations of state that can be used for real gases (e.g., Van der Waal's, Beattie-Bridgeman, Nobel-Abel and

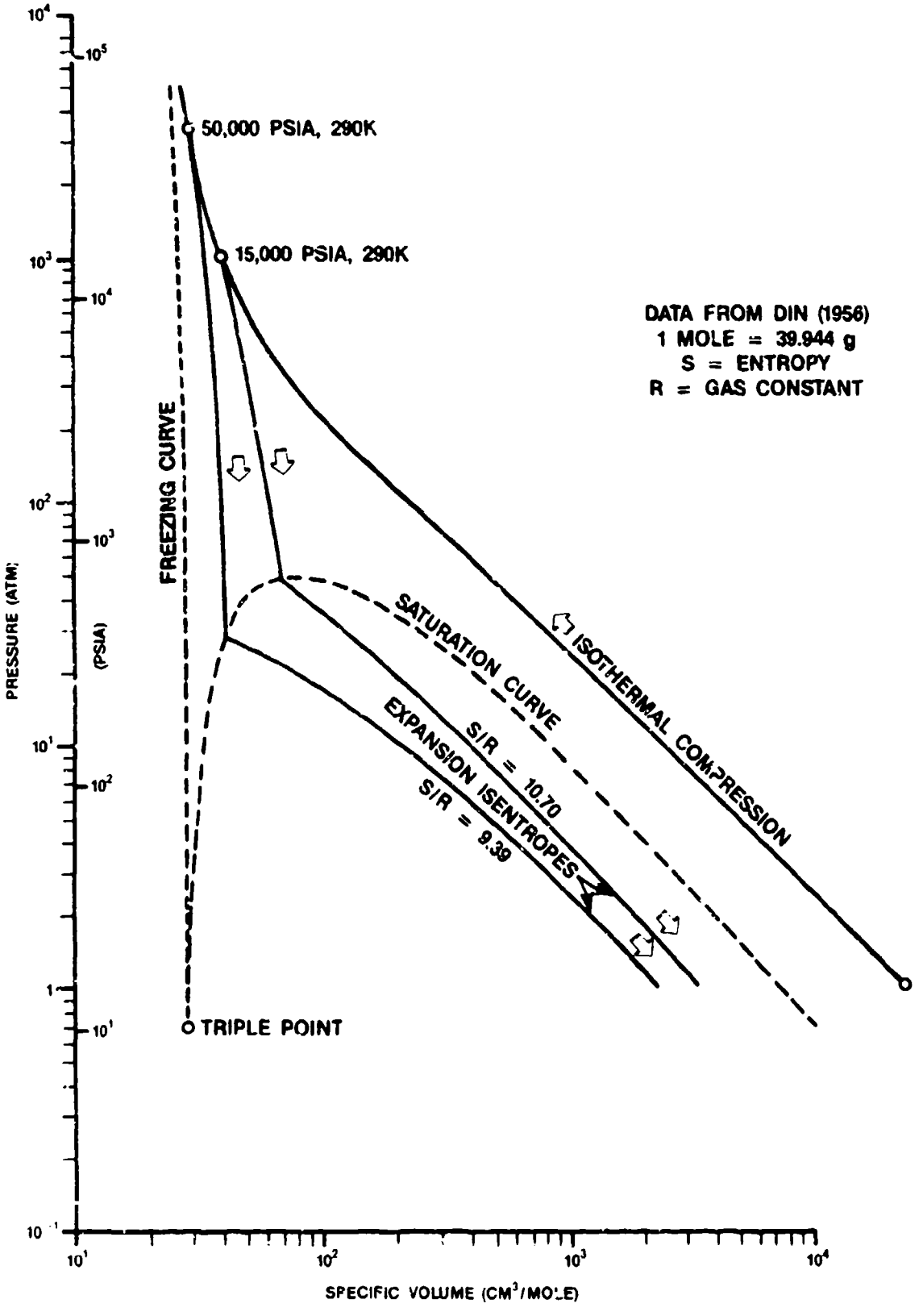

[8]

Figure 2-4. Argon P-V Compression and Expansion Paths for Cold Tanks

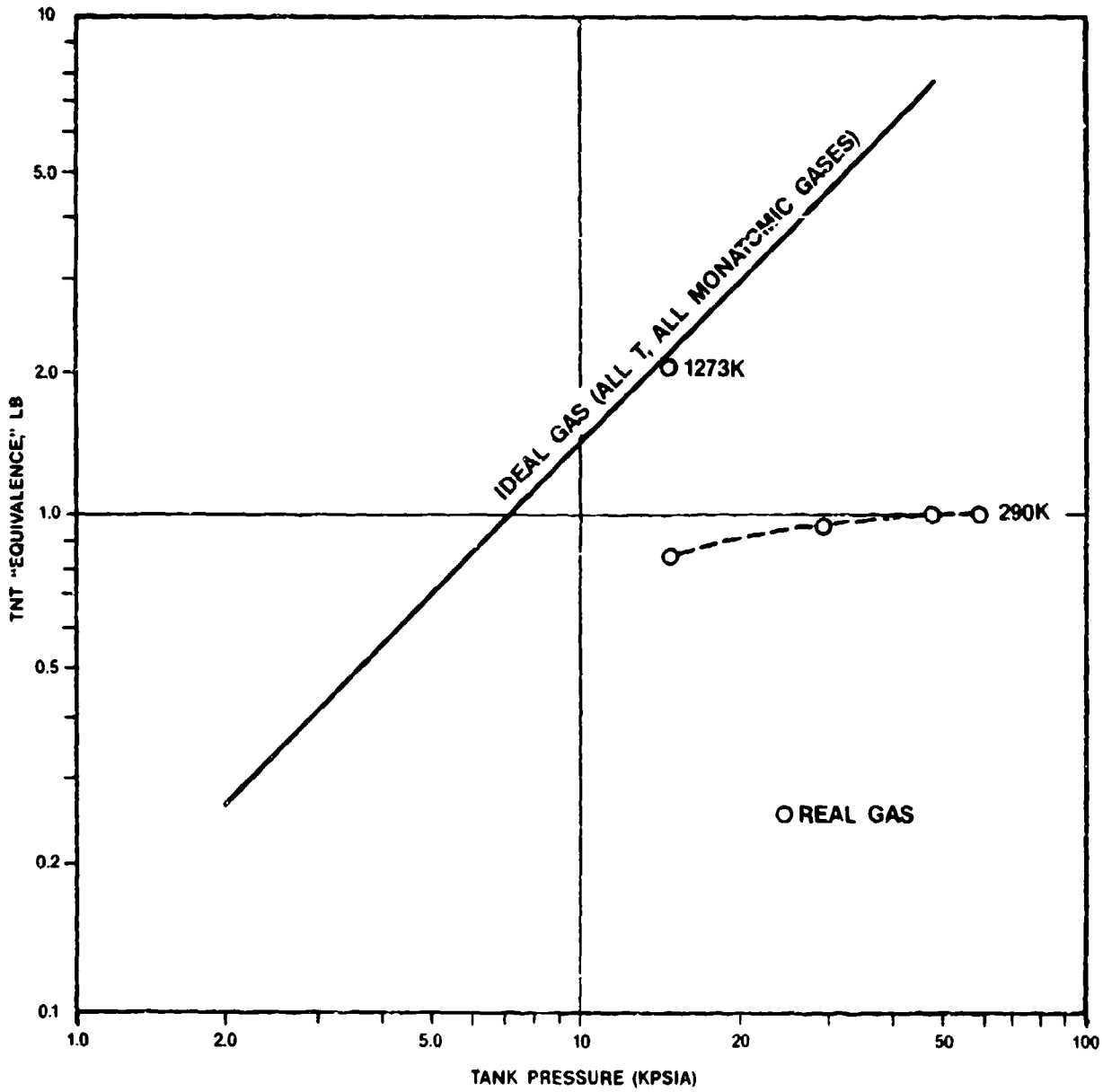

[8]

Figure 2-5. TNT Energy Equivalence of One Cubic Foot Pressurized Argon Tanks

Redlich-Kwong) using empirical coefficients for the appropriate gas [25]. One simple real gas equation of state involves a compressibility factor Z, which is defined as:

$$Z = \frac{Pv}{RT}$$

Since RT/P is the ideal gas specific volume (v ideal), the compressibility factor may be considered a measure of the ratio of the actual specific volume to ideal gas specific volume. For an ideal gas, the compressibility factor is unity, but for actual gases it can be either less than or greater than unity. Hence, the compressibility factor measures the percent deviation of an actual gas from ideal gas behavior. Applying this concept to equations 10, 17, and 27, we get expansion energy relationships for real gases as follows:

Isentropic:
$$\frac{W}{V} = \frac{P_1}{Z\left(\frac{K-1}{K}\right)}\left[1 - \left(\frac{P_2}{P_1}\right)^{\frac{K-1}{K}}\right] \qquad (28)$$

Adiabatic:
$$\frac{W}{V} = \frac{P_1}{Z\left(\frac{K-1}{K}\right)}\left(1 - \frac{P_2}{P_1}\frac{\rho_1}{\rho_2}\right) \qquad (29)$$

Isothermal:
$$\frac{W}{V} = \frac{P_1}{Z} \ln \frac{P_1}{P_2} \qquad (30)$$

Equations 28 and 30 present the isentropic and isothermal expansion energies, respectively, for a real gas. This section will compare the results of these equations for vessel failures with initial pressures ranging from 50 psi to high pressures typically used at various facilities. Table 2-2 shows calculated values for equations 28 and 30. The following are assumptions made to support the calculations:

1. Vessels are at ambient temperature (540 R)
2. P_z is atmospheric pressure (14.7 psia) in all cases
3. Gas: GN2
4. K = 1.4 for GN2
5. For GN2: T_c = 227 R and P_c = 33.5 atm
6. $P_R = P/P_c$ and $T_R = T/T_c$. Absolute pressures, and temperatures in degrees Kelvin or Rankine, must be used.

The curves are graphed in Figure 2-6. For purposes of comparison, the values were calculated per unit volume.

Table 2-2. Comparison of Isentropic and Isothermal Expansion Energies for Real Gas (GN2)

Vessel Pressure (psia)	Z	Isentropic Energy, Eq (28) $\frac{ft\text{-}lb_f}{ft^3}$	Isothermal Energy, Eq (30) $\frac{ft\text{-}lb_f}{ft^3}$
0	1.0	0	0
50	1.0	8040	13807
100	1.0	18334	33933
500	1.0	118204	263540
750	.99	188159	439537
1000	.98	261578	631360
1500	.97	412613	1042267
2500	.99	704007	1880835
5000	1.16	1262253	3630679
7500	1.37	1642305	4926213
10000	1.56	1952744	6030971

2.3 TNT Equivalence

In Sections 2.1 and 2.2, the energy release associated with a pressure vessel burst is theoretically predicted for the following processes: isothermal, adiabatic, and isentropic for both ideal and real

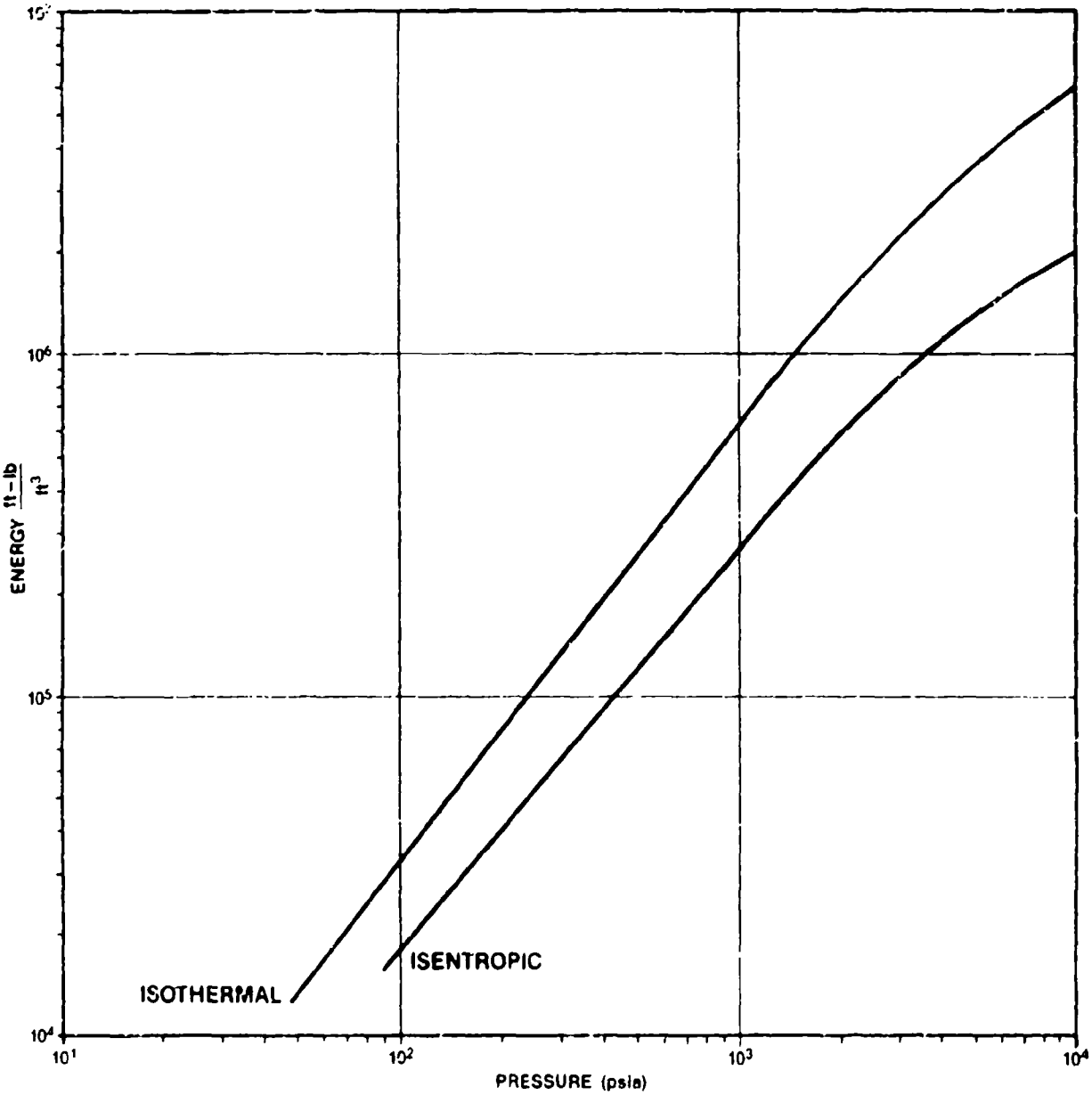

Figure 2-6. Comparison of Isentropic and Isothermal Expansion Energies for Real Gas

gases. In this section, it will be shown how TNT equivalency can be used to approximate a relative measure (e.g., pounds of TNT) of explosive magnitude for a bursting pressure vessel. Once the TNT equivalence is determined, then the effects of a pressure vessel failure can be converted to overpressure at various distances from the source.

2.3.1 Determining TNT Equivalence

The magnitude of an explosion is established by the amount of energy released. This can be expressed directly in energy units such as ft-lb, joules, or calories. To express explosions numerically a standard, TNT (symmetrical 2,4,6 - trinitrotoluene), was established. This is because TNT is a chemically pure material, it is readily available for calibration purposes, it is relatively safe to handle, and for specimens of known density and crystalline nature, its explosive effects are quite reproducible [4]. In Kinney [4], the standard pound (gram) of TNT is defined as the energy of 1.545×10^6 ft-lb (4610 J). This will be the standard for equating energy to equivalent pounds of TNT throughout this report. A further discussion of conversion factors will appear in Section 2.3.2. The energy expansion equations derived in Sections 2.1 and 2.2 will show how this energy from a bursting pressure vessel is equated to a TNT equivalence.

Example

Given: cylindrical vessel
hemispherical heads
horizontal geometry
gas: GN2
V_1 = 10 ft^3 T_c = 227 R P_o = 33.5 atm
P_1 = 2000 psi
P_2 = atmospheric = 14.7 psia

Assumptions: K = 1.4
isentropic expansion
real gas

Find: TNT equivalence

$$W = \frac{P_1 V_1}{Z(K-1)}\left[1 - \left(\frac{P_2}{P_1}\right)^{\frac{K-1}{K}}\right]$$

$$W = 5.43 \times 10^6 \text{ ft-lb}_f$$

TNT equivalence = 3.52 pounds TNT

Therefore, the energy from a burst pressure vessel of the dimensions given in the example can be equated to the energy from a charge of 3.52 pounds of TNT. This can be repeated for all sizes and pressures of pressure vessels. Figure 2-7 is a plot of the relationship between TNT equivalence in pounds TNT per cubic foot and vessel pressure in psi. The plot shows two curves relating to the energy expansion equations (e.g., isothermal and isentropic). However, of concern at this time is the fact TNT energy may differ from pressure vessel failure energy because not all of the vessel energy is directed into the blast wave as is the case for TNT energy. A significant portion of the vessel energy may be used to tear the vessel metal and propel fragments. This can only be resolved by further experimental work.

2.3.2 Overpressure vs. Distance for TNT

If the vessel burst energy is to be equated to a charge of TNT, a means to convert pounds of TNT to peak overpressure is needed. Overpressure is defined as the peak pressure above ambient conditions. Kingery [9] contains a compilation of experimental blast parameters versus distance that were measured on 5 -, 20 -, 100 -, and 500-ton TNT surface bursts. The data from all four tests were first processed to obtain the "as read" values of peak overpressure, arrival time, positive duration, and positive impulse. Cube root scaling and altitude corrections were applied to these values to bring them to standard sea-level conditions and the equivalent of a one-pound TNT charge. The peak overpressures were obtained from direct measurements provided by pressure transducers. The scale values were then used to determine the

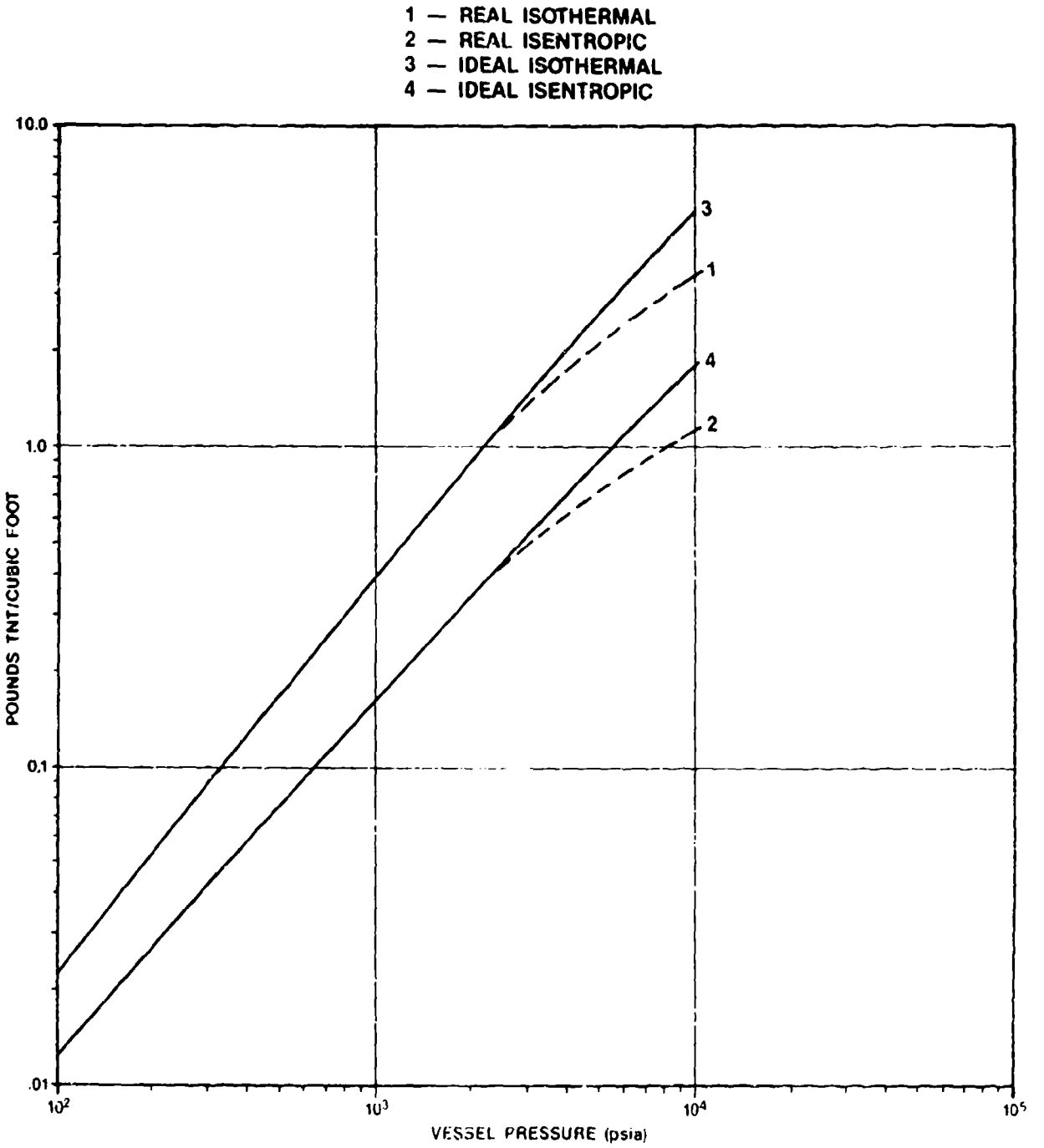

Figure 2-7. TNT Equivalence vs. Vessel Pressure for Ideal and Real GN2

curve in Figure 2-8 and data in Table A-I of Appendix B; λ = scaled distance $D/W^{1/3}$ where D = distance from ground zero (ft) and $W^{1/3}$ = cube root of TNT equivalence ($lb^{1/3}$) and ΔP_s = peak overpressure (psi). From the TNT equivalence, one can determine the peak overpressure at various distances from ground zero (point of vessel burst).

Cube root scaling can also be applied to bursts which occur above ground in order to, for example, minimize ground reflection [26]. The scaling equation is analogous to that used for the horizontal range.

$$\lambda_h = H/W^{1/3}$$

where λ_h = scaled burst height
H = height of burst (ft)
W = TNT equivalence (lbs)

As mentioned earlier in Section 2.3.1, the standard for equating vessel burst energy to equivalent weight TNT will be:

1.545×10^6 ft-lb energy = one pound of TNT for this report. This value comes from Kinney [4] who gives the basis for this value as follows:

> "The standard gram TNT is defined as the blast energy of 4610 J (1100 cal). This dates to early days of nuclear devices when a standard ton TNT was defined as the energy release of one million kilocalories."

Although we choose to use Kinney's conversion factor, there is no agreement in the industry as to a standard. The following are other conversion factors used in the industry:

- Brown, S., et al, "Energy Release Protection - ASME - SC6000,"
  Draft No. 1, August 1983.
  1.426×10^6 ft-lb = 1 pound TNT

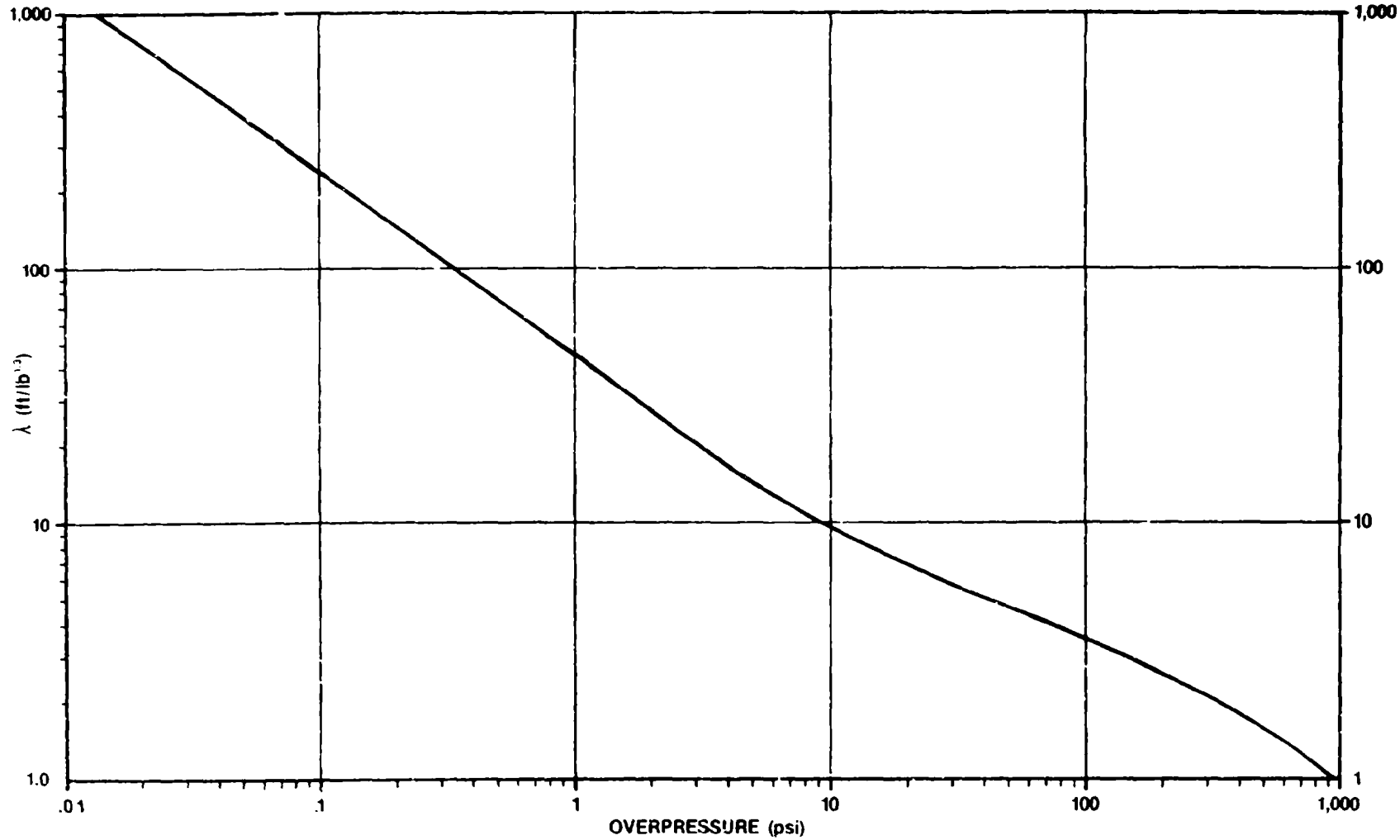

Figure 2-8. Overpressure vs. Scaled Distance, Kingery [9]

- Brown, S., et al, "Protection Against Pressure Vessel And Piping Explosions/Ruptures," Table 2.
  (4520 J/g TNT)
  1.515 x 10^6 ft-lb = 1 pound TNT

- Pittman, J.F., "Blast And Fragment Hazards From Bursting High Pressure Tanks," 17 May 1972.
  (1018 Cal/g TNT)
  1.428 x 10^6 ft-lb = 1 pound TNT

- Brown, S., "Pressurized Systems Energy Release Protection," NAS1-17278, May 1986.
  (1832.4 Btu/lb TNT)
  1.425 x 10^6 ft-lb = 1 pound TNT

- Baker, W.E., et al, "Workbook For Predicting Pressure Wave and Fragment Effects of Exploding Propellant Tanks and Gas Storage Vessels," NASA CR-134906, November 1975.
  1.4 x 10^6 ft-lb = 1 pound TNT

- Kinney, G.F., et al, "Explosive Shocks In Air," 1995
  1.545 x 10^6 ft-lb = 1 pound TNT

- U.S. Air Force, "Air Force System Command Design Handbook 1-6," December 1982.
  1.6 x 10^6 ft-lb = 1 pound TNT

As shown above, there are many conversion factors. The average of these seven is 1.477 x 10^6 ft-lb per pound TNT. Kinney's value differs by 4.4 percent from the average. By using 1.545 x 10^6 ft-lb/pound TNT (i.e., Kinney), a smaller TNT equivalence is obtained and, therefore, lower overpressures. Although this is not the conservative approach, it is felt that being able to relate to the standard definition where a ton of TNT is defined as the energy release of one million kilocalories is a good approximation. Further vessel burst experimentation should settle this debate.

2.3.3 Comparison of Experimental Data with TNT Equivalence

In order to perform a comparison between Pittman's experimental data [10 & 11] and TNT equivalence, tables (Appendix A) were developed using Pittman's data, vessel burst energy (isothermal and isentropic), TNT equivalence, and overpressures from Kingery data. The following is the sequence for performing the comparison:

1) The Pittman data of vessels, vessel volume, vessel burst pressure, vessel material, and burst medium were input on the tables.
2) The vessel burst energy from the expansion equations (isothermal and isentropic) was calculated and input on the tables.
3) The TNT equivalence was calculated based on 1.545×10^6 ft-lb per pound TNT from Kinney [4] and input to the table. Pittman had calculated a TNT equivalence for his vessels but used an earlier approximation of 1.428×10^6 ft-lb per pound TNT, resulting in the differences shown in the tables.
4) The TNT equivalence was converted to overpressure data at distances equal to the Pittman data. This was performed using the table Kingery [9] developed (see table A-I in Appendix B). Kingery's table uses a term (λ) defined as the scaled distance from ground zero in units of ft/lb $^{1/3}$ TNT. Taking the distances from Pittman and the cube roots of the TNT equivalence, (λ) was calculated. Entering Kingery's table A-I with (λ), a corresponding overpressure (ΔP_s) in psi was obtained. These values of ΔP_s were recorded on the tables.
5) From this data, overpressure versus distance curves were plotted and compared against actual Pittman data. Figures 2-9 and 2-10 show representative plots with the remaining plots being contained in Appendix C.

Figures 2-9 and 2-10 plot overpressure versus distance for real argon (Figure 2-9) and ideal argon (Figure 2-10) for both isentropic and isothermal expansion of the gas. The same 9 data points from Pittman (vessel 6) appear on each figure. The curves assume that all of the energy from the burst goes into the blast wave. Both the isothermal and

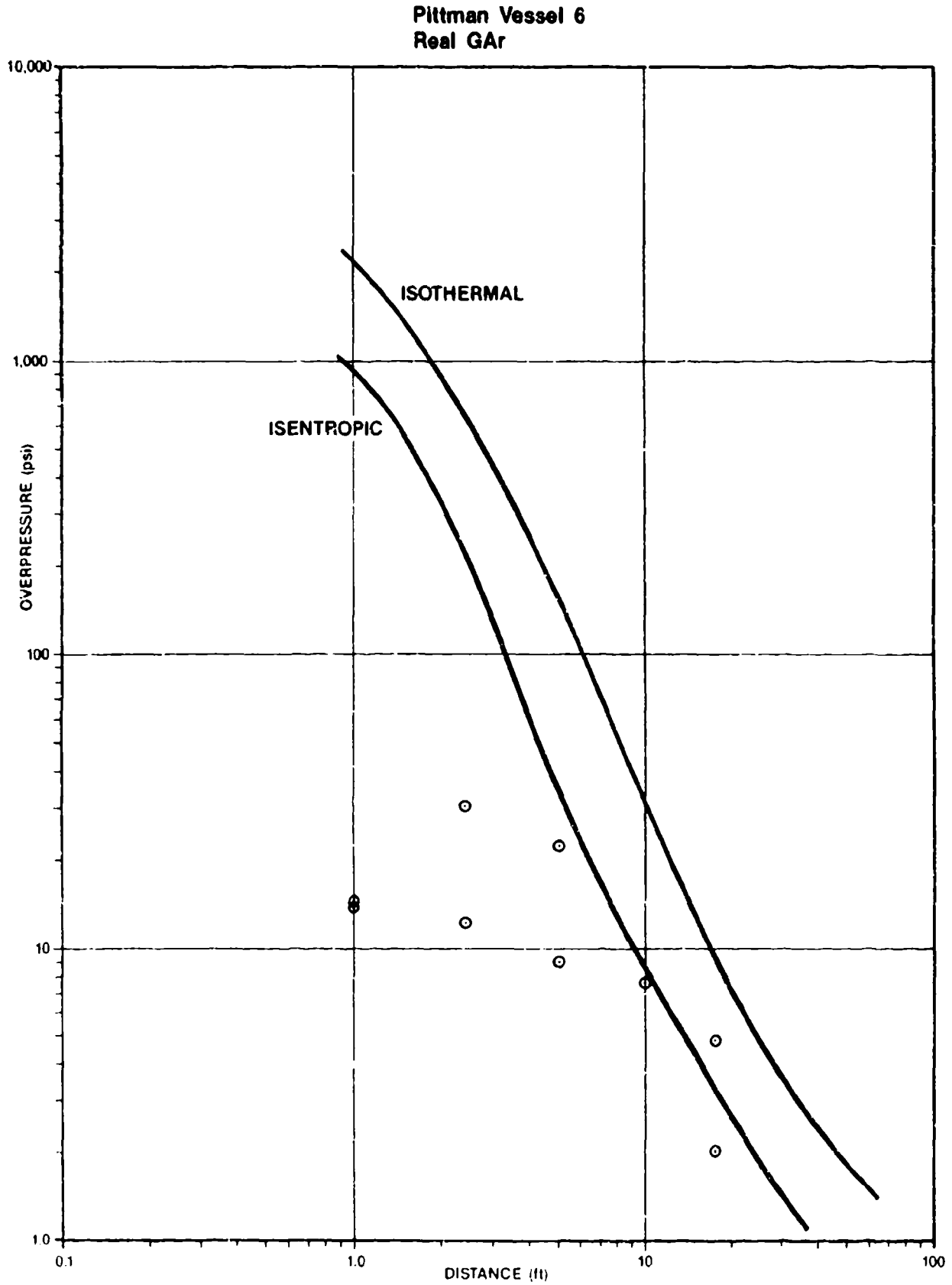

Figure 2-9. Overpressure vs. Distance

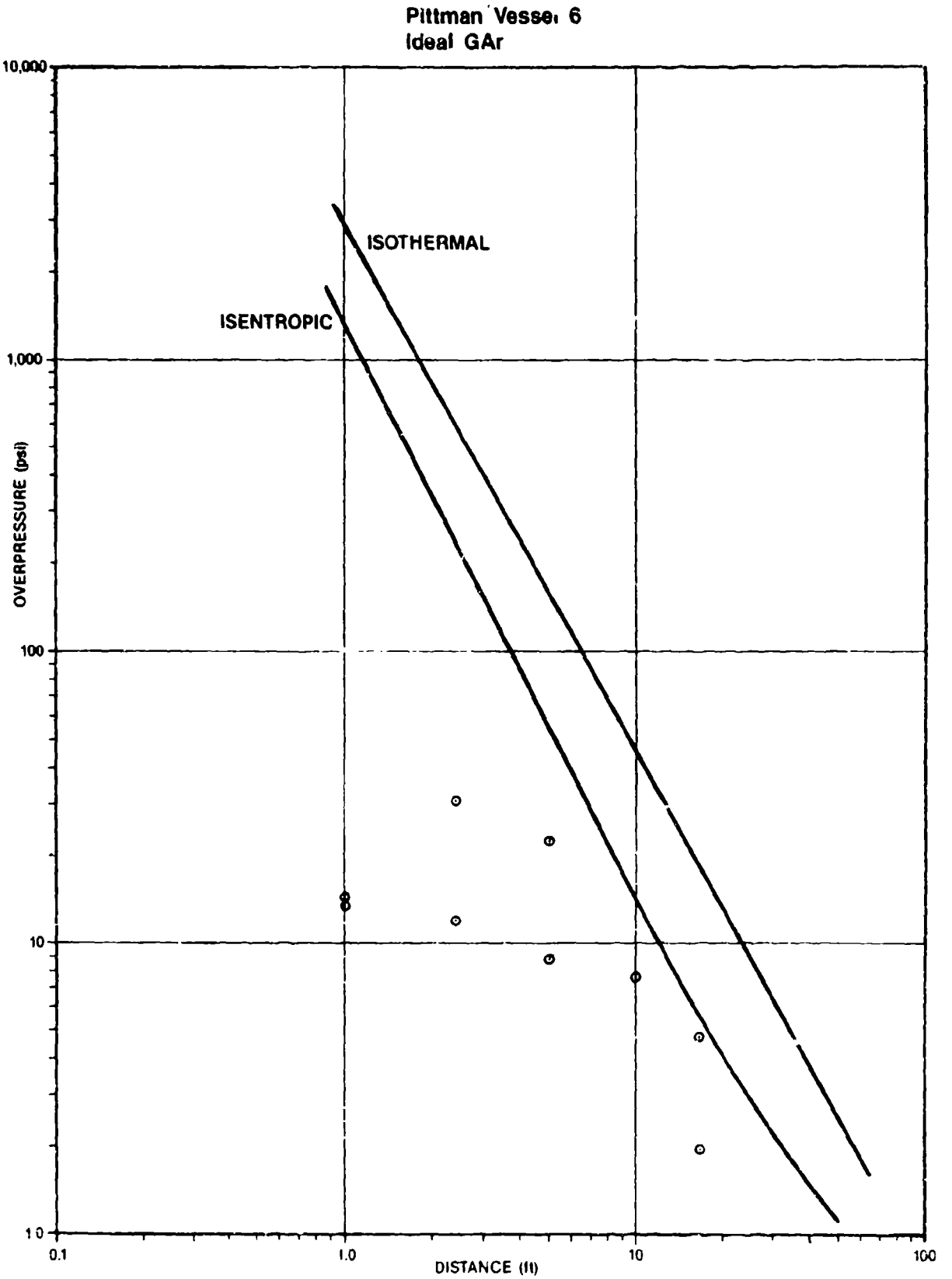

Figure 2-10. Overpressure vs. Distance

isentropic curves overestimate the pressure seen at a given distance from the burst. The isentropic expansion case for real argon predicts the experimental data most nearly accurately.

The following conclusions can be drawn from Figures 2-9, 2-10, and Appendix C: 1) Overpressure vs. distance curve for a pressure vessel rupture does not correspond to that for a TNT explosion of equivalent energy. 2) Using TNT burst data from hemispherical charges is not accurate for use with cylindrical vessels because a blast wave from a pressure vessel rupture is strongly influenced by burst geometry. 3) The factor controlling the magnitude of the airblast overpressure from pressure vessel rupture in the Pittman tests was the jetting direction of the high pressure gases. 4) No allowance was made in the calculations for the reduction of energy available to the blast wave resulting from the energy expended in vessel tearing and fragment acceleration. Brown [6] states that anywhere from 20 to 80 percent of the burst energy goes into the blast wave.

Estimates of the energy available to the blast wave based on theory and experiment, for munitions, are reported in literature. The most common estimate, according to Fugelso [12], of the energy available to the blast wave is the modified Fano formula (Joint Munitions Effectiveness Manual, 1970).

$$\frac{Weff}{W} = 0.6 + 0.4 \left(1 + \frac{2}{C/M}\right)^{-1}$$

Where: Weff is the energy available for blast. C/M is the charge weight-to-metal weight ratio. The charge weight is taken as the equivalent TNT weight.

These different estimates for the amount of energy available to the blast wave have to be verified with additional vessel burst data.

2.4 Experimental Approach and Computer Codes

2.4.1 Experimental Approach

The Department of the Air Force is concerned with the integrity of both flight and ground support pressure vessels and any hazards that result from their use. Additionally, they must be able to accurately predict the potential damage if a pressure vessel were to burst. As shown in earlier sections, an accurate method to relate vessel burst energy to blast wave overpressure does not exist. Nor is there enough existing experimental data to validate computer codes. Therefore, an experimental approach should be used to produce empirical data on which estimates of overpressure damage can be based or validated.

Pittman's experimental approach [10 & 11] for bursting pressure vessels and collecting data uses a methodology that follow-up studies performed today, could use. In the 10 years since Pittman's experiments, there have been advances in technology with regards to instrumentation such as transducers used to measure blast wave phenomena. These advances in technology can be integrated into Pittman's methodology to upgrade the experimental approach to today's standards. However, a few problems still exist in today's technology with regards to blast wave measurement. These include calibration of the blast gages and measurement of peak overpressure. Blast gages are typically piezoelectric-type pressure transducers intended for dynamic situations. These may be capable of only semi-static use, whereas static transducer calibrations are typically the most precise. The extra effort for dynamic calibrations may be desireable to check rise time and ringing which would affect accuracy in measuring peak overpressure. The most precise measurement of overpressure requires ideally an inertialess pressure sensing element with zero time delay. In contrast, arrival times may be more simply and precisely measured. Compromises can be made between the desired characteristics and what feasibly can be obtained without degrading the experimental results.

2.4.2 Computer Codes

Figures 2-11 and 2-12 are representative of the types of curves that can be generated by computer modeling of the blast wave from a bursting pressure vessel. The codes used to generate these curves are two of the available codes that have been used to model blast effects from explosives and pressure vessels. The two codes examined by this study are the Wondy V Code and the Sharp Shock Wundy Code.

The Wondy V Code was selected because Pittman had used an earlier version of the code in his first study [10]. The Sharp Shock Wundy Code was used because it includes a modification that may more accurately predict the sharp shock peak at the leading edge of the blast wave. (This is evident by examining the shape of the two curves in Figure 2-12, and comparing them to theoretical blast wave curves or to actual test curves from vessel burst tests.) Differing opinions exist as to the actual shape of this curve. Some contend that a vessel burst blast wave is characterized by a sharp rise to a peak pressure and an exponential decay thereafter see Figure 2-1a, while others say there is a less rapid rise to a less distinct peak with a gradual decay to ambient, see Figure 2-1b. This also will have to be resolved by more testing, because peak pressure is a major concern in assessing the effects of blast waves.

Figure 2-11 shows the peak pressure that would be observed at any radial location from the vessel as determined using the Sharp Shock Wundy Code. Another way to explain this curve would be to connect the peaks in Figure 2-2 and a curve similar to Figure 2-11 would be obtained. Figure 2-12 shows peak pressure (overpressure) versus distance for a specific instance in time after the vessel burst, as determined using both computer codes. The Wundy Sharp Shock Code was used for nitrogen and the Wondy V Code was used for argon. These curves

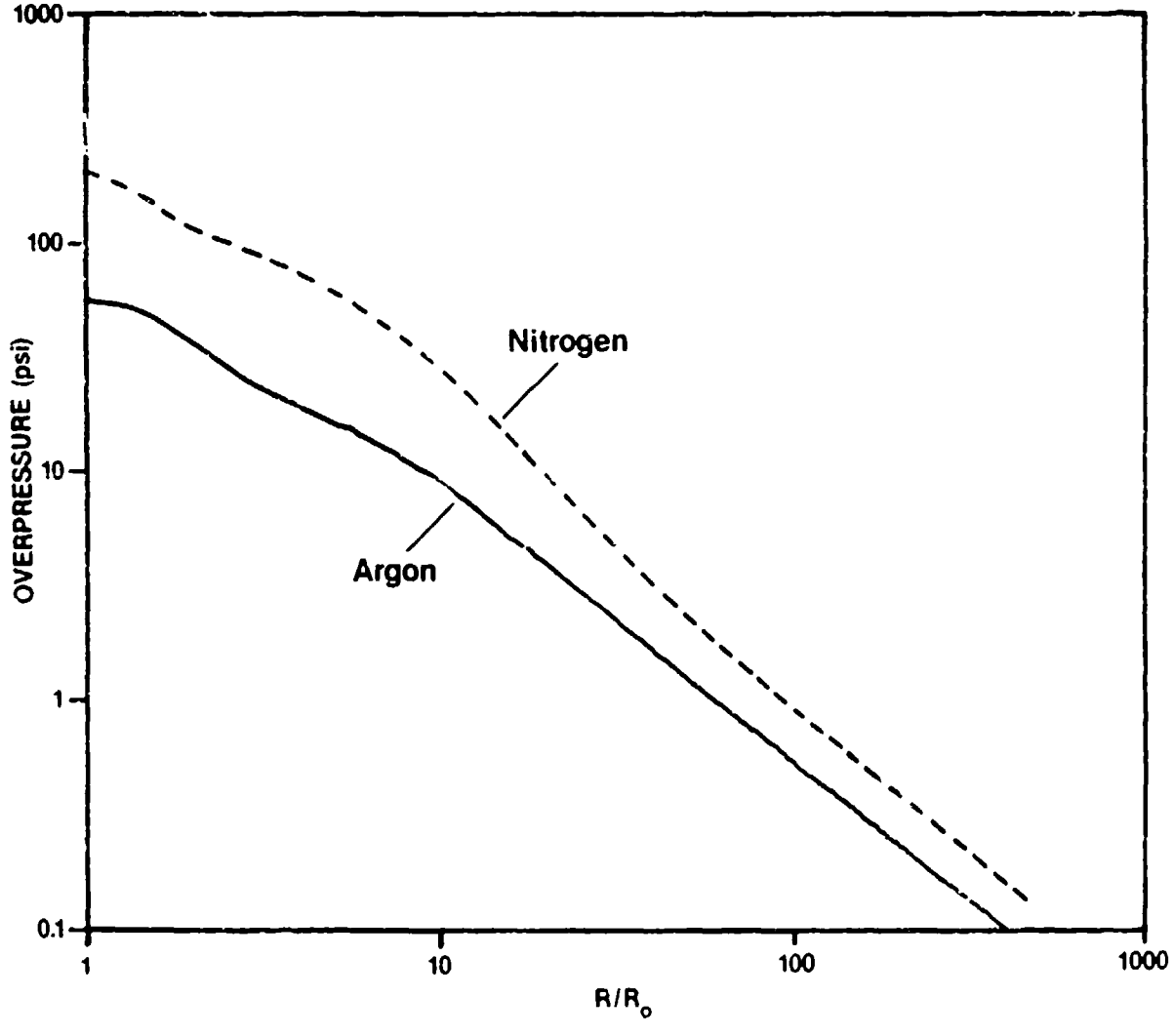

Figure 2-11. Overpressure vs. Scaled Distance for Argon and Nitrogen Tanks Pressurized to 8000 psi in a 17C Environment. (from ATR, 1987)

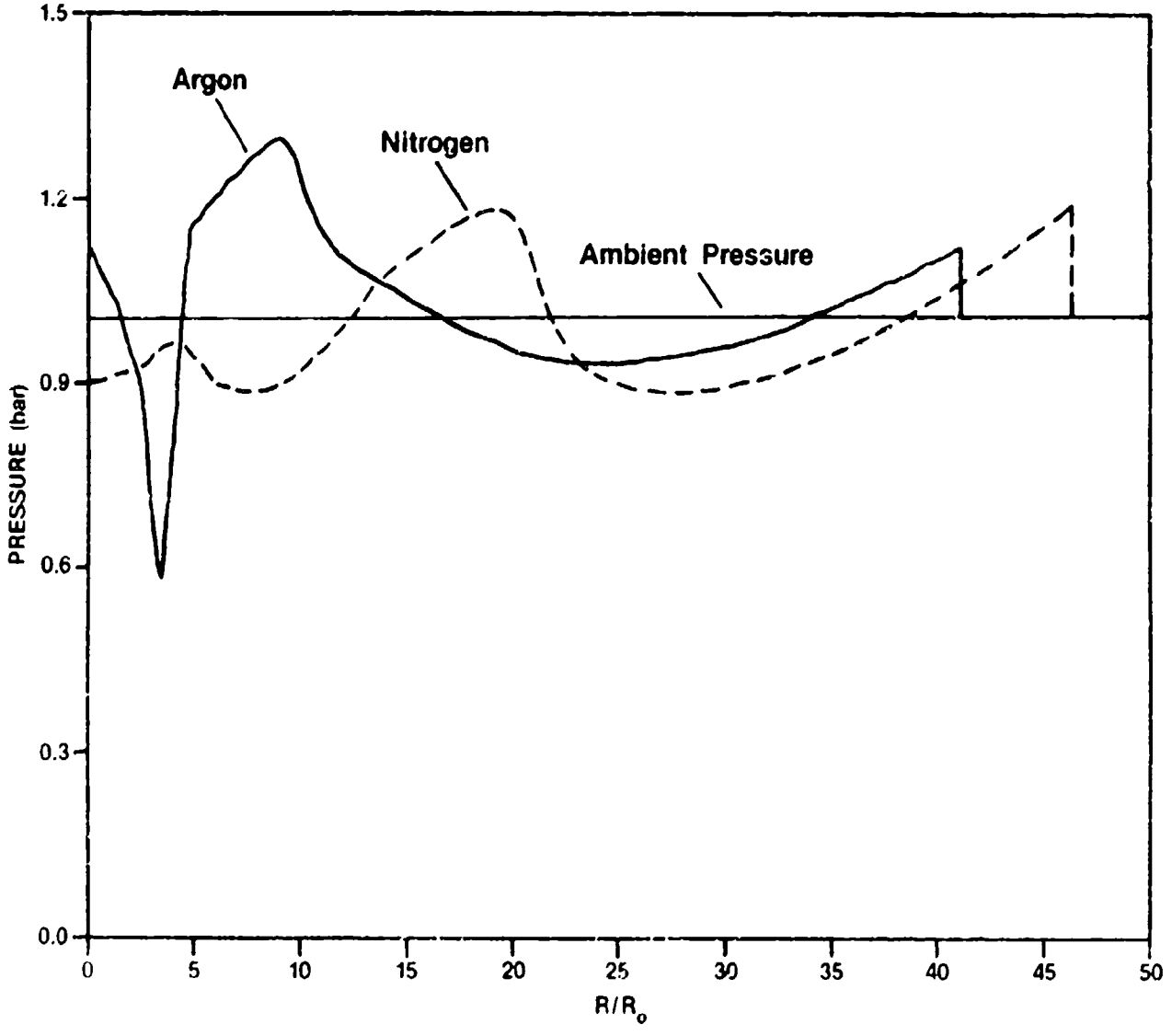

Figure 2-12. Pressure vs. Scaled Distance for Argon and Nitrogen at approximately 1025 μ sec/cm. (From ATR, 1987)

were developed for a vessel which is similar to the vessels used by Pittman. The following are the vessel characteristics used in the computer code example:

Spherical
Volume - 6 ft³
Fluid - gaseous nitrogen (GN2), gaseous argon (GAr)
Burst pressure - 8000 psig
Fluid temperature - 17°C (63°F)

Figure 2-11 shows a very high overpressure (>100 psi) at the vessel surface $R/R_o = 1$, which rapidly decays. However, it is evident from the graph that significant overpressure exists farther out than 113 ft ($R/R_o = 100$). In this case, "significant" means overpressure that could break windows, which is possible with fairly low overpressures. If a minimum acceptable overpressure of 0.5 psi is used, then the separation distance from this graph would be about 170 ft ($R/R_o = 150$). This is considerably less than the minimum criteria of 1250 ft required by current practice [13].

An additional aspect to be considered with these curves is the assumptions made in doing the computer calculations. First, the blast wave was assumed to be one-dimensional (1-D) (i.e., the energy from the blast wave dissipates equally in a circle from the blast center). Second, the calculation assumes that all the energy available in the pressurized gas is dissipated through the blast wave. Neither of these assumptions are completely accurate in a real situation. These assumptions, along with ways of accounting for them, are the subjects of the following paragraphs.

The first assumption, that the blast is 1-D, assumes that the vessel breaks up into two equal halves with the blast wave being released equally in a circle; see Figure 2-13. This is an underconservative assumption, because most vessels fail at a localized area of high stress. Because the initial failure would occur at a specific location, a large portion of the energy stored in the vessel

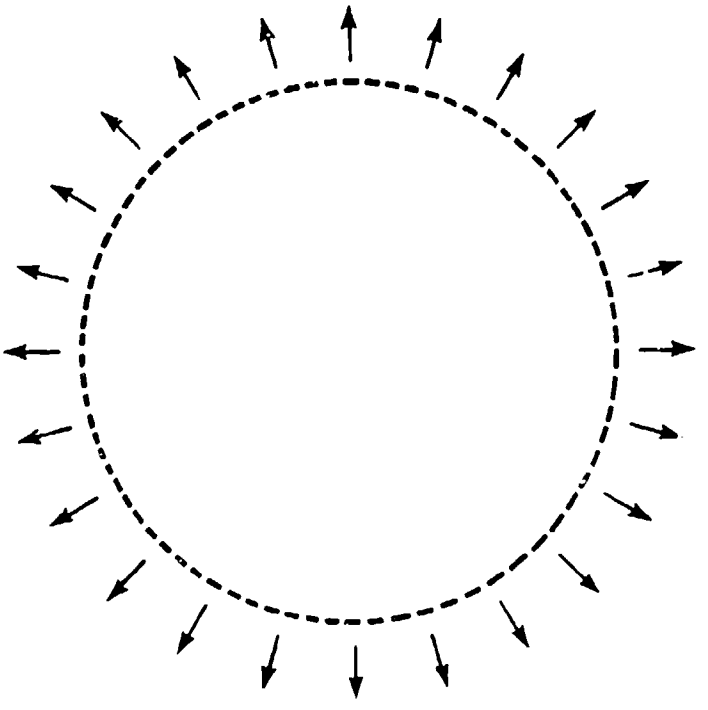

One-Dimensional Blast

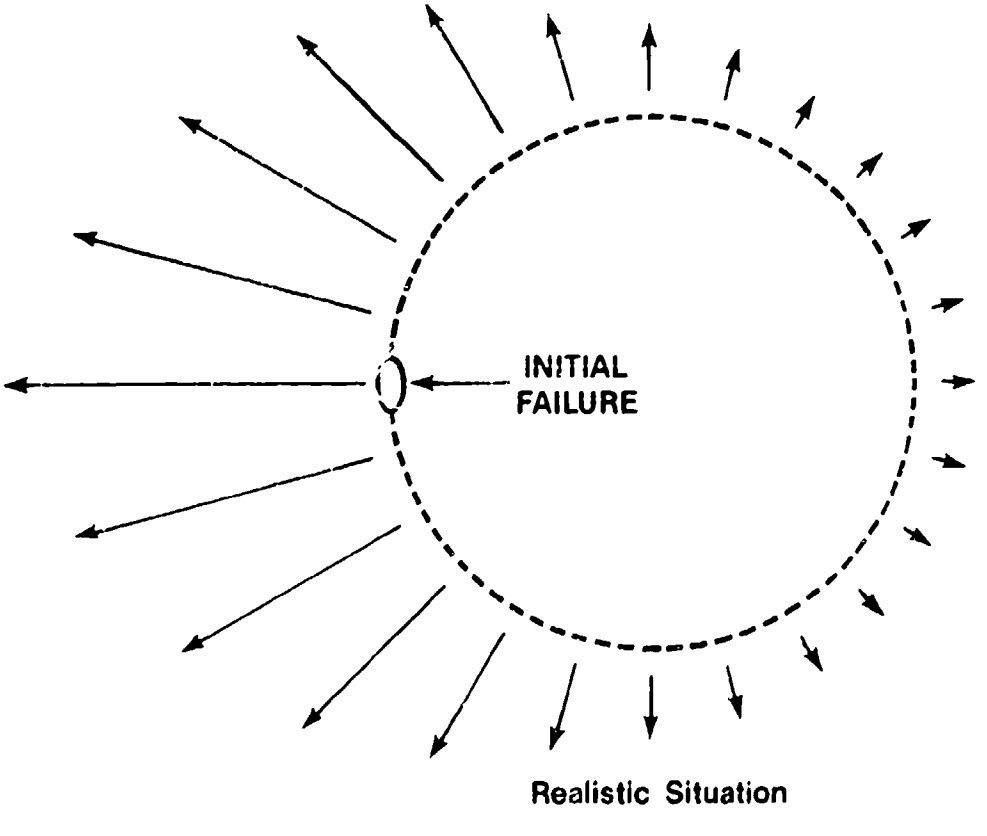

Realistic Situation

Figure 2-13. One Dimensional Blast vs. Realistic Situation

would be released through the initial failure, in one general direction, and not evenly in all directions; see Figure 2-13. Pittman made the following observation based on his 1976 experiments [8]:

> The blast field from pressure vessel rupture is strongly influenced by burst geometry. The vessels used in this investigation burst into two pieces creating strong argon motion along a line defined by the vessel's center and the point on the vessel where rupture first occurred. Airblast overpressures measured along the line of this jet were more than a factor of 4 greater than those measured in the opposite direction.

To still use a simple 1-D Code, it would be necessary to multiply the energy available for the 1-D Code by a correction factor to compensate for the directionalization of the energy release in a realistic situation. Different types of vessels may require different correction factors. To determine what correction factor would be necessary, a testing program would have to be conducted which would compare computer runs to burst tests. An alternative method to using such a correction factor would be to use a more complex two- or three-dimensional computer code to predict overpressure. But a two- or three-dimensional code could only be "run" on a supercomputer. This option was not pursued.

The second assumption, that all the energy is dissipated in the blast wave, is an overconservative assumption. It was stated earlier in Section 2.1.2 and again in 2.3.3 that only 20-80 percent of the energy is dissipated through the blast wave. This overconservative assumption may or may not compensate for the underconservative assumption discussed above. In either case, predictions must be compared to tests of various shapes, sizes, materials and pressures of vessels before an accurate prediction method can be developed.

2.5 Evaluation

The two principal models used to predict the blast wave generated by a pressure vessel burst employ isentropic expansion and isothermal

expansion, respectively, of the contained gas. In each model, the energy released by the vessel burst is determined by calculating the work performed by the expanding gas. All of this work is assumed to supply energy to the blast wave. The expansion of the contained gas is neither isothermal nor isentropic, but the isentropic expansion approximation appears to model the blast wave more closely, using Pittman's data.

Assuming that the expanding gas is ideal predicts greater overpressures than if real gas equations are used. In both cases, however, the predicted overpressures exceed those obtained experimentally.

It is convenient to equate the energy released by a vessel burst to that produced by an explosion of a given amount of TNT. This is a useful comparison since there is a much larger body of experimental data for TNT explosions than for pressure vessel bursts. Unlike TNT explosions, however, a significant amount of the energy produced by a vessel burst is expended in breaking the vessel and in accelerating fragments.

There is a limited amount of available data to compare the blast wave methodologies to experimental or accidental vessel bursts. Additional testing is required to validate a methodology.

Two one-dimensional blast wave computer codes are available to model the overpressure as a function of distance from the point of vessel burst. The one-dimensional codes assume that the blast wave progresses radially, that is, the overpressure at a given distance is the same in any direction. Since vessels can be expected to fail at a flaw, a jetting effect should be produced with much higher overpressure along the line of the jet than in other directions.

SECTION 3. FRAGMENTATION

The purpose of this section is to review the current methodologies available to predict the properties of the fragments generated by the burst of a high pressure pneumatic vessel. The section begins with an introduction, which briefly describes some of the most important studies on pressure vessel fragmentation, and which is followed by a discussion of terminology relevant to fragmentation.

Most analyses to predict the initial velocities of fragments are based upon a work by Taylor and Price. This analysis and subsequent analyses, which generalize Taylor-Price or adapt it to special cases, are reviewed. Each analysis is evaluated and compared to experimental data, where applicable. One model is also discussed which utilizes a real gas instead of an ideal gas which the other models use; a comparison between real and ideal gas effects on fragment velocity is made.

Once the initial velocity of a fragment is determined, it is desirable to calculate its range. This is accomplished using the established ballistics equations of physics; computer codes are identified which determine fragment range, given the initial velocity. Some upper limits on fragment range are identified for special cases.

Experimental data on fragmentation is presented and evaluated. The lack of available data on the distribution of fragments (the number produced and their masses) is identified.

A discussion of a probabilistic determination of fragment generation and trajectories is addressed. This methodology involves determining probability functions, based on experimental data, for fragment number, size, shape, mass, initial velocity and range. A lack of available experimental data currently limits the use of this methodology.

3.1 Introduction

The failure of a pressure vessel not only generates a blast wave but also produces fragments, usually with very high velocities. These fragments constitute a significant hazard to personnel, systems, components and structures in the vicinity. A study of the hazards associated with the failure of a vessel must include consideration of the range and potential impact energy of each of the fragments produced.

Brown [6] and Baker [14] have both written summaries of the current (circa 1984) state of the art in fragmentation.

Determining the velocities of fragments from pressure vessel ruptures has been undertaken by several authors. Taylor and Price (1971) developed equations for velocities of the fragments for a spherical pressurized gas vessel bursting into 2 halves. Their analysis was expanded by Bessey and Kulesz (1976) to allow for the rupture of either a sphere or a cylinder into any number of fragments. Baker (1975) developed two computer codes, SPHER and CYLIN, based upon the Taylor-Price analysis, to determine the fragment velocities for a sphere and cylinder, respectively, bursting into a given number of fragments (which must be assumed); the computer code FRAG 2, also based upon Taylor-Price, determines fragment velocity and other parameters for a vessel bursting into two equal fragments. Baker, et al, (1978) developed the code UNQL to calculate fragment velocities when a spherical or cylindrical vessel bursts into two unequal fragments.

Jager (1981) derived the fragment velocity for two cases: a jet propelled fragment torn off of a moored pressure vessel and a self propelled fragment such as a rocketing cylinder. Baum (1983) modified the work of Kulesz, et al, (1979) to determine upper limits on fragment velocity by analyzing gas properties and the effect of the rarefaction wave generated within the gas by the motion of the accelerating fragments.

Bessey (1974) also extended the Taylor-Price analysis to spherical vessels containing liquid propellants. The [illegible] and oxidizer are assumed to come into contact and partially det[illegible]. He compares his

results to those of Taylor-Price for pressurized gases. Similarly, Kulesz (1978) derived equations for the rocketing effect of a large portion of a liquid propellant vessel, and developed the computer code THRUST.

Determination of the range of a fragment from its initial velocity is well understood. Ballistics equations from physics can be used to determine fragment trajectories; these require knowledge of initial target speed and elevation angle and also the drag (or lift) coefficient for its orientation in flight. Two computer codes, TRAJE and FRISB, were developed by Baker, et al, (1975 & 1978) to determine the ranges of drag type and lift type fragments, respectively.

Presently, there is no theory to predict the distribution or dispersion of fragments; that is, the number, size and mass of fragments must be determined empirically.

3.2 Terminology [27]

One of the primary hazards from vessel failure is due to the fragments that are generated. Fragments can be accelerated to very high speeds and threaten nearby personnel, systems and components. Additionally, fragments can penetrate nearby storage vessels, causing vessel(s) to fail and possibly leading to detonation of liquid propellant.

Primary fragments are portions of the vessel or its attachments that are accelerated due to the internal pressure of the vessel upon failure. As few as one fragment may be produced in the failure of a ductile vessel. Vessels which fail in a brittle manner or which fail due to the partial detonation of a liquid propellant will generally produce more fragments.

Secondary fragments, or appurtenances, are produced due to the action of the blast wave on nearby objects, such as tools, components and parts of buildings. An important secondary fragment is broken glass which is a hazard to personnel and can also penetrate thin-skinned objects nearby.

Fragments will follow a trajectory until they impact an object or strike the ground. The forces which act upon them are gravity and the fluid dynamic forces: drag and lift. The drag or fluid force acting on a fragment is given by:

$$F = 1/2\ C\ \rho\ Av^2$$

where ρ = air density
v = fragment speed
A = surface area

and C is either the drag coefficient C_D or the lift coefficient C_L, as appropriate. The lift and drag coefficients must be empirically determined and graphed or tabulated.

Fragments with lift coefficient greater than drag coefficient are called lift type fragments; they are usually disk shaped. Fragments with drag coefficient greater than lift coefficient are called drag type fragments. They are usually chunked shaped, that is, all of the dimensions are of the same order of magnitude. Trajectory calculations are performed differently for lift type fragments and drag type fragments.

The relative hazard that a fragment presents is dependent upon both its trajectory parameters and its impact effects. A fragment can cause damage by either penetrating or rebounding from an object. If the fragment passes entirely through the object, the process is called perforation. If the fragment fails to pass entirely through the object, but displaces a portion of it, it is termed penetration. Spalling is the process by which the impact induces compression waves in the object, causing a tension failure.

3.3 Determination of Initial Fragment Velocity

3.3.1 Taylor - Price Analysis

The velocities of 2 fragments generated by the rupture of a spherical pressure vessel were predicted by Taylor and Price [15] in a 1971 ASME paper. Their work was based upon that of Grodzovskii and Kukanov (1965) but removed two restrictions: (1) the speed of the gas,

and therefore, the fragments are small, relative to the sonic escape velocity and (2) the volume between the separating fragments as they are accelerating does not change significantly from the original volume.

The Taylor-Price analysis assumes that the two fragments move in opposite directions in a vacuum and that an ideal gas escapes perpendicularly to the motion of the fragments. The velocities are determined for the fragments for two cases: isothermal and adiabatic.

The isothermal case yields higher velocities for the fragments than does the adiabatic case. This is not surprising since the isothermal case predicts higher available energy from the blast. Both cases predict lower velocities than those obtained by Grodzovskii and Kukanov.

In the isothermal case, they determined that as the dimensionless mass $\alpha = \frac{P_o V_o}{M_t a_o^2} = \frac{C_o}{KM_t}$ becomes large, the maximum possible fragment velocity v_{max} approaches a constant: $v_{max} = a_o \sqrt{\frac{2}{K-1}}$

where a_o = sonic velocity of gas
C_o = mass of gas
K = ratio of specific heats
M_t = total mass of vessel and gas

This maximum fragment velocity corresponds to the maximum velocity attainable in nozzle expansion. Note that α is large in highly stressed, lightweight vessels.

The analysis by Taylor and Price has been used, extended or modified by several other authors in order to improve on the assumptions or to adapt the analysis to other cases.

One such extension of Taylor-Price was performed by Baker, et al, (1975), and covers cylinders as well as spheres.

3.3.2 Modifications to Taylor - Price

Baker [5] assumed that, in the case of a sphere, it fragments into n fragments of circular projection which travel radially without tumbling. A cylinder shell is assumed to fragment into n lengthwise strips which travel radially; motion of the two heads is not considered. The energy of the contained gas is partitioned between the kinetic energy of the fragments, the energy of the escaping gas and the energy of expansion of the gas. Strain energy in the vessel walls prior to burst is neglected; however, for steel vessels containing gas at pressures of several thousand psi, this energy is on the order of 0.1% - 0.2% of the gas energy.

Baker developed the computer codes SPHER and CYLIN to solve for the nondimensional velocities of the fragments for the spherical and cylindrical vessels, respectively. Both codes use the Runge-Kutta integration technique to solve simultaneous nonlinear differential equations for the velocities. The number of fragments generated by the burst must be assumed and used as an input parameter. Baker used these codes to solve for the velocities in a large number of cases. These solutions were used to generate curves which could be employed to determine fragment velocities.

The solutions demonstrated that as the number of fragments produced increases, the maximum fragment velocity increases to a maximum; this occurs when 10-30 fragments are produced.

The SPHER code was run, and the curves were also used, to calculate fragment velocities for 4 cases which were measured by Pittman [10] (discussed in Section 3.5). The SPHER code and curves underestimate the velocity of the smaller sphere by about 10%. They underestimate the velocity of the larger sphere by 20-25% as measured by the breakwire system but are very close as measured by the strobe photographic system.

The measured and calculated velocities are:

Sphere Characteristics		Pressurizing Gas		Initial Fragment Velocities		
Radius	Wall Thickness		Pressure	V(Pittman)	V(Code)	V(Curves)
cm	cm	Type	Pa	m/s	m/s	m/s
11.7	0.274	N_2	5.51×10^7	366±15	352	338
34.3	0.919	N_2	5.51×10^7	342±30[1]	339	322
34.3	0.919	N_2	5.51×10^7	426±27[2]	339	322
34.3	0.919	N_2	5.51×10^7	448±30[2]	339	322

[1]This value was based on velocity measurements using a strobe photographic technique.
[2]These values were based on velocity measurements using breakwire measurement techniques.

Baker also modified the Taylor-Price method to solve for fragment velocities when a vessel, sphere or cylinder, bursts into two equal halves. The following assumptions were made:

(1) Vessel breaks into two equal halves along a plane perpendicular to cylindrical axis and the fragments are driven in opposite directions.
(2) Contained gas obeys the ideal gas laws.
(3) Escaping gas travels perpendicular to the direction of motion of the fragments with local sonic velocity, and enters a vacuum.
(4) Energy necessary to break the vessel walls is negligible compared to the total system energy.
(5) Drag and lift forces are negligible during the time period in which the fragments attain their maximum velocities.

A computer code, FRAG 2, was developed to solve for velocity, acceleration, distance, time and ambient pressure. The program was run, varying input parameters, for the following conditions:

(1) Vessel is made of titanium or titanium alloy.
(2) Vessel walls are of uniform thickness.
(3) Vessel has hemispherical heads.

The following conclusions can be drawn:

(1) As pressure increases, fragment velocity increases at a decreasing rate.
(2) As gas density increases, sonic velocity increases, fragment velocity increases, and the rate of change of velocity with respect to pressure (dv/dP) decreases.
(3) As vessel thickness to diameter decreases (i.e., for thinner wall vessels), fragment velocity increases and the rate of change of velocity with respect to pressure (dv/dP) decreases.
(4) As vessel length to thickness decreases, fragment velocity increases, particularly at lower pressures.

Gases that were chosen for the calculations were air, hydrogen, xenon and carbon dioxide.

3.3.3 Self-Propelled and Jet-Propelled Fragments

Jager [16, 17] derived some relatively simple equations to determine the maximum velocity that a fragment might obtain for two cases. The first case covers self propelled fragments such as a rocketing gas cylinder; the second case addresses jet propelled fragments such as a flange torn off of a moored vessel.

The analysis ignores gravity over the time period during which the fragment is accelerated to its final velocity. It is assumed that both the choked flow velocity and density decrease exponentially as the vessel discharges with time.

The maximum velocity attainable by a self propelled fragment is given by

$$v = a_1 \sqrt{\frac{2}{K-1}\left[1 - \left(\frac{P_e}{P_i}\right)^{\frac{K-1}{K}}\right]} \ln\left(\frac{m_g + m_g}{m_g}\right)$$

where m_g = mass of gas initially in vessel
m_r = mass of rocketing fragment
K = ratio of specific heats
a_i = gas sonic speed (initial)
P_o = ambient pressure
P_i = initial pressure in vessel

3.3.4 Limiting Case Energy Considerations

Baum [18] (1984) considers limiting cases to determine fragment velocities. If a gas at initial pressure P_o and initial volume V_o expands adiabatically, the maximum expansion work E is given by

$$E = \frac{P_o V_o}{K-1}$$

where K is the ratio of the specific heats.

In the case of an ideal gas (i.e., initial pressure is sufficiently low that molecular forces and finite molecular size do not influence behavior of the gas, and condensation does not occur at the end of expansion), the maximum proportion k of this energy which could appear as kinetic energy is

$$k = \left[1 - \left(\frac{P_e}{P_o}\right)^{\frac{K-1}{K}}\right] + (K-1)\left(\frac{P_e}{P_o}\right)\left[1 - \left(\frac{P_e}{P_o}\right)^{-1/K}\right]$$

where P_e is the pressure external to the vessel.

The maximum kinetic energy available for fragments is obtained by multiplying the proportion k by the available energy:

$$KE_{max} = \frac{P_o V_o}{K-1} \quad k$$

Baum [21] (1988) has also performed burst tests for a number of different cases of fragment types and vessel contents for both spherical and cylindrical vessels. Initial fragment velocities were measured and evaluated. In general, initial fragment velocity is a function of:

- velocity of sound in the gas
- initial fragment acceleration
- ratio of initial internal vessel pressure and external pressure
- vessel length to radius ratio
- isentropic expansion coefficient of gas

Based upon results from his own experiments and those performed by others, Baum recommends upper limits on fragment velocities for several cases. Cases for vessels containing ideal gases are summarized below:

Vessel Geometry	Failure Type[1]	Fragment Type	Upper Limit Velocity[2,3]
cylindrical	D or D/B	end cap	$2\ a_o (F)^{1/2}$
cylindrical	D or D/B	rocket	$2.18\ a_o \left(F \left(\frac{L}{R} \right)^{1/2} \right)^{2/3}$
cylindrical	D/B or B	multiple fragments from vessel disintegration	$0.88\ a_o\ (F)^{0.55}$
spherical	B	multiple fragments from vessel disintegration	$0.88\ a_o\ (F)^{0.55}$
cylindrical	D	whole vessel with axial split	$0.17\ (2E/m)^{1/2}$

Notes:

(1) Failure type is ductile (D), brittle (B) or ductile/brittle (D/B)

(2) F is the dimensionless initial fragment acceleration given by

$F = \frac{P_o A R}{m a_o^2}$ where

P_o = initial pressure

A = fragment projected area

R = vessel radius

m = fragment mass

a_o = velocity of sound in gas

(3) other terms

L = vessel length

E = maximum expansion work

3.3.5 Real Gas Effects

Wiedermann [19] employed a quasi-steady expanding cavity model similar to Baum to evaluate the effects that a real gas has upon fragments. Each of the preceding models assumed that the gas in the vessel was ideal. This is a good assumption for low pressure gases. At higher pressures, real gas effects are more significant. Where Baum used the ideal gas law, Wiedermann employs the Nobel-Abel and Van der Waals equations of state.

Wiedermann developed non-dimensional equations which he solved for non-dimensional fragment velocity. The equations were solved for a range of values for the following dimensionless parameters:

acceleration,
co-volume (difference in volume between real gas and its associated ideal gas),
ratio of specific heats (adiabatic exponent), and
gas volume factor.

The results indicated a significant reduction in fragment velocity for real gas in the bursting vessel as opposed to an ideal gas.

3.4 Determination of Fragment Range

3.4.1 Theory

Once the initial velocity of a fragment has been determined, its range may be determined through ballistics calculations. The equations of motion for a fragment can be written in x and y coordinates where x is the horizontal range and y is the altitude.

For a drag type fragment, the acceleration that it experiences is due to gravity (in the -y direction) and drag (opposing the velocity).

$$\frac{F_x}{m} = \ddot{x} = -\frac{C_D A_D \rho}{2m} v^2 \cos\theta$$

$$\frac{F_y}{m} = \ddot{y} = -\frac{C_D A_D \rho}{2m} v^2 \sin\theta - g$$

where m = mass of fragment

$\ddot{x}$ = horizontal acceleration

$\ddot{y}$ = vertical acceleration
C_D = drag coefficient
A_D = area exposed to drag or reference area
ρ = air density
v = velocity
θ = trajectory angle
g = acceleration due to gravity
F = net force acting on the fragment

In the case of a lift type fragment, C_D and A_D are replaced by C_L and A_L, the lift coefficient and area exposed to lift, respectively. If lift and drag are of the same order of magnitude, both terms might be used in the equations.

The initial conditions (boundary values) are as follows. At time $t = 0$:

$$\dot{x}(0) = v_o \cos\theta_o$$

$$\dot{y}(0) = v_o \sin\theta_o$$

where $\dot{x}$ = horizontal velocity

$\dot{y}$ = vertical velocity
v_o = initial velocity
θ_o = initial trajectory angle

The velocity v may be related to the horizontal velocity $\dot{x}$ and the vertical velocity $\dot{y}$ by

$$v = (\dot{x}^2 + \dot{y}^2)^{1/2}$$

The trajectory of the fragment is determined by solving the two differential equations simultaneously. This is generally done through the use of a computer code.

The solutions will generally give velocity and horizontal and vertical distances as functions of time. The range would be the horizontal distance when the vertical distance is 0.

3.4.2 Computer Codes for Fragment Range

Kulesz, et al [5] developed the computer codes FRISB and TRAJE to determine the ranges of fragments. FRISB is used for disc shaped fragments with diameter at least 5 times greater than thickness; lift effects are considered by FRISB. TRAJE is used for chunky shaped fragments with all three dimensions of the same order of magnitude. Lift effects are ignored in TRAJE. The FRISB code can also be used for chunky shaped objects by setting the lift coefficient equal to zero.

FRISB and TRAJE both employ the Runge-Kutta method to simultaneously solve two second order differential equations for fragment velocities. The velocities are numerically integrated in order to determine the range.

The TRAJE code can access a subroutine that allows for rotor effects such as a helicopter blade would demonstrate.

Kulesz ran the code TRAJE for different values of the input variables:

initial trajectory angle,
initial velocity,
mass,
area, and
aspect ratio (diameter/thickness)

The computer run results were used to generate curves that allow for graphical determination of range. Sample checks were run by interpolating results from curves and comparing these results to the TRAJE predictions. The error ranged from 5% to 80%. The greatest errors occurred for low ratios of fragment mass/area.

3.4.3 Upper Limits on Range

Baum [18] (1984) recommends upper limits on range similar to the upper limits for initial fragment velocity. In the case where the drag force is less than the fragment's weight and the lift force is negligible, an upper limit on range can be determined by solving the ballistics equations by setting drag and lift coefficients equal to zero and assuming the optimal initial trajectory angle of 45°. Then the range is given by:

$$x = \frac{v_o^2}{g}$$

For non-tumbling fragments with significant lift force but drag force still less than weight, the upper limit on range is given by:

$$x = \frac{3\ v_o^2}{g}$$

The upper limit on range for a large fragment from the ductile failure of a vessel can be determined by assuming that the kinetic energy of the fragment is 20% of the maximum expansion work available (E) and that the fragment's mass is one tenth of the mass (M) of the vessel.

$$x = \frac{4\ E}{Mg}$$

The upper limit on range for any of the small fragments generated by the brittle failure of a vessel can be determined by assuming that the total kinetic energy of the fragments is 40% of the maximum expansion work and that each of the fragments has the same initial velocity.

$$x = \frac{0.8\ E}{Mg}$$

3.5 Experimental Data

3.5.1 Pittman, 1972

In 1972, Pittman [10] burst five vessels of titanium alloy (Ti-6Al-4V); three of these were spheres used to store high pressure gas while two were cylinders used to store liquid propellant. Design burst pressures were 7500 psig or 8000 psig for the spherical vessels and 460 psig for the cylindrical vessels. All five vessels were pressurized with gaseous nitrogen to burst.

The fragment recovery system utilized thirty 6-inch thick wallboard panels to stop the fragments. Two fragment velocity measurement systems were used. The first system used breakwires in the panels to trip electric counters. The second system used two cameras with strobes. Speed was estimated by computing the difference in position for each identifiable fragment between two stroboscopic flashes assuming straight line fragment travel. At least one of the velocity measurement systems functioned for each vessel burst.

The number of fragments that each vessel burst into was estimated by calculating the percentage of the vessel weight that was recovered and taking the ratio of the number of fragments recovered to the total vessel weight. Results for the vessels are as follows:

Vessel	Usual Content	Number of Fragments
A	A-50	61
B	Oxidizer	57
C	GHE	38
D	GHE	47
E	GHE	48

Upon detailed analysis of the fragments produced, Pittman concluded:

- The method of estimating the number of fragments is incorrect.
- The fragment distribution is not homogeneous over a solid angle described by a spherical shell.
- Fragments found within the arena went straight up and fell back.

Measured fragment velocities are recorded in Table 3-1.

3.5.2 Pittman, 1976

Pittman [11] in 1976 pressurized seven spherical vessels constructed of T-1 steel with argon until each failed. Each had a capacity of 1 cubic foot. The design burst pressures were 15 ksi, 30 ksi and 50 ksi. Each vessel burst into 2 fragments. Of the 14 fragments, 10 were recovered. Data for the remaining 4 fragments were estimated. The weights of the fragments varied from 51 pounds (from a 15 ksi vessel) to 271 pounds (from a 50 ksi vessel).

The fragment recovery and velocity measurement system was designed assuming that the vessels would fail in a brittle manner, and produce several fragments. Velocity screens were set up to stop the fragments. Breakwires in the screen would trip electric counters upon impact, allowing velocity to be determined from the arrival time.

Tank	Breakwire Velocity	Fragment Number	Strobe System Velocities		
			Time Interval (ms)	Distance Traveled (ft)	Velocity VA *
A	No Data	1	0 to 1.50	1.52	1010
			1.50 to 3.00	1.56	1040
			3.00 to 5.00	1.50	750
			0 to 5.00	4.58	918
		2	0 to 1.50	1.56	1040
			1.50 to 3.00	1.61	1070
			3.00 to 5.00	1.86	930
			0 to 5.00	5.03	1000
		3	0 to 3.00	3.10	1030
			3.00 to 5.00	1.73	865
			0 to 5.00	4.83	967
B	1215 ±50	1	0 to 3.00	2.76	920
			3.00 to 4.50	1.29	860
			0 to 4.50	4.05	900
		2	0 to 3.00	2.96	986
			3.00 to 4.50	1.32	880
			0 to 4.50	4.28	950
C	1270 ±80	1	0 to 3.00	3.60	1200
			3.00 to 4.50	1.53	1020
			0 to 4.50	5.20	1150
D	1400 ±90	No Strobe Data			
E	1470 ±100	No Strobe Data			

* VA - Average velocity in ft/sec over the time interval given

Table 3-1. Pittman 1972 Fragment Data [10]

All of the vessels failed in a ductile manner and burst into 2 fragments. Only 1 of the 14 fragments tripped the breakwire to record a velocity. Velocities of the other fragments were measured based on a pressure-temperature history.

Fragment weights, measured velocities and ranges are as follows.

SHOT #	VESSEL DESIGN BURST PRESSURE (PSI)	FRAGMENT WEIGHT (POUNDS)	FRAGMENT VELOCITY (FEET/SEC)		DISTANCE FRAGMENT TRAVELED (FEET)
1	15,000	52.4	310[1]		
1		52.4	321[1]	BOTTOM HALF	665[3]
		TOP HALF NOT FOUND			1680[4]
2	15,000	52.75	324[1]		
2		52.75	330[1]	BOTTOM HALF	
2			317[1]		552[3]
		TOP HALF NOT FOUND			1380[4]
3	30,000	147.5	354[1]		
3		147.5	373[1]	BOTTOM HALF	INSIDE THE
3		147.5	348[1]		ARENA
3		147.5	338[1]		
		TOP HALF NOT FOUND			1136[4]
4	50,000	258	215[1]		
4		258	216[1]		INSIDE THE
4		258	210[1]	LARGE PORTION	ARENA
4		258	221[1]		
		SMALL PORTION NOT FOUND			722[4]
5	50,000	271	270[2]		INSIDE THE
5		142			ARENA
6	15,000	51.1	NONE		
6		51.1	NONE		
7	30,000	108	290[1]		INSIDE THE
7		108	250[1]		ARENA
7		93.5	NONE		

Notes:

(1) VELOCITY MEASUREMENTS MADE FROM P-T HISTORIES

(2) VELOCITY MEASUREMENTS MADE FROM BREAKWIRE SYSTEM

(3) MEASURED DISTANCE TRAVELED

(4) ESTIMATED DISTANCE TRAVELED

Table 3-2. Pittman 1976 Fragment Data

3.5.3 Jager, 1981

Jager [17,20] in 1981 measured the velocities of single fragments jet propelled from 26 steel compres ed air bottles. Prior to the experiments, contours of the desired fragments were machined into each bottle. The fragments were either 5cm by 5cm squares or 15cm by 15cm squares. Masses ranged from 0.16kg to 150kg. In some cases, however, the vessel was cut in half in order to obtain a self propelled fragment. The bottles were anchored in place to minimize movement.

Velocities were measured by photographing the fragments as they moved past scaled distance marks. The fragments moved past the scale in 15 of 26 tests.

Fragment velocities ranged from 20 m/s to 280 m/s. The table following lists both measured velocities and velocities calculated using equations developed by Jager (discussed in Section 3.3.3).

3.6 Fragment Distribution

There are currently no theories to predict the number, sizes and masses of fragments produced as a result of a pressure vessel burst. Studies in this area have centered on statistically curve fitting data from the experiments by Pittman.

Baker, et al [5] analyzed data Pittman [10] obtained by bursting titanium vessels. They found that the logarithms of the fragment masses follow a normal, or Gaussian, distribution. They plotted two mass distribution curves---one for the percentage of fragments with a weight < W versus weight W and the other for the mean fragment weight versus normalized yield. Normalized yield = PV/E_o where P and V are vessel pressure and volume, respectively, and E_o is the energy of detonation of 1 gram of TNT (4190 joules). There were insufficient data points on the latter curve to determine if it was a straight line on a log-log scale.

Test no.	p_1 (bars)	ρ_1 (kg/m³)	V_1 (liter)	m_G (kg)	m_p (kg)	F.100 (m²)	v_p (m/s) calc.	v_p (m/s) meas.	REMARKS
			JET PROPELLED FRAGMENTS						
a) Fragments 15±15 cm²									
1	100	116	50	5.8	1.43	2.5	205	206	
2	100	117	50	5.9	1.38	2.5	206	201	
3	172	215	50	10.7	1.35	2.5	226	212	vessel burst in 3 pcs.
b) Fragments 5±5 cm²									
4	100	116	50	5.8	0.16	0.35	270	178	impact before meas.
5	140	174	50	8.7	0.16	0.35	267	158	not clearly identified
6	300	381	50	19.0	0.16	0.35	277	280	burst into 2 pcs.
c) Vessel bottom (purely jet-propelled, no plug-type phase)									
7	100	127	50	5.9	12.0	3.5	97	84	no rigid support
8	200	254	50	11.7	12.66	3.5	129	119	no rigid support
9	285	357	50	16.5	12.49	3.5	148	125	no rigid support
10	25	30	220	6.6	21.8	18.4	96	90	rigid support
			ROCKETING FRAGMENTS						
11	100	127	50	3.1	33.2	3.5	57	53	1/2 vessel
12	294	340	50	8.2	31.6	3.5	161	156	1/2 vessel
13*	100	119	50	2.0	25.1	3.5	50	60	1/3 vessel
14	25	30	220	6.2	119.5	18.4	30	26	whole vessel without bottom
15	25	31	220	6.8	156	>30	24	16	vessel cut open lengthwise, flying sideways and rotating

*Flying third of vessel treated as jet-propelled from remaining 2/3-vessel (with m_G=3.9 kg) would give calculated v_p=59 m/s.

Symbols: p_1 - pressure of gas in vessel, ρ_1 - density of gas in vessel, V_1 - volume capacity of vessel, m_G - mass of gas in vessel or vessel portion, m_p - mass of fragment, v_p - peak velocity of fragment.

[17]

Table 3-3. Jager Fragment Data

3.7 Probabilistic Methodology

Rather than base a study of fragmentation on analytical methods and a "worst case" scenario, a probabilistic methodology might be employed. The probabilistic methodology relies upon empirical data in order to generate probabilistic densities or curves for damage sustained as a consequence of a bursting vessel's fragments. The validity of a probabilistic assessment is a function of the availability and accuracy of the data and also the choice for an acceptable level of damage to be sustained.

A probabilistic assessment for damage as a result of vessel fragmentation has been performed by Sundararajan and Rooker [23] (1984). Their approach divides the assessment into two phases:

1. generation of fragments
2. fragment trajectories

In the first phase, the failure probability of a pressure vessel is examined for a hypothetical failure, the distribution of the number of fragments and their weights, sizes and shapes, and fragment velocities (including ejection angles) are analyzed to develop probability functions.

The second phase, determination of fragment trajectories, could be accomplished through one of two approaches: a Monte Carlo simulation method or a semi-analytical method. The Monte Carlo simulation method consists of performing a series of trials to determine the ranges of fragments by sampling input fragment speeds and ejection angles according to the probability density functions obtained in the first phase. From the series of trials, a strike probability contour map is drawn; this contour map allows determinations to be made for the relative hazards of locating personnel or equipment around the vessel.

The semi-analytical method, alternatively, might be used to determine probability density functions of impact velocity, fragment orientation and weight for targets located near the vessel.

A probabilistic assessment has been performed by Huang [23] to determine the impact effect of debris from a building due to the detonation of stored munitions. Since much data is available on munitions blasts, it is possible to develop a probabilistic assessment whereas for vessel bursts, insufficient data is available. This methodology might be applied to vessel bursts given data following testing.

3.8 Evaluation

Studies into fragmentation began in earnest in the 1940's, centering almost exclusively on the fragmentation hazard presented by munitions blasts. Much classified work was performed to analyze the hazard presented by shrapnel and debris to personnel. These early studies are of very limited usefulness to this current study which analyzes the effects of fragments produced by the failure of a pressurized vessel.

A munitions blast tends to produce many more smaller fragments than a vessel failure due to overpressure. The increase in the number of fragments produced, however, may not have that great an impact on the maximum velocity achieved by any fragment.

There has also been a fair amount of research into the failure of vessels containing liquid propellant. This is of primary concern in the case of a rocket on a launch pad. Fragments generated by the partial detonation of the propellant pose a hazard to ground support equipment and may also lead to the failure of nearby liquid propellant vessels.

Literature on actual failures of liquid propellant vessels was researched to compare their fragmentation with that of pressurized gas vessels and also munitions blasts. Liquid propellant vessels tend to produce fewer, but larger, fragments than munitions blasts and more, but smaller, fragments than gas pressurized vessel bursts. Only the pressurized gas vessel burst is considered in this review.

The Taylor-Price analysis is the basis for most models which determine the velocity of fragments generated by a pressure vessel burst. Several important models and computer codes have been presented which have modified the Taylor-Price analysis to improve the assumptions, or have

applied assumptions to analyze a special case, or have generalized the assumptions to make the analysis more universal. These models and codes cover a wide range of useful applications. The biggest drawback is limited data to verify their accuracies.

There has been very little data published on fragmentation measurements. Currently, research is being performed by Baum to measure fragment velocities and derive equations for worst case fragment velocities for a large variety of different vessel burst cases. It is expected that he will publish data in the future.

The most widely used fragmentation data, currently, is that of Pittman. However, there are drawbacks to both of his sets of data.

In the 1972 bursts of 5 titanium vessels, only 2 vessel bursts were measured by both the breakwire system and the stroboscopic cameras. In one of these 2 bursts, the velocity measurement systems differed by about 25% on fragment velocity. Additionally, Pittman concluded that the method for estimating the number of fragments produced was incorrect. One important conclusion is that fragments are not propelled from the burst uniformly in all directions.

The results of the 1976 bursts of 7 vessels made of T-1 steel surprised Pittman. It was anticipated that the vessels would fail in a brittle manner and generate a large number of fragments. The fragment recovery and velocity measurement system was designed accordingly. Instead, each vessel failed in a ductile manner and burst into 2 fragments. Four of the 14 fragments were not recovered and were assumed to have traveled many hundreds of feet, leaving the area. Only in the case of 1 of the 14 fragments was a velocity measured. In all other cases, velocity was deduced by analyzing the pressure - temperature history recorded for the blast wave analysis.

Another matter raised by this experiment is the question of how a given vessel will fragment depending upon its failure mechanism. The failure mechanism could very well play a key role in determining the number, size, mass and velocity of fragments produced. To date, there has not been any research into this area.

Once a velocity has been determined for a fragment, calculation of its range is not particularly difficult. The ballistics equations have been used in a wide variety of applications with success. The most critical task in determining the range is determining the drag coefficient. Drag coefficients have been measured empirically and tabulated for a variety of objects. The choice of the drag coefficient presupposes that the fragment size and shape are known.

Determining the distribution of fragments produced by a vessel burst involves cataloging the size, shape, mass, speed and direction of travel of fragments. As has been discussed, there is no model or theory to predict this; studies have centered on statistically analyzing experimental results.

The only usable data in this regard is the 1972 failures of 5 titanium vessels by Pittman. The data from Pittman is not sufficient to draw any real conclusions beyond the fact that the mass distribution appears to follow a log normal curve.

More experimental failures of vessels and an analysis of the mechanism of failure will be needed to determine fragment distributions.

SECTION 4. CONCLUSIONS AND RECOMMENDATIONS

4.1 Summary

As described in this report, this study was conducted to (1) determine and summarize existing methodologies for, and experimental confirmation of, energy release processes (both blast and fragmentation) from the failure of pneumatic pressure vessels, (2) determine inconsistencies in, or lack of information on, these processes, thus developing requirements for future study, and (3) develop a plan of action to resolve inconsistencies, or generate required data, to establish an effective model of energy release from failed pneumatic pressure vessels. The theoretical approach for the process of pressure vessel failure has not been consistently applied, modelled, or experimentally validated. This results in a significant number of basic questions raised as a result of this study which require further investigation. It also results in questions raised over our understanding of the effects of failed vessels in aerospace applications. This has particular importance to the siting and operation of vessels on permanent manned and unmannned orbiting platforms. Therefore, the conclusions and recommendations which follow, although originally prompted by a study of ground support equipment (GSE), have direct application to both GSE and aerospace vehicle equipment (AVE). The recommended course of action, if implemented, should establish a consistent set of validated models for energy release processes, and subsequent effect on surrounding equipment, for the failure of pressurized vessels.

4.2 Conclusions

4.2.1 Blast Wave Methodologies

As presented in this report, any of several blast wave methodologies (isentropic, adiabatic or isothermal) may be used to model the expansion of gas following the failure of a vessel. The applicability of the methodologies depends on the failure environment and may depend on proximity to the source of the failure; for example, a different methodology may apply in the region directly adjacent to the failure (near field), as compared to a region more distant from the failure (far field).

Available experimental burst data indicates that current standards used to predict blast wave characteristics may be overly conservative in near field. These methods, which use an isothermal expansion model coupled with a TNT energy equivalency, may also be underconservative in the far field. The actual expansion of a vessel's contents following rupture is proposed to be more closely approximated by an adiabatic process rather than an isothermal process. However, due to irreversibilities in the process, the use of the adiabatic expansion equation is not practical. Therefore, an isentropic process appears to be the most applicable model available for future study. Modifications may be appropriate as experimental results are obtained and analyzed. Evaluation of the overall effect of using ideal or real gas assumptions must also be included in future study.

Experimental data available to validate existing computer models and standard approaches is generally unavailable. As illustrated in Figure 4-1, the body of related experimental data consists of 11 burst tests, only two of which were made under an 8000 psi burst pressure. In addition, no data is available in the far field. Evaluation of this data against available models does not yield consistent conclusions.

Two computer models exist to simulate the expansion of the gas following failure of the vessel. These models, titled "Wondy" and "Wundy" (both available in several modified versions), although used to predict blast wave characteristics, have not been validated by any burst tests.

Based on the limited experimental vessel burst data, the following additional items remain unaddressed, requiring further study as part of the recommendations.

1. Blast wave characteristics - Since the shape of the overpressure wave front may vary significantly from that predicted by equivalency with TNT, an evaluation should be undertaken to model and measure shape characteristics from failed pneumatic overpressure vessels.

PRESSURE RANGES	CYLINDRICAL VESSEL	SPHERICAL VESSEL
VERY LOW PRESSURE (< 350)	NO DATA	NO DATA
LOW PRESSURE (350 - 3000 PSI)	640 PSI (1.3)* 615 PSI (1.6)	NO DATA
MEDIUM PRESSURE (3000 - 7000)	NO DATA	NO DATA
HIGH PRESSURE (7000 - 10,000)	NO DATA	8145 PSI (6.0) 8015 PSI (0.2) 8015 PSI (6.0)
ULTRA HIGH PRESSURE (>10,000 PSI)	NO DATA	14,965 PSI (1.02) 14,765 PSI (1.02) 13,415 PSI (1.02) 13,815 PSI (1.02) 50,415 PSI (1.02) 50,415 PSI (1.02)

* (VOLUME IN CUBIC FEET)

Figure 4-1. Pittman Burst Tests

2. Burst energy components - Minimal information is currently available which would allow evaluation of the maximum, and most probable, percentage of internal energy available to produce the blast wave. This uncertainty may yield significant variations in prediction of blast wave energies and damage potential. Experimental envelopes should be developed for distribution of energies between blast wave, fragmentation, vessel distortion, and crack initiation and propagation.

3. Jetting direction correction factor - Since nonuniform blast wave generation is most probable in vessel failure, an evaluation of the effect of jetting on the items addressed above should be undertaken. This effect may result in a significant increase in blast wave energies along one radial direction from the vessel. Since no experimental data exists to address this effect, data should be taken to develop a model, practice or a correction factor.

4. TNT conversion factor - TNT equivalency is currently used to relate failed pressure vessel blast waves to blast wave effects on equipment, facilities and personnel. Although TNT blast effects are well defined and experimentally confirmed, the relationship between stored energy in a pneumatic vessel and an equivalent amount of TNT has not been experimentally confirmed. In fact, the literature includes a number of different values for this conversion. Experimental confirmation of the applicability of this relationship should be addressed in future studies.

In summary, there is a significant lack of complete experimental data, and associated validation of available computer models. It appears that current prediction methods may be overconservative in some applications, while underconservative in other applications. Since these methods are used to site high pressure vessels and systems at government missile and space complexes, along with applications to orbiting

platforms, it is prudent to address these issues of uncertainty as soon as practical and resolve discrepancies between current standardized methods and actual blast effects.

4.2.2 Fragmentation Methodologies

As summarized in this report, the study of fragmentation mechanisms and effects have been studied extensively since the 1940s, with initial emphasis on the fragmentation hazard presented by the detonation of munitions. The failure of vessels containing liquid propellants has also been studied extensively, however, not until the early 1970s have pressurized gas vessels been addressed. The Taylor-Price analysis, presented in this report, is the basis for most models which determine the velocity of fragments generated by a pressure vessel burst. This approach, modified to address a variety of applications, has not been satisfactorily validated. The primary conclusion of the few experimental results available is the fact that the fragmentation is a function of its failure mechanism. That is, the failure mechanism may play a significant role in determining the energy imparted (velocity), number, size/shape, and mass of fragments produced. This lack of information creates a significant problem in using these models as a predictive tool. The existing models are useful, however, when evaluating failed vessels when number and size of fragments are known. Validation of models should address energy distribution between blast wave and fragmentation, along with ability to predict resulting effects of vessel failure.

4.3 Recommendations

4.3.1 Short Term Recommendations

As described above, additional data is required from actual burst tests to validate both blast wave and fragmentation models. This validation would include the modification of available models to predict blast wave and fragment propagation, thus assisting in the ability to more accurately locate vessels in ground support and orbiting platform applications. Short term goals include:

- obtain additional experimental data to validate and assist in modification of existing computer models by:
  - establishing vessel selection criteria for burst testing a wide variety of ground and flight vessels
  - inventorying candidate vessels for burst testing

- develop logistics engineering support for burst testing by:
  - evaluating test site(s)
  - identifying test support requirements
  - developing cost estimates for test support
  - developing detailed test criteria
  - developing test schedules
  - developing test plans

- establish baseline computer models to be evaluated for blast wave and fragmentation validation by:
  - obtaining current versions of blast wave and fragmentation computer programs
  - running computer models for a variety of initial conditions to establish envelopes for experimental parameters

4.3.2 Long Term Recommendations

Based on the short term recommendations described above, the following long term recommendations have been developed:

- implement a series of burst test programs, including both flight and ground support vessels, designed to validate computer models
- modify computer models or theoretical bases for blast wave and fragmentation
- evaluate relationship between TNT equivalency and pressure vessel burst characteristics
- determine validity of on-line monitoring, crack propagation prediction, fracture mechanics analysis, blast and fragmentation effects, as applied to flight and ground support vessels.

4.3.3 Preliminary Test Plan Matrix

A "strawman" test plan matrix was developed to conceptualize the considerations necessary to implement a full scale vessel burst test program. Figure 4-2, the Preliminary Test Program Matrix for Experimental Vessel Burst Assessments, presents an initial evaluation of burst configurations, pressures and volumes, along with a variety of other test parameters. The following paragraphs describe the logic behind the selection of these preliminary test programs. Each of the seven test programs described, may be comprised of several test runs, that is, several burst tests may be required under each test program. In addition, an initial trial test may be required to confirm operation of the test facility, including instrumentation.

4.3.3.1 Initial Burst Test Program (Tests 1-4)

Proposed Test Plans 1 through 4 are designed to provide a baseline envelope for blast wave and fragment generation. This is achieved by controlling (1) the failure initiation mechanism, (2) burst pressure, (3) number of fragments produced, and (4) symmetry of blast wave and fragmentation pattern produced. This control is a result of the use of shaped charges to initiate failure, removing sufficient wall thickness to allow the resulting inadequate remaining wall to fail. Each of these four test plans may consist of several individual test trials. This approach can also be utilized to (1) validate and modify existing computer models for the prediction of blast wave and fragment generation and propagation, (2) develop a model for prediction of the distribution of energy between blast wave, fragmentation, and material distortion, and (3) modify the test facility to more accurately measure the required experimental parameters.

As illustrated in Figure 4-2, Test Plan 1 is proposed to be conducted using flight weight vessels with a volume of less than 5 cubic feet and a burst pressure of approximately 1000 psi. As described above, since these tests are initiated by a shaped charge, the actual design pressure for these vessels may cover a wide range of values. The primary objective of Test Plan 1 is to validate and modify the Wundy blast wave computer code

DESCRIPTION	TEST PLAN 1	TEST PLAN 2	TEST PLAN 3	TEST
TYPE OF VESSEL	SPHERE (AVE)	CYLINDER (GSE)	SPHERE (AVE)	CYLIN
APPROXIMATE BURST PRESSURE	1000 psi	1000 psi	5000 psi	1000
APPROXIMATE BURST VOLUME	1-5 cu ft	25 cu ft	1-5 cu ft	25
BURST CONFIGURATION	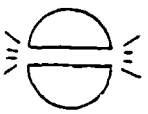	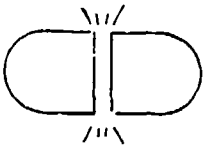	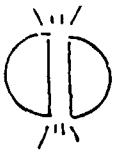	
VESSEL CONTENTS	GN2	GN2	GN2	GN
VESSEL MATERIAL	(TBD)	Carbon Steel	(TBD)	Carbo
BURST INITIATOR	Shaped Charge	Shaped Charge	Shaped Charge	Shape
PARAMETERS MEASURED	Overpressure 3 Arrays, 120° Gas Temp, Press	Overpressure 3 Arrays, 180°/90° Gas Temp, Press Frag Vel, Mass	Overpressure 2 Arrays, 180° Gas Temp, Press Frag Vel, Mass	Overp 3-180 Gas T Frag
BLAST WAVE COMPUTER CODE	Blast, Wundy Code	Blast, Wundy Code	Blast, Wundy Code	Blast Wundy
FRAGMENTATION COMPUTER CODE	None	FRAG 2, CYLIN	TBD	TBD
FRACTURE MECH PERFORMED	No	No	No	No
ACOUSTIC EMISSIONS OR STRAIN GAGES	No	No	No	No
OTHER EXPERIMENTS CONDUCTED	Blast Effects	Blast Effects	Blast Effects	Frag Blast
RELATED TESTS	-	-	Tests 1 & 2	Test
RESULTS EVALUATED	Computer Codes Validated/Mod., Instrumentation	Computer Codes Validated/Mod., Instrumentation	Computer Codes Validated/Mod., Instrumentation	Comput Valida Instru

TEST PLAN 4	TEST PLAN 5	TEST PLAN 6	TEST PLAN 7
CYLINDER (GSE)	CYLINDER (GSE)	CYLINDER (GSE)	CYLINDER (GSE)
1000 psi	1000 psi	5000 psi	10,000 psi
25 cu ft	25 cu ft	25 cu ft	25 cu ft
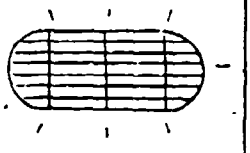			
GN2	GN2	GN2	GN2
Carbon Steel	Carbon Steel	Carbon Steel	Carbon Steel
Shaped Charge	Machined Flaw	Machined Flaw	Machined Flaw
Overpressure 3-180°/90° Gas Temp,Press Frag Vel, Mass	Overpressure 3-180°/90° Gas Temp,Press Frag Vel, Mass	Overpressure 3-180°/90° Gas Temp,Press Frag Vel, Mass	Overpressure 3-180°/90° Gas Temp,Press Frag Vel, Mass
Blast, Wundy Code	Blast, Wundy Code	Blast, Wundy Code	Blast, Wundy Code
TBD	TBD	TBD	TBD
No	Yes	Yes	Yes
No	Yes	Yes	Yes
Frag Impact Blast Effect	None Defined	None Defined	None Defined
Test 2	Tests 2 & 4	Tests 2,4 & 5	Tests 2,4,5 & 6
Computer Codes Validated/Mod., Instrumentation	Also Evaluate AET,FM, etc.	Also Evaluate AET,FM, etc.	Also Evaluate AET,FM, etc.

Figure 4-2. Preliminary Test Program Matrix for Experimental Vessel Burst Assessments

with secondary objectives of (1) validation of fragmentation computer codes for the simplest two fragment case, and (2) evaluation and modification, if necessary, of the test array orientation and configuration. The circumferential failure, initiated by the shaped charge, should produce a symmetrical blast wave which would be measured in a plane parallel to the failure initiation point. This configuration should also yield the maximum blast wave energy, with the minimum energy imparted to the two fragments and with minimum material distortion prior to failure. This should be used to begin to establish the upper envelope for the blast wave energy.

Test Plan 2 introduces failures in ground support pressure vessels under the same conditions as described in Test Plan 1. The blast wave is reoriented to a plane perpendicular to the horizontal, with the two fragments propagating at 90° to the blast wave. The results should again be used to validate and modify the respective computer codes and adjust test facility configuration.

Test Plan 3 is proposed to use flight weight vessels at a burst pressure of 5000 psi with failure plane oriented perpendicular to the horizontal. As described in Test Plans 1 and 2, two fragments would be produced from the failure. This program should complete preliminary evaluation of two fragment, symmetric blast wave failures and establish baseline envelopes for the remaining plans.

Test Plan 4 initiates multiple fragmentation using shaped charges to cause failure. These tests, performed on ground support (or flight) vessels, should be used to estimate the partition of energy between blast wave and fragmentation when multiple fragments are involved. Validation of computer models should continue with expansion to multiple fragment models. This test plan is designed to directly compare to Test Plan 2 establishing the related envelope which should be the basis of future test comparisons.

Test Plans 1 through 4 should establish the validity of existing computer models and provide needed data for modification of these models. These tests also establish an upper and lower bound envelope for the

partition of energy between blast wave and fragmentation. In addition, results of the tests are used to reconfigure the test facility and instrumentation for future burst tests initiated by machined flaws.

4.3.3.2 Immediate Follow-on Burst Test Program (Tests 5-7)

Proposed Test Plans 5 through 7 are designed to simulate actual vessel failures using machined flaws. These plans, with burst pressures at 1000, 5000 and 10,000 psi, are designed to address several significant issues including:

- propagation of flaw during failure and ability to predict fragmentation pattern, number and size
- validity of fracture mechanics in predicting flaw growth and approach to failure
- ability of acoustic emissions testing to predict flaw growth and onset of failure
- validity of blast wave and fragmentation computer codes under actual failure conditions
- validity of energy partition envelope for blast wave and fragmentation
- blast wave effects on code predictions including jetting, unsymmetric blast wave distributions, location of barriers, etc.
- fragmentation effects

Details for Test Plans 5 through 7 would be developed as part of the initial burst test program, and as such only major goals or objectives are described here.

4.3.3.3 Long Term Follow-on Burst Tests (Test 8- end of program)

Specific unresolved issues may be raised as part of the initial or immediate follow-on tests which should be addressed in longer term programs. These would be developed on a case-by-case basis and may be incorporated, as appropriate, into existing programs. In addition, any of the test programs described may be reordered, modified, deleted and replaced, or adjusted due to the results of prior tests.

4.3.4 Summary of Recommendations

A test program should be initiated to address several major issues raised as part of this study. These issues have wide applicability to the location of vessels on manned or unmanned space platforms and as ground support equipment. The proposed "strawman" Test Program should be used as a basis for discussion of the implementation of this program. Numerous related research efforts may be incorporated into this program such as on-line monitoring in space and ground environments, failure effects and barrier design options. This preliminary evaluation should establish a point of discussion for future coordinated full scale vessel failure prediction.

REFERENCES

REFERENCES

1. Department of the Air Force, "System Safety," AFSC DH 1-6, December 1, 1982.

2. Department of the Air Force, "System Safety," AFSC DH 2-5, March 30, 1985.

3. Dawson, V.C., et al, "Failure Damage Assessment Techniques for High Pressure Gas Containment Vessels," NOLTR 70-208, Naval Ordnance Lab, White Oak, Maryland, September 18, 1970.

4. Kinney and Graham, "Explosive Shocks In Air," Second Edition Springer Verlag, 1985.

5. Baker, W.E., et al, "Workbook for Predicting Pressure Wave and Fragment Effects of Exploding Propellant Tanks and Gas Storage Vessels," NASA Contract Number 134906, Southwest Research Institute, San Antonio, Texas, November 1975.

6. Brown, S.V., "Energy Release Protection for Pressurized System. Part I - Review of Studies into Blast and Fragmentations," Applied Mech. Review, Vol. 38, No. 12, ASME, December 1985.

7. Wark, K., "Thermodynamics," Second Edition, McGraw - Hill Book Company, 1971.

8. Pittman, J.F., "Blast and Fragments From Pneumatic Pressure Vessel Rupture to 345 MPa," Naval Surface Weapons Center, White Oak, Maryland.

9. Kingery, C.N., "Air Blast Parameters Versus Distance for Hemispherical TNT Surface Bursts," Report No. 1344, Ballistic Research Laboratories, Aberdeen Proving Ground, Maryland, September, 1966.

10. Pittman, J.F., "Blast and Fragment Hazards From Bursting High Pressure Tanks," Naval Ordnance Laboratory, White Oak, Maryland, May 17, 1972.

11. Pittman, J.F., "Blast and Fragments From Superpressure Vessel Rupture," Naval Surface Weapons Center, Silver Spring, Maryland, February 1976.

12. Fugelso, L.E., et al, "A Computational Aid For Estimating Blast Damage From Accidental Detonation of Stored Munitions," General American Research Division, General American Transportation Corporation, Niles, Illinois, November 1972.

13. Department of the Air Force, "Safety - Explosives Safety Standards," Air Force Regulation 127-100, May 20, 1983.

14. Baker, W.E., "Blast and Fragments From Bursting Pressure Vessels," ASME PVP Volume 82, 1984.

15. Taylor, D.E. and Price, C.F., "Velocities of Fragments From Bursting Gas Reservoirs," Journal of Engineering for Industry, November 1971.

16. Jager, E.H., "Simple Calculation of Pressurized-Gas Conventional Vessel Fragment Velocity," 1981.

17. Held, M. and Jager, E.H., "Assessment of Gas Pressure Vessel Burst Hazard," ASME PVP Volume 62, 1982.

18. Baum, M.R., "The Velocity of Missiles Generated by the Disintegration of Gas Pressurized Vessels and Pipes," ASME PVP Volume 82, 1984.

19. Wiedermann, A.H., "Air-Blast and Fragment Environments Produced by the Bursting of Vessels Filled With Very High Pressure Gases," ASME PVP Volume 106, 1986.

20. Jager, E.H. and Junge, W., "Measurement of Pressurized-Air Vessel Fragment Velocity," 1981.

21. Baum, "Disruptive Failure of Pressure Vessels: Preliminary Design Guidelines for Fragment Velocity and the Extent of the Hazard Zone", Transactions of the ASME - Journal of Pressure Vessel Technology, May 1988.

22. Sundararajan and Rooker, "Probabilistic Assessment of Pressure Vessel Missile Generation and Damage Potential," ASME PVP Volume 82, 1984.

23. Huang, "Theory and Computer Program for the Multiple Debris Missile Impact Simulation (MUDEMIMP)," Naval Civil Engineering Laboratory, Technical Note N-1701, June 1984.

24. Hilsenrath, et al, "Tables of Thermal Properties of Gases," National Bureau of Standards Circular 564, 1955.

25. Sonntag and Van Wylen, "Introduction to Thermodynamics: Classical and Statistical," Wiley and Sons, 1971.

26. Swisdak, M. M., "Explosion Effects and Properties, Part I - Explosion Effects in Air," White Oak Laboratory, Naval Surface Weapons Center NSWC/WOL/TR 75-116, October 1975.

27. Baker, Cox, Westine, Kulesz, and Strehlow, "Explosion Hazards and Evaluation," Elsevier, Amsterdam, 1983.

APPENDIX A

DEVELOPMENT OF TNT EQUIVALENCE FROM DATA

Table 1. Pittman Data from [10 & 11]

VESSEL NUMBER	VESSEL SHAPE	VESSEL VOLUME (FT^3)	VESSEL BURST PRESSURE (PSI)	VESSEL MATERIAL	VESSEL MEDIUM
1	Cylindrical	1.34	640	Ti 6-Al 4-V Alloy	GN2
2	Cylindrical	1.68	615	Ti 6-Al 4-V Alloy	GN2
3	Spherical	0.238	8015	Ti 6-Al 4-V Alloy	GN2
4	Spherical	6	8015	Ti 6-Al 4-V Alloy	GN2
5	Spherical	6	8145	Ti 6-Al 4-V Alloy	GN2
6	Spherical	1.02	14965	T-1 Steel	GAr
7	Spherical	1.02	14765	T-1 Steel	GAr
8	Spherical	1.02	34415	T-1 Steel	GAr
9	Spherical	1.02	31815	T-1 Steel	GAr
10	Spherical	1.02	50415	T-1 Steel	GAr
11	Spherical	1.02	50415	T-1 Steel	GAr

Table 2. Expansion Energy — Ideal Gas

VESSEL NUMBER	ISOTHERMAL ENERGY ($FT\text{-}LB/FT^3$)	ISENTROPIC ENERGY ($FT\text{-}LB/FT^3$)
1	0.35×10^6	0.15×10^6
2	0.33×10^6	0.14×10^6
3	7.25×10^6	2.41×10^6
4	7.25×10^6	2.41×10^6
5	7.39×10^6	2.45×10^6
6	14.9×10^6	3.01×10^6
7	14.6×10^6	2.97×10^6
8	38.3×10^6	7.06×10^6
9	35.1×10^6	6.5×10^6
10	58.9×10^6	10.42×10^6
11	58.9×10^6	10.42×10^6

Table 3. TNT Equivalence[1] - Ideal Gas

VESSEL NUMBER	TNT EQUIVALENCE FROM ISOTHERMAL (pounds TNT)	TNT EQUIVALENCE FROM ISENTROPIC (pounds TNT)	TNT EQUIVALENCE FROM PITTMAN[2] (pounds TNT)
1	0.300	0.132	0.138 (0.127)
2	0.358	0.158	0.169 (0.156)
3	1.104	0.366	0.324 (0.299)
4	28.17	9.352	10.1 (9.33)
5	28.70	9.510	10.1 (9.33)
6	9.83	1.95	0.82 (0.757)
7	9.26	1.92	0.82 (0.757)
8	25.28	4.56	0.95 (0.878)
9	23.17	4.21	0.95 (0.878)
10	38.88	6.74	1.0 (0.924)
11	38.88	6.74	1.0 (0.924)

1 - Based on 1.545×10^6 ft-lb$_f$ per pound TNT from Kinney

2 - Pittman data assumed 1018 Cal per gram TNT. The values in parentheses assume 1.545×10^6 ft-lb$_f$.

Table 4. Peak Overpressure — Ideal Gas

VESSEL NUMBER	DISTANCE FROM BURST (ft)	OVERPRESSURE FROM ISOTHERMAL (psi)	OVERPRESSURE FROM ISENTROPIC (psi)
1	3.3	44.10	23.90
	5.5	14.37	8.458
	12.0	3.534	2.386
2	3.3	50.21	27.228
	5.5	16.23	9.44
	12.0	3.87	2.587
3	3.3	116.98	50.96
	5.5	36.67	16.47
	12.0	7.31	3.90
4	7.3	213.5	95.166
	12.0	70.15	31.49
	18.0	28.62	13.07
5	7.3	216.1	96.66
	12.0	71.22	31.94
	18.0	28.47	13.226
6	1.0	2763.6	1363.0
	10.0	48.54	14.9
	16.5	16.5	5.75
	60.0	1.849	0.93

Table 4. Peak Overpressure — Ideal Gas (Continued)

VESSEL NUMBER	DISTANCE FROM BURST (ft)	OVERPRESSURE FROM ISOTHERMAL (psi)	OVERPRESSURE FROM ISENTROPIC (psi)
7	1.0	2700.42	1225.6
	10.0	46.43	14.8
	16.5	15.37	5.7
	60.0	1.804	0.93
8	1.0	3984.24	1997.1
	10.0	98.26	27.27
	16.5	31.58	9.6
	60.0	2.856	1.3
9	1.0	3852.6	1931.0
	10.0	91.96	25.8
	16.5	29.61	9.2
	60.0	2.73	1.28
10	1.0	4643.5	2377.1
	10.0	135.03	36.5
	16.5	43.42	12.4
	60.0	3.03	1.57
11	1.0	4643.5	2377.1
	10.0	135.03	36.5
	16.5	43.12	12.4
	60.0	3.03	1.57

Table 5. Expansion Energy (ft–lb/ft^3) — Real Gas

VESSEL NUMBER	ISOTHERMAL ENERGY	ISENTROPIC ENERGY	
3	4.9 x 10^4	1.65 x 10^4	
4	4.9 x 10^4	1.65 x 10^4	
5	4.9 x 10^4	1.64 x 10^4	
6	8.7 x 10^4	1.76 x 10^4	
7	8.6 x 10^4	1.76 x 10^4	
	TNT EQUIVALENCE (pounds TNT)		
3	0.76	0.25	
4	19.26	6.41	
5	19.26	6.38	
6	5.75	1.16	
7	5.7	1.16	
	PEAK OVERPRESSURE (psi)		DISTANCE (ft)
3	88.17	38.6	3.3
	27.63	12.67	5.5
	5.82	3.24	12.0
4	717.1	395 9	3.3
	299.9	135.9	5.5
	52.7	23.3	12.0
5	717.1	395.9	3.3
	299.9	135.9	5.5
	52.7	23.3	12.0
6	2208.8	926.85	1.0
	32.4	8.82	10.0
	11.17	3.69	16.5
	1.47	0.66	60.0
7	2208.8	926.85	1.0
	32.4	8.82	10.0
	11.17	3.69	16.5
	1.47	0.66	60.0

APPENDIX B

TABLE A-I
from Kingery [9]

λ		ΔP		λ		ΔP		λ		ΔP
2000		6952.	4	7500	1	1718	2	1800	3	1523
2500		5599	4	8000	1	1501	2	1900	3	1409
3000		4624	4	8500	1	1323	2	2000	3	1314
3500		3897	4	9000	1	1182	2	2200	3	1148
4000		3341	4	9500	1	1059	2	2400	3	1016
4500		2904	4	10,00	2	9615	1	2600	3	9079-01
5000		2553	4	1100	2	8029	1	2800	3	8186-01
5500		2264	4	1200	2	6825	1	3000	3	7430-01
6000		2022	4	1300	2	5920	1	3250	3	6640-01
6500		1818	4	1400	2	5186	1	3500	3	5980-01
7000		1645	4	1500	2	4665	1	3750	3	5430-01
7500		1497	4	1600	2	4177	1	4000	3	4960-01
8000		1368	4	1700	2	3797	1	4500	3	4200-01
8500		1255	4	1800	2	3488	1	5000	3	3620-01
9000		1157	4	1900	2	3208	1	5500	3	3170-01
9500		1070	4	2000	2	2984	1	6000	3	2800-01
1000	1	9935	3	2200	2	2596	1	6500	3	2500-01
1100	1	8602	3	2400	2	2299	1	7000	3	2260-01
1200	1	7544	3	2600	2	2061	1	7500	3	2050-01
1300	1	6678	3	2800	2	1867	1	8000	3	1870-01
1400	1	5923	3	3000	2	1706	1	9000	3	1580-01
1500	1	5334	3	3250	2	1537	1	1000	4	1370-01
1600	1	4782	3	3500	2	1397	1			
1700	1	4322	3	3750	2	1279	1			
1800	1	3919	3	4000	2	1178	1			
1900	1	3540	3	4500	2	1015	1			
2000	1	3207	3	5000	2	8876				
2200	1	2630	3	5500	2	7857				
2400	1	2180	3	6000	2	7023				
2600	1	1834	3	6500	2	6328				
2800	1	1558	3	7000	2	5742				
3000	1	1337	3	7500	2	5222				
3250	1	1117	3	8000	2	4769				
3500	1	9438	2	9000	2	4041				
3750	1	8064	2	1000	3	3484				
4000	1	6958	2	1100	3	3047				
4500	1	5316	2	1200	3	2692				
5000	1	4184	2	1300	3	2405				
5500	1	3376	2	1400	3	2162				
6000	1	2782	2	1500	3	1970				
6500	1	2334	2	1600	3	1793				
7000	1	1989	2	1700	3	1647				

APPENDIX C

OVERPRESSURE VS. DISTANCE FOR COMPARISON OF PITTMAN DATA

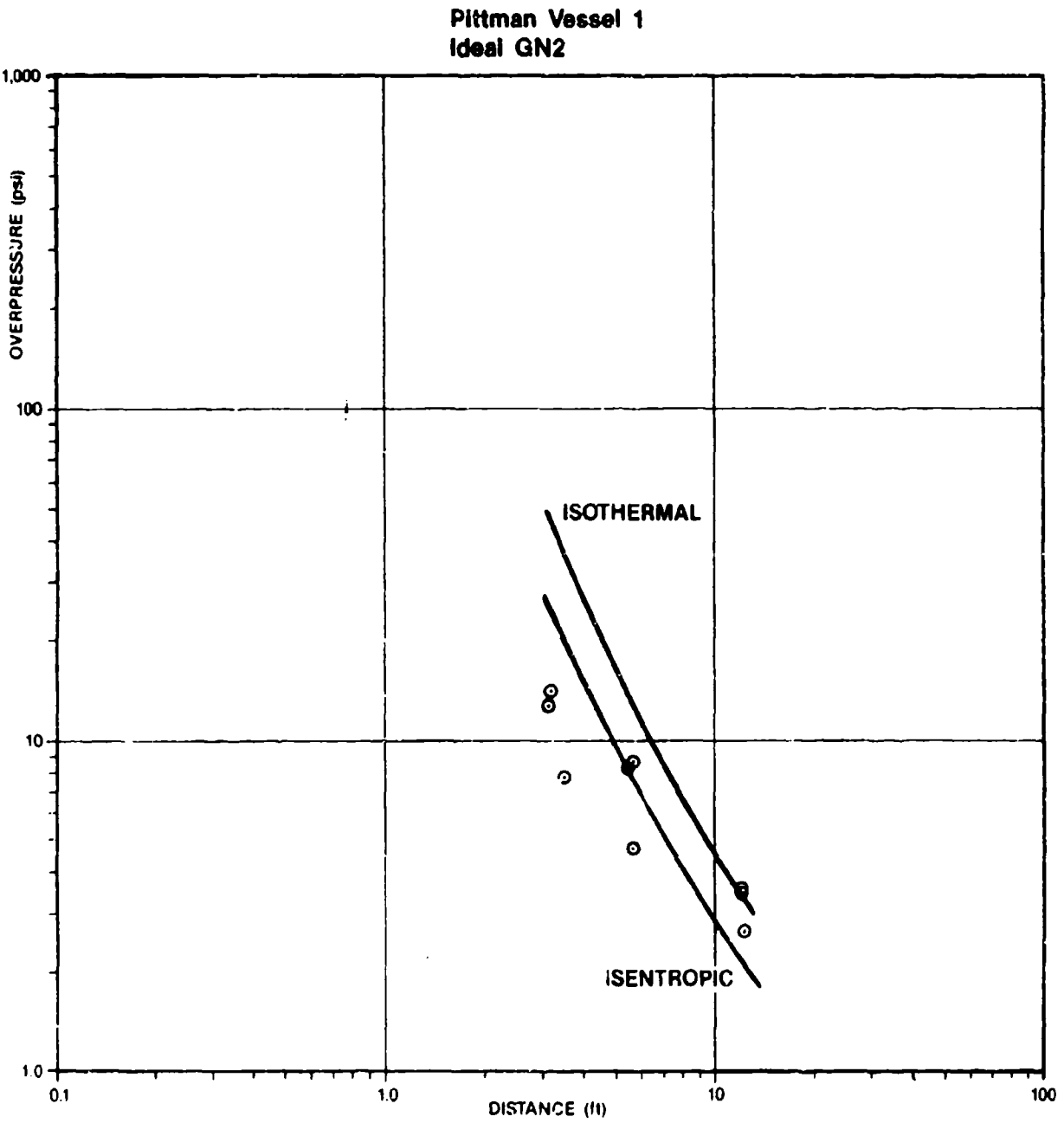
Pittman Vessel 1
Ideal GN2
1,000
100
10
1.0
OVERPRESSURE (psi)
ISOTHERMAL
ISENTROPIC
0.1
1.0
10
100
DISTANCE (ft)

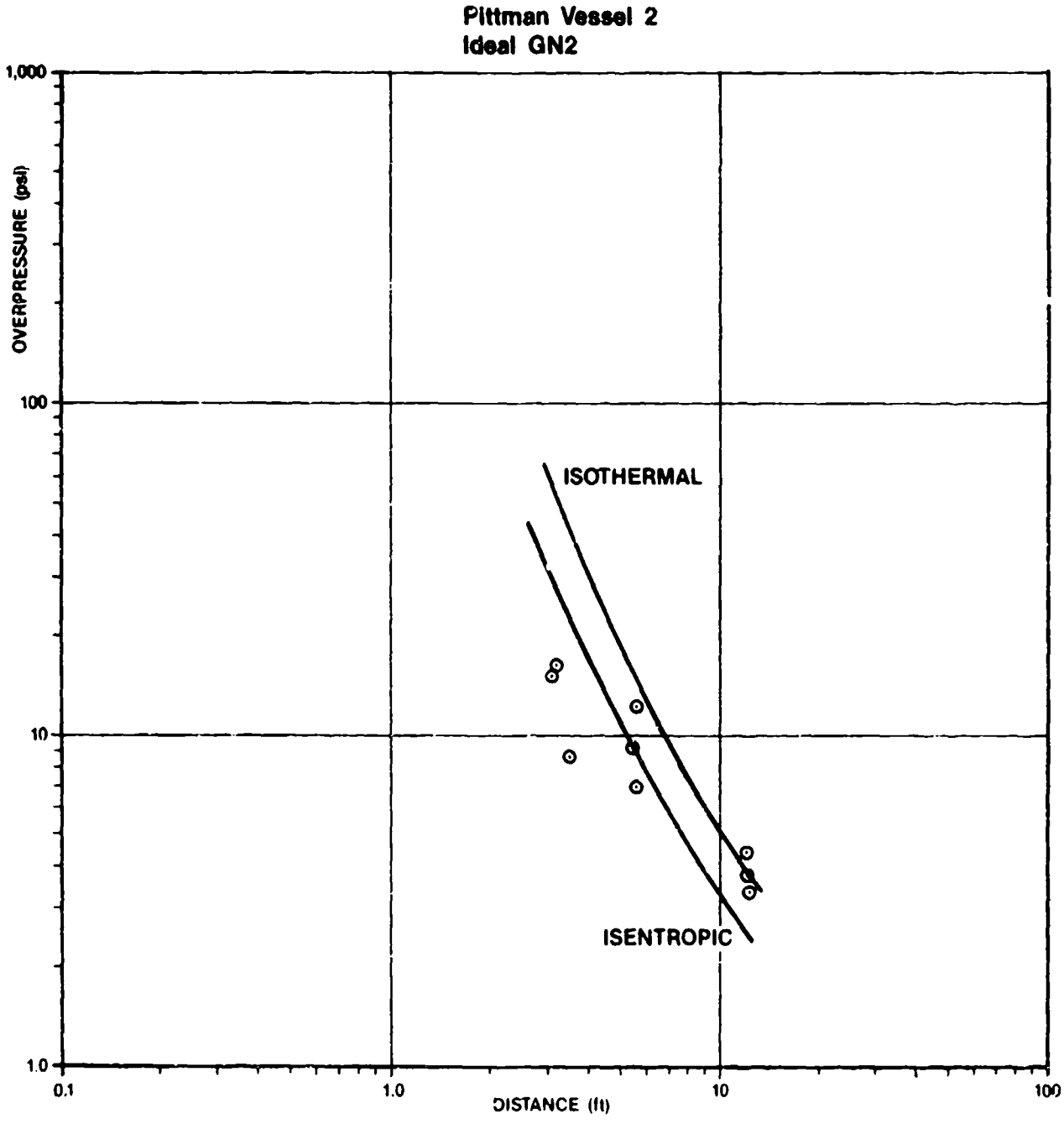
Pittman Vessel 2
Ideal GN2
1,000
100
10
1.0
OVERPRESSURE (psi)
ISOTHERMAL
ISENTROPIC
0.1
1.0
10
100
DISTANCE (ft)

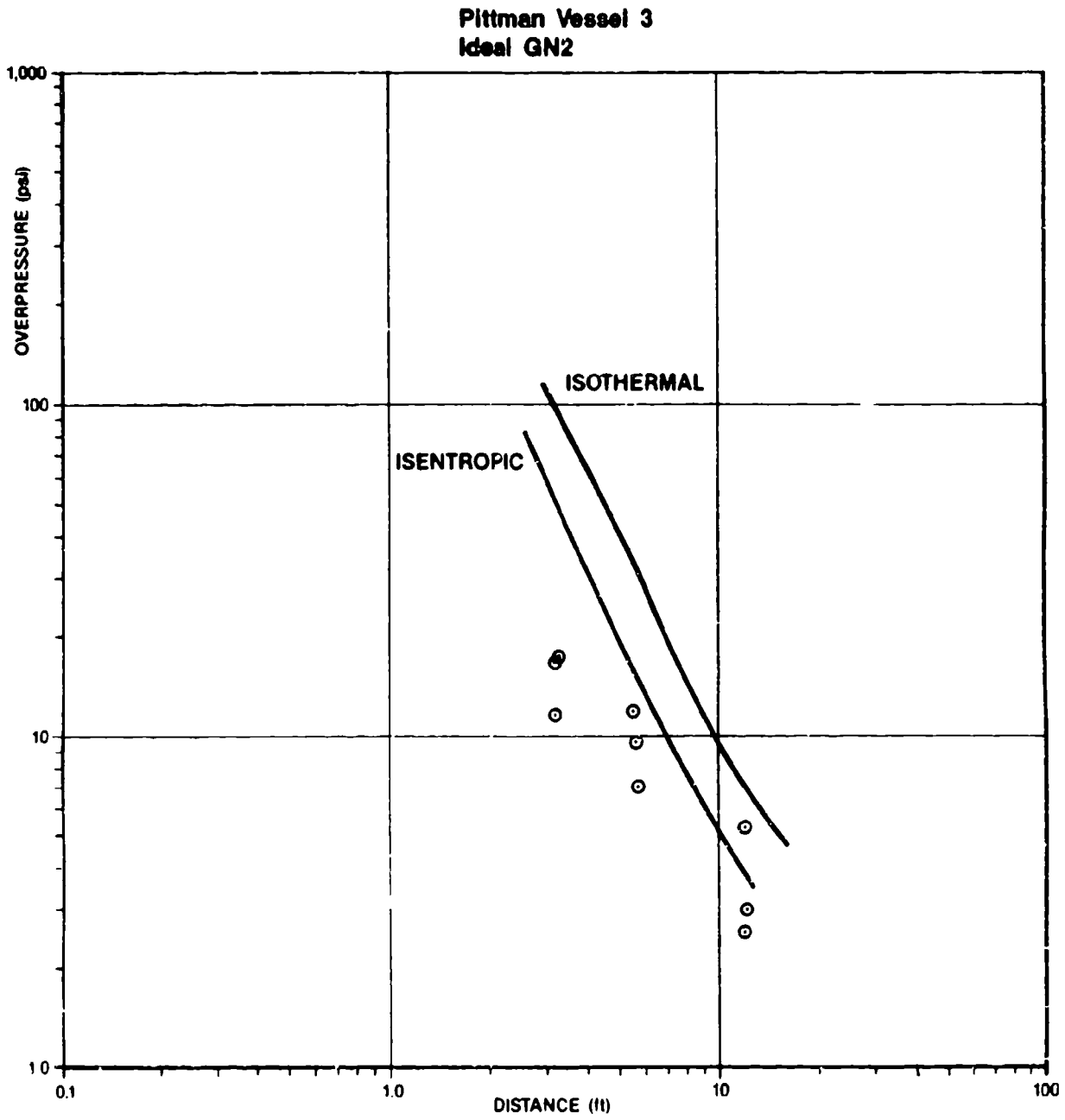
Pittman Vessel 3
Ideal GN2
OVERPRESSURE (psi)
1,000
100
10
1.0
ISOTHERMAL
ISENTROPIC
0.1
1.0
10
100
DISTANCE (ft)

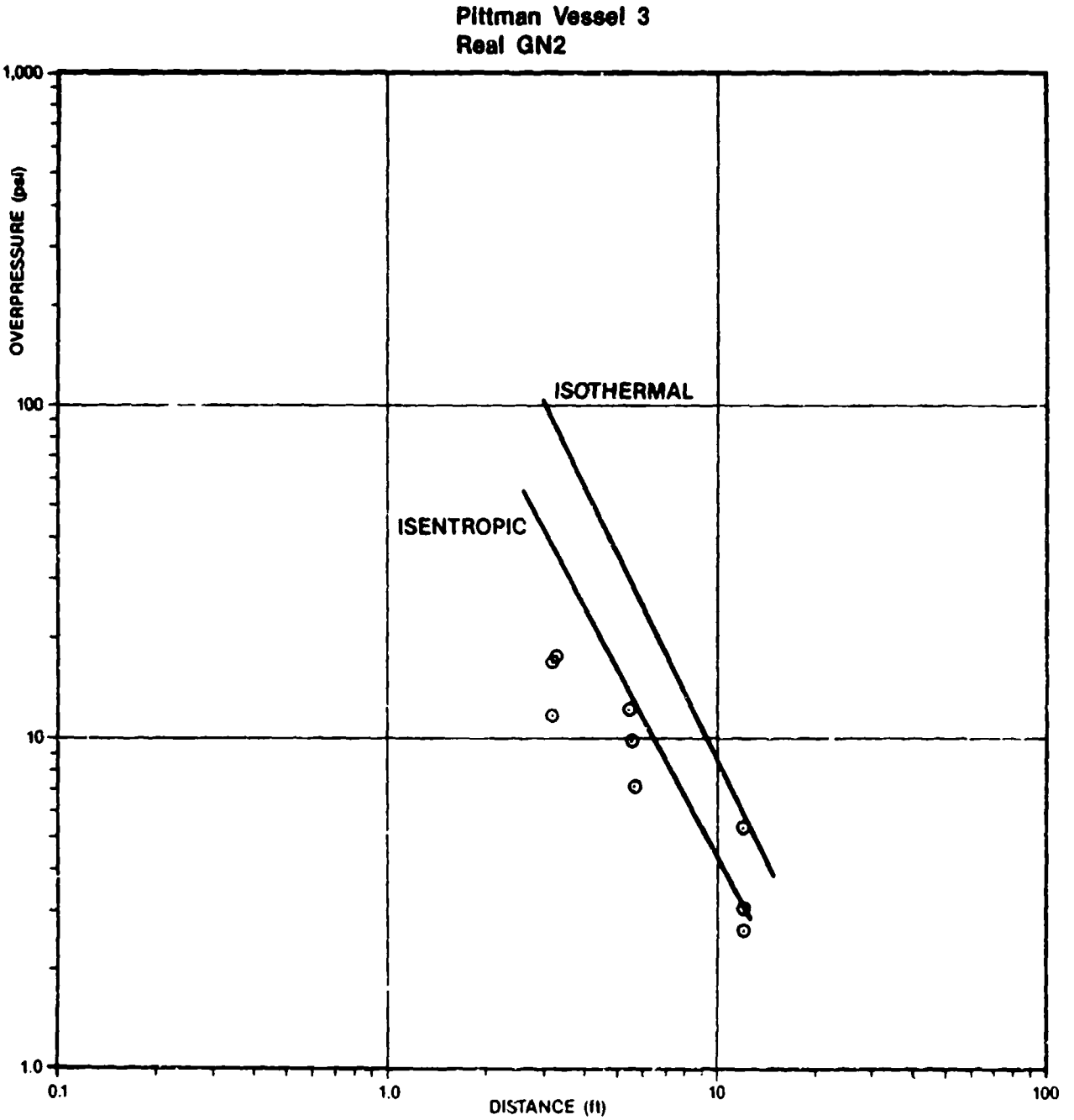
Pittman Vessel 3
Real GN2
1,000
100
10
1.0
OVERPRESSURE (psi)
ISOTHERMAL
ISENTROPIC
0.1
1.0
10
100
DISTANCE (ft)

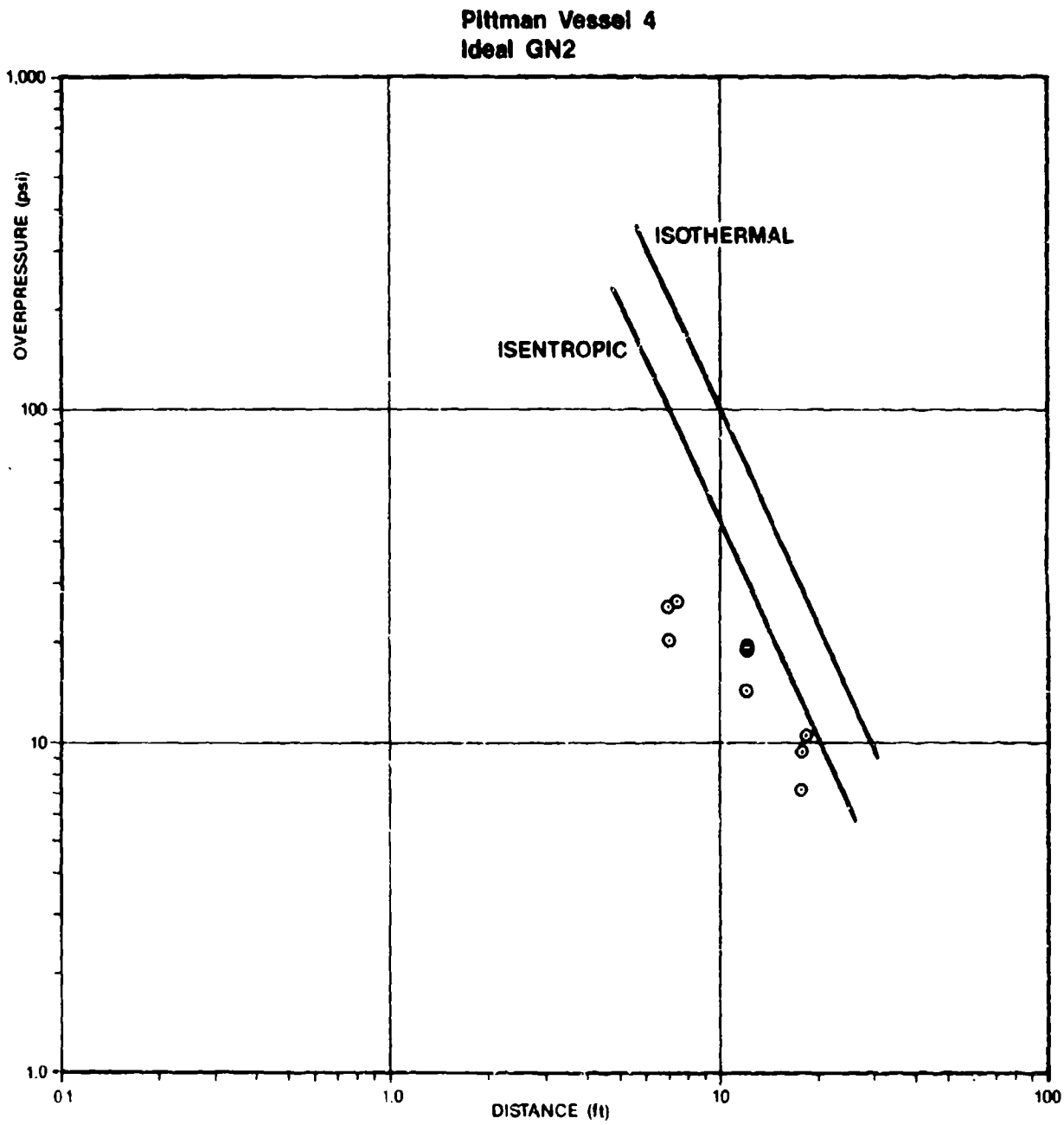
Pittman Vessel 4
Ideal GN2
1,000
100
10
1.0
OVERPRESSURE (psi)
ISOTHERMAL
ISENTROPIC
0.1
1.0
10
100
DISTANCE (ft)

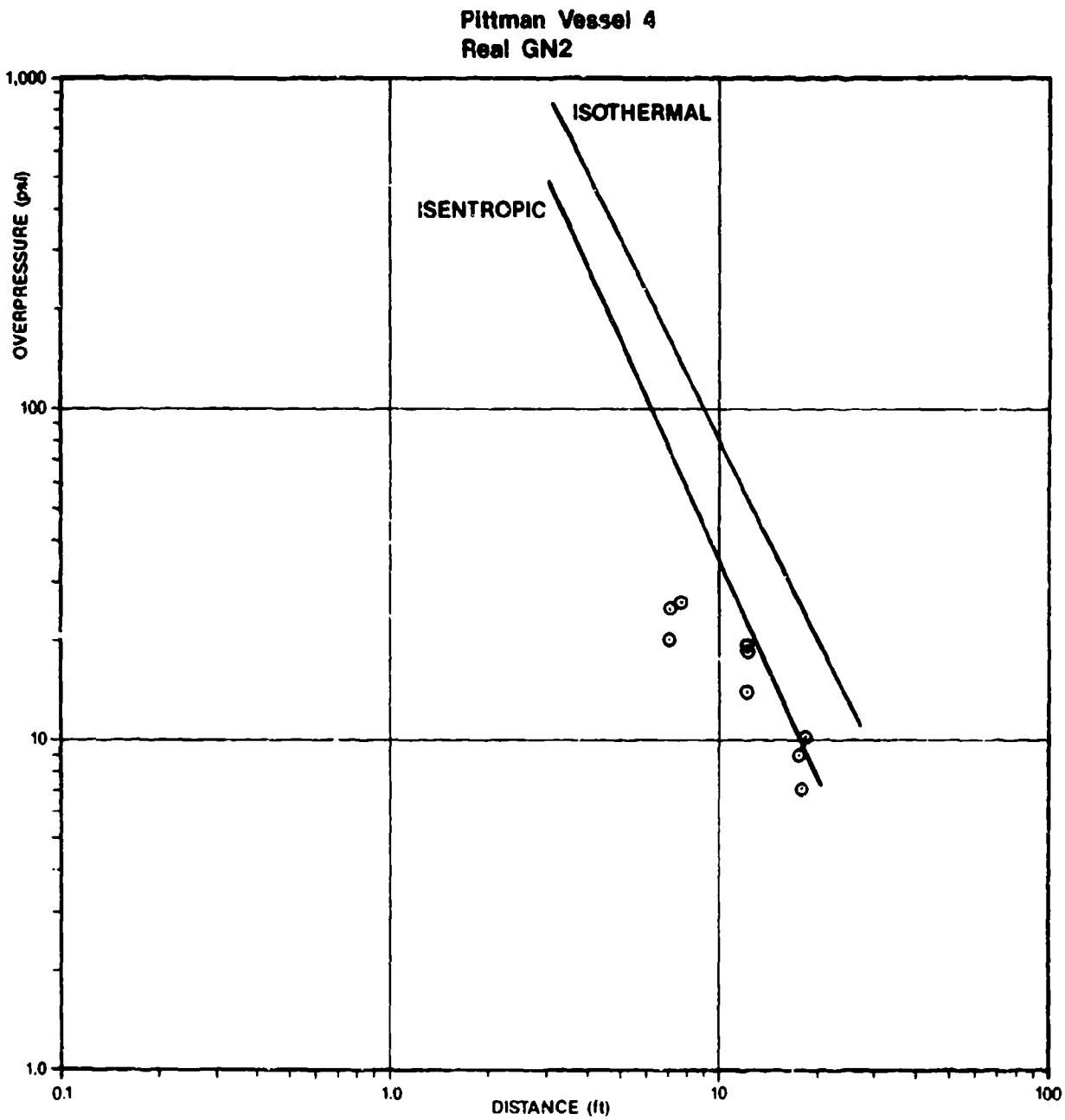
Pittman Vessel 4
Real GN2
ISOTHERMAL
ISENTROPIC
OVERPRESSURE (psi)
1,000
100
10
1.0
0.1
1.0
10
100
DISTANCE (ft)

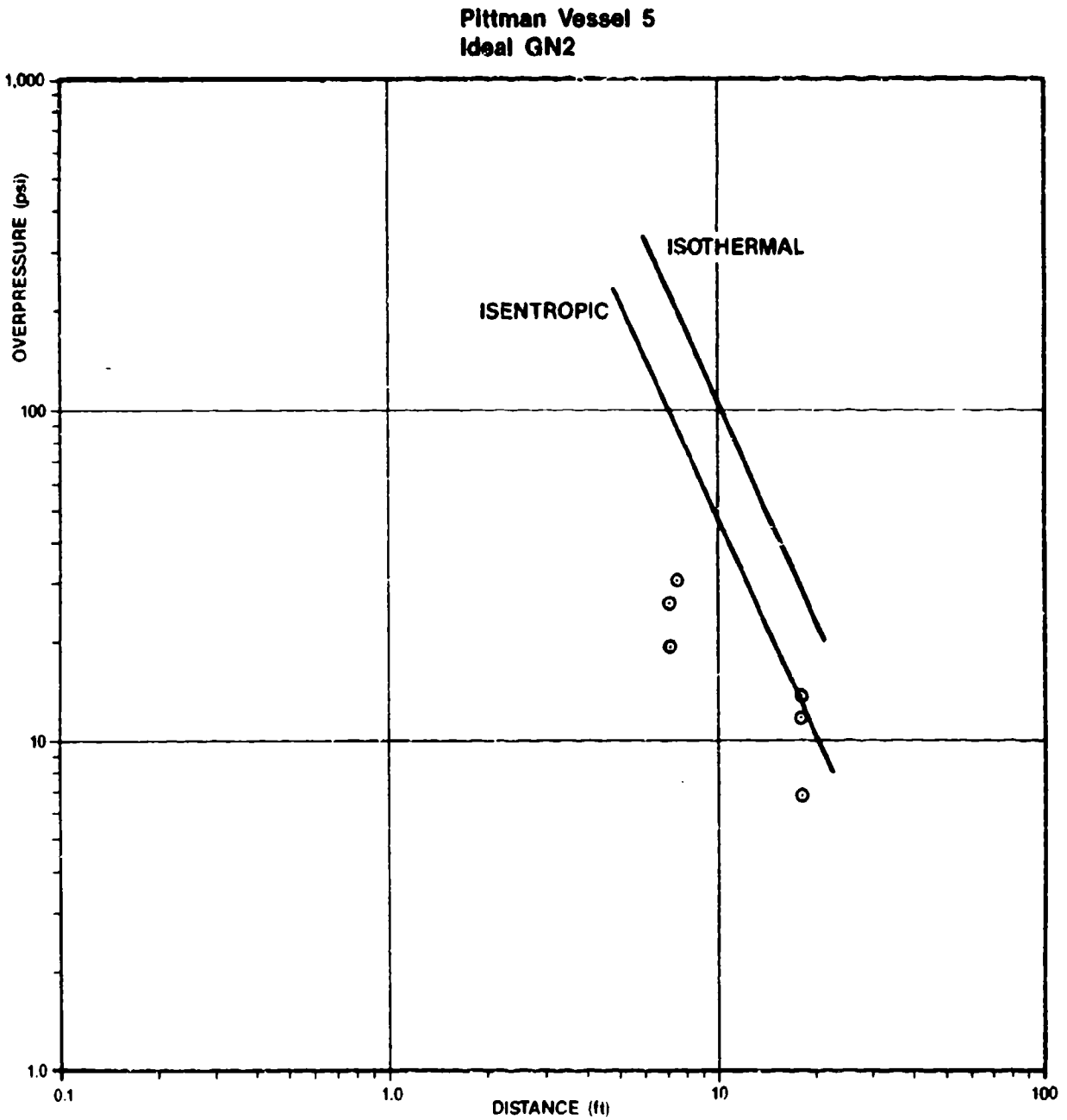
Pittman Vessel 5
Ideal GN2
1,000
100
10
1.0
OVERPRESSURE (psi)
ISOTHERMAL
ISENTROPIC
0.1
1.0
10
100
DISTANCE (ft)

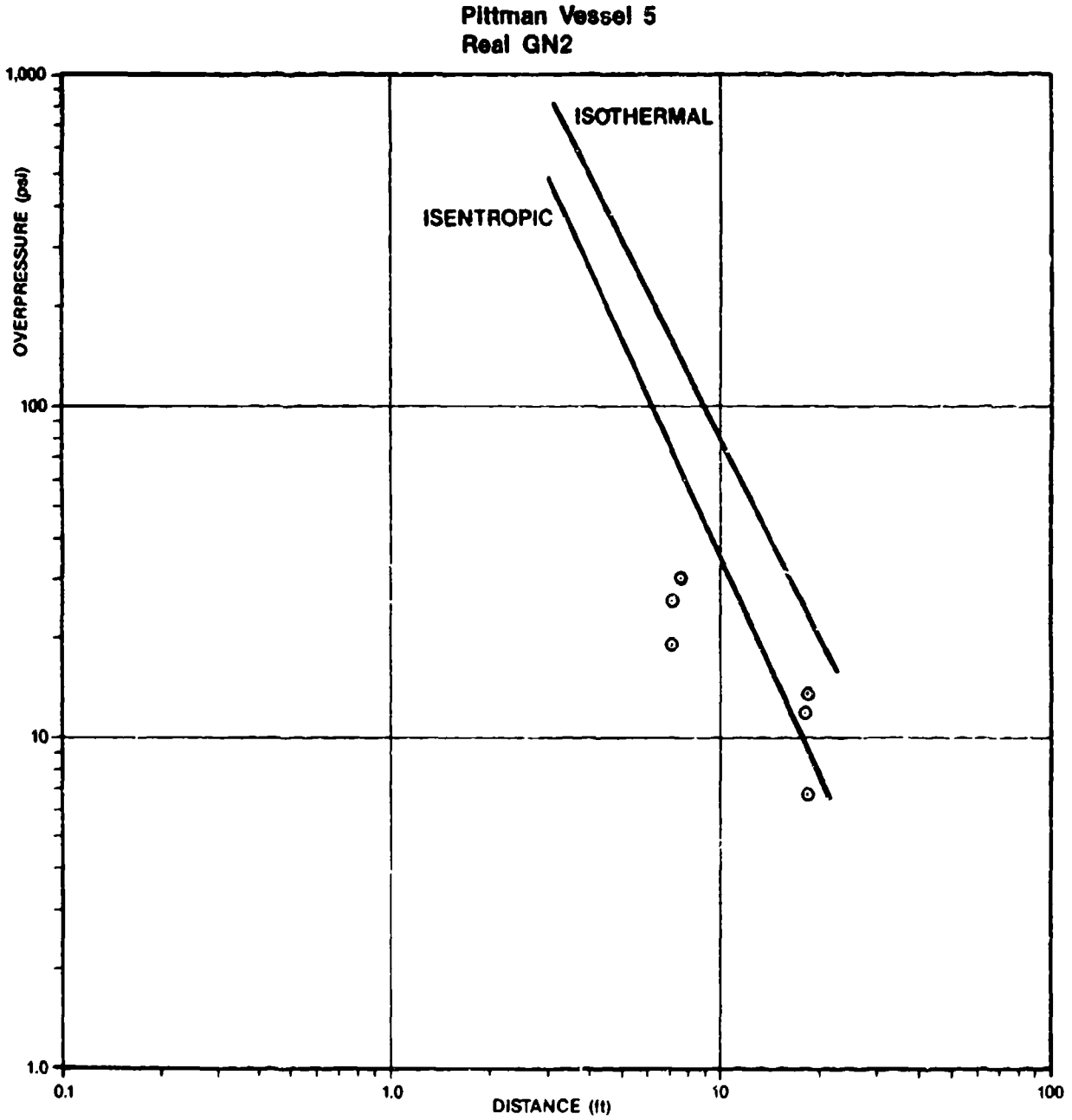
Pittman Vessel 5
Real GN2
1,000
100
10
1.0
OVERPRESSURE (psi)
ISOTHERMAL
ISENTROPIC
0.1
1.0
10
100
DISTANCE (ft)

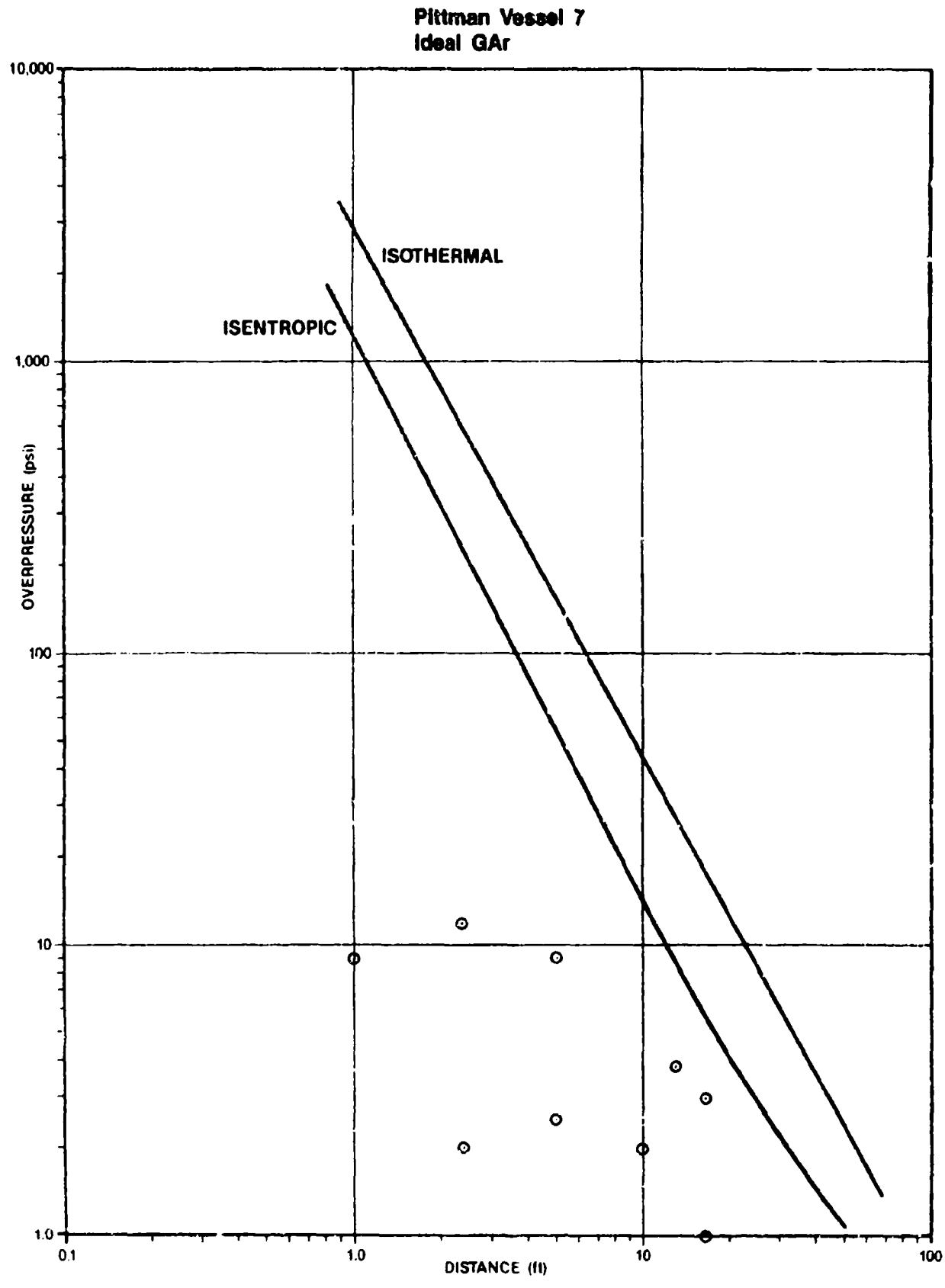
Pittman Vessel 7
Ideal GAr
10,000
1,000
100
10
1.0
OVERPRESSURE (psi)
ISOTHERMAL
ISENTROPIC
0.1
1.0
10
100
DISTANCE (ft)

Pittman Vessel 7
Real GAr

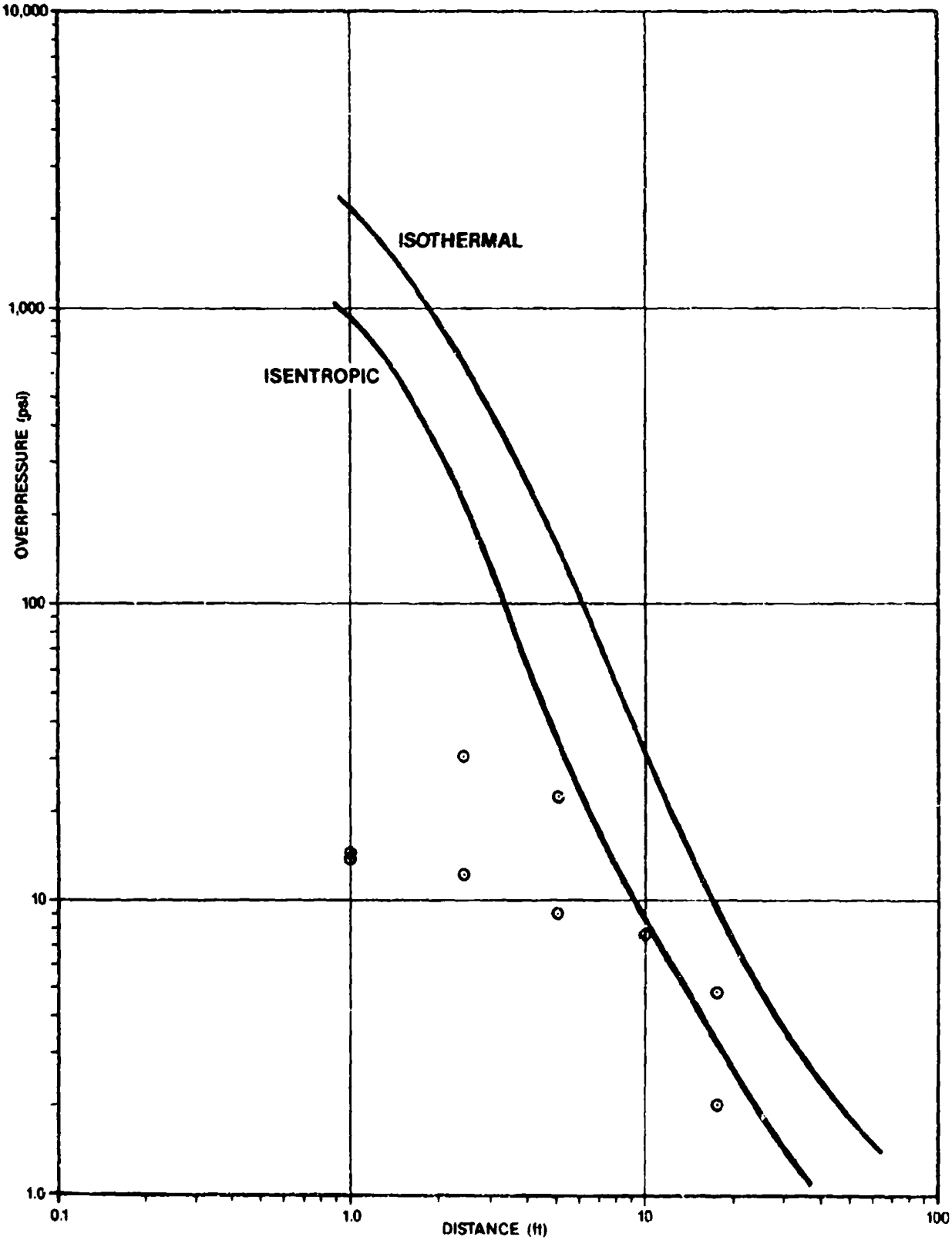

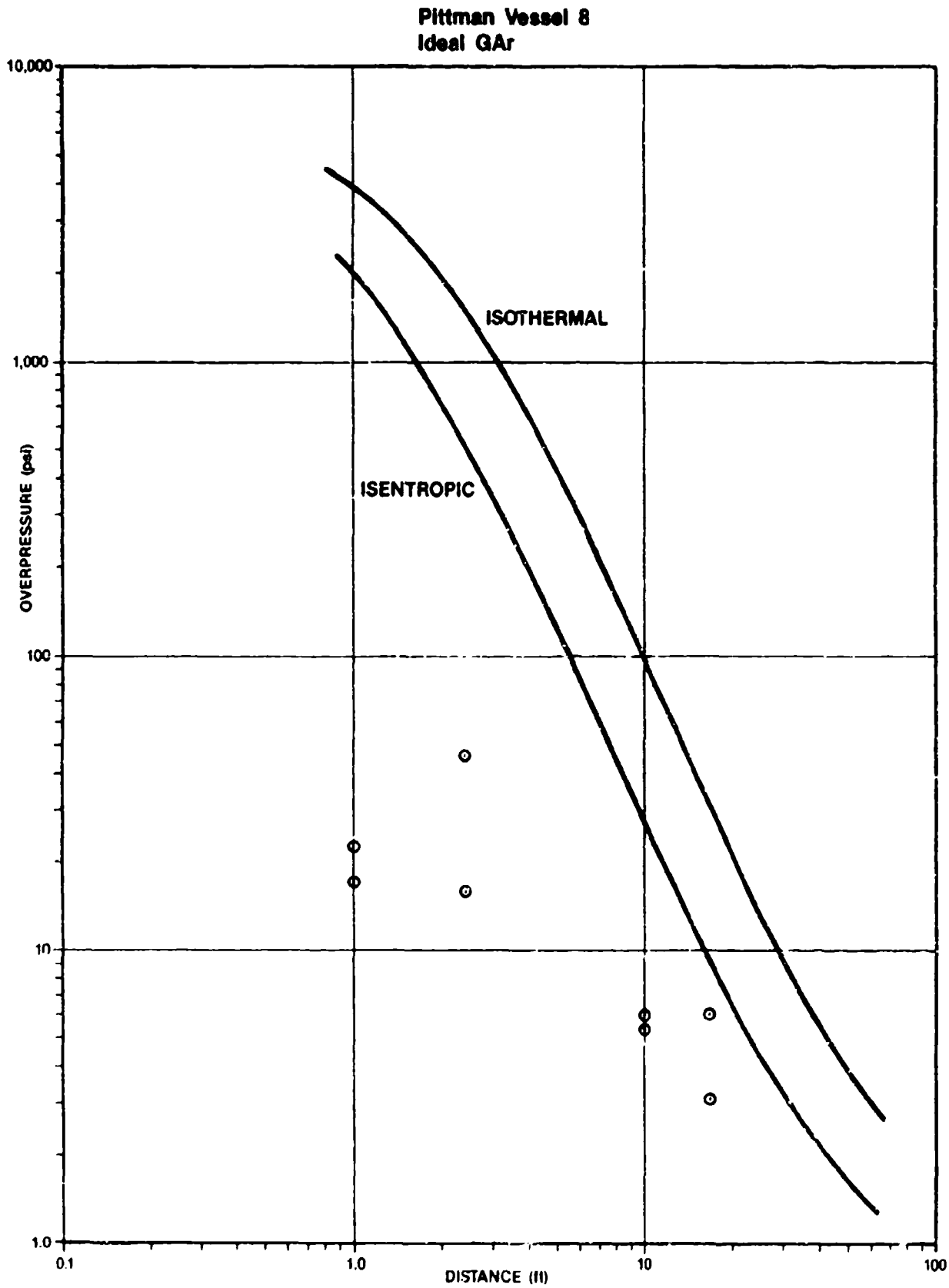
Pittman Vessel 8
Ideal GAr
10,000
1,000
100
10
1.0
OVERPRESSURE (psi)
ISOTHERMAL
ISENTROPIC
0.1
1.0
10
100
DISTANCE (ft)

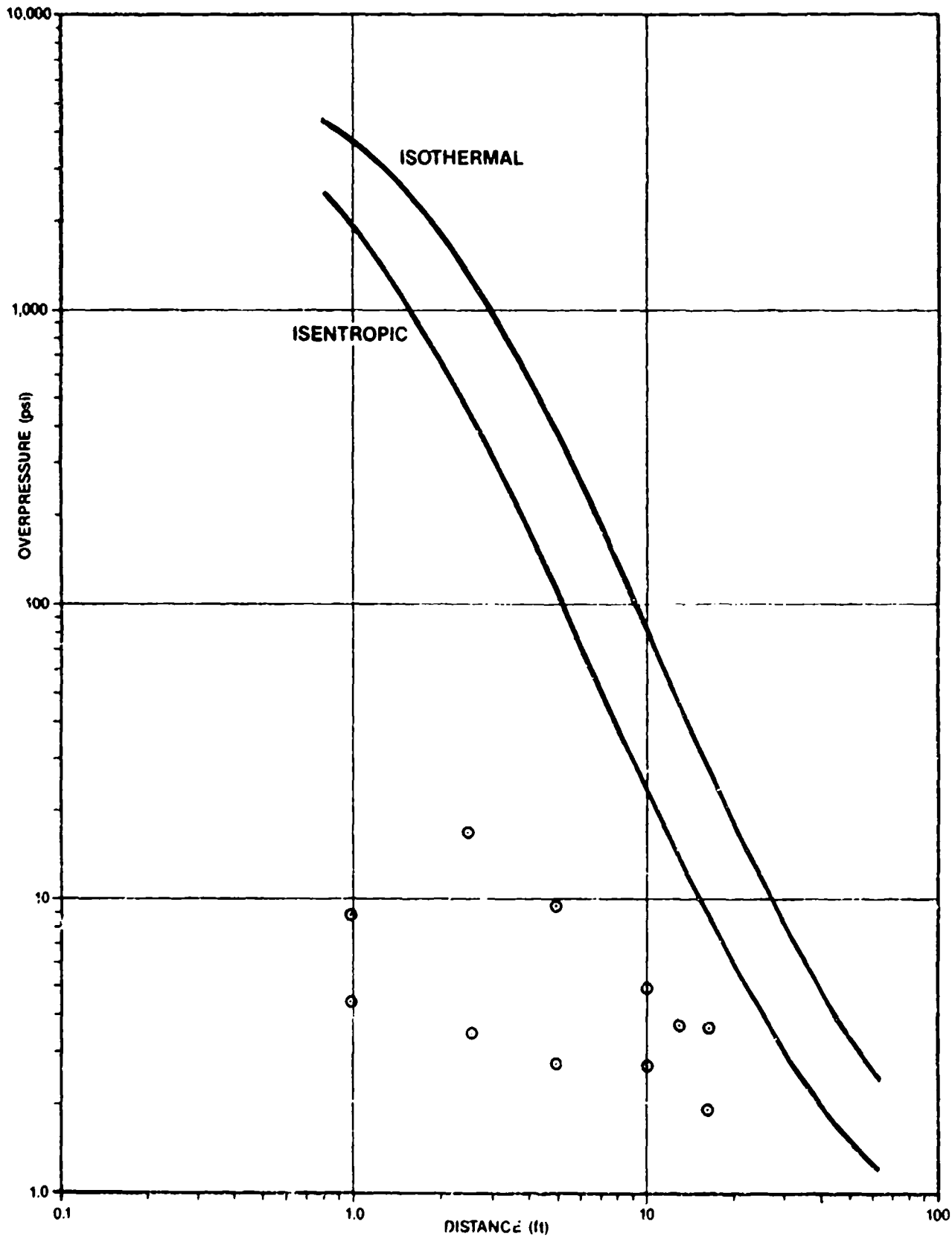
Pittman Vessel 9
Ideal GAr
10,000
1,000
100
10
1.0
ISOTHERMAL
ISENTROPIC
OVERPRESSURE (psi)
0.1
1.0
10
100
DISTANCE (ft)

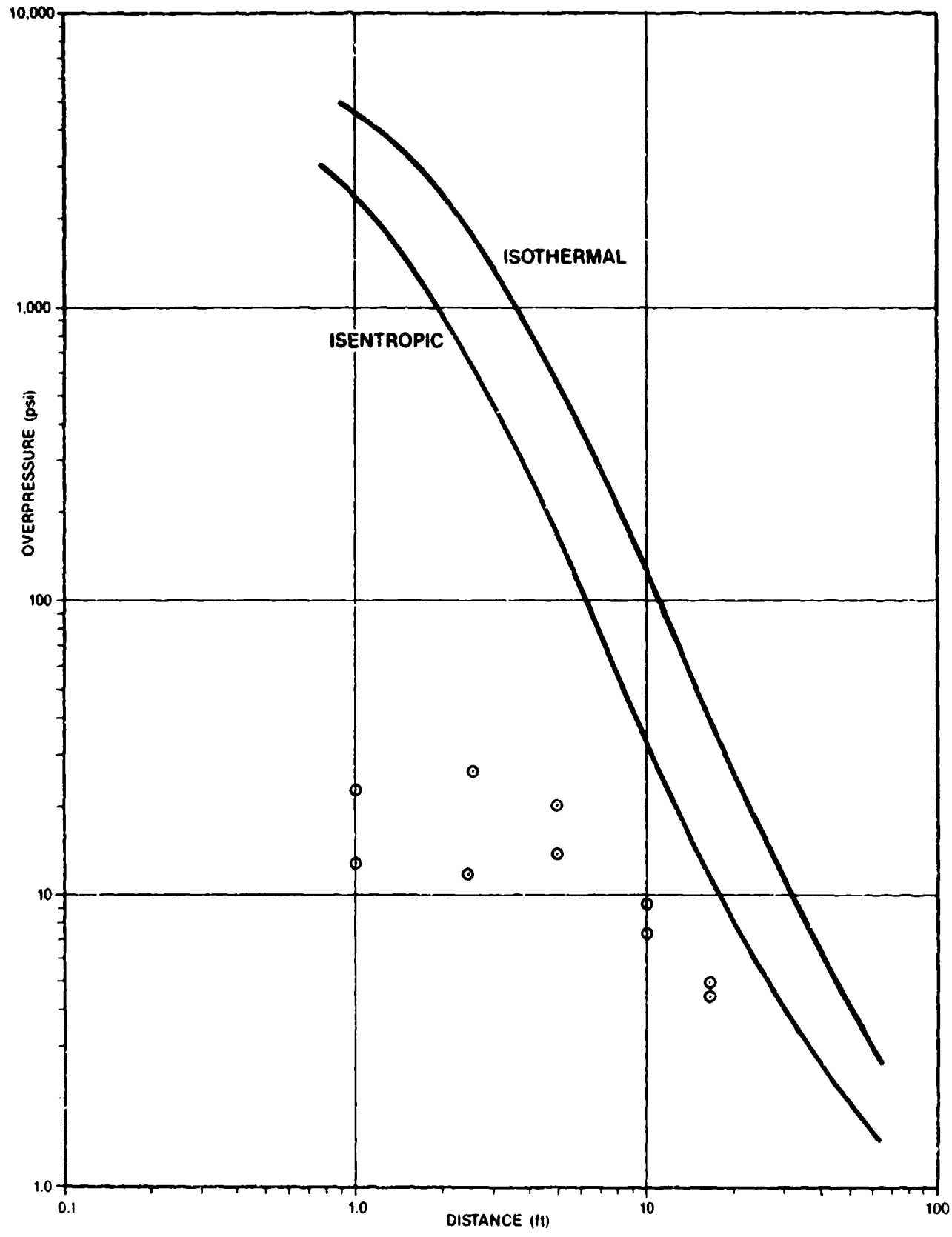
Pittman Vessel 10
Ideal GAr
10,000
1,000
100
10
1.0
OVERPRESSURE (psi)
ISOTHERMAL
ISENTROPIC
0.1
1.0
10
100
DISTANCE (ft)

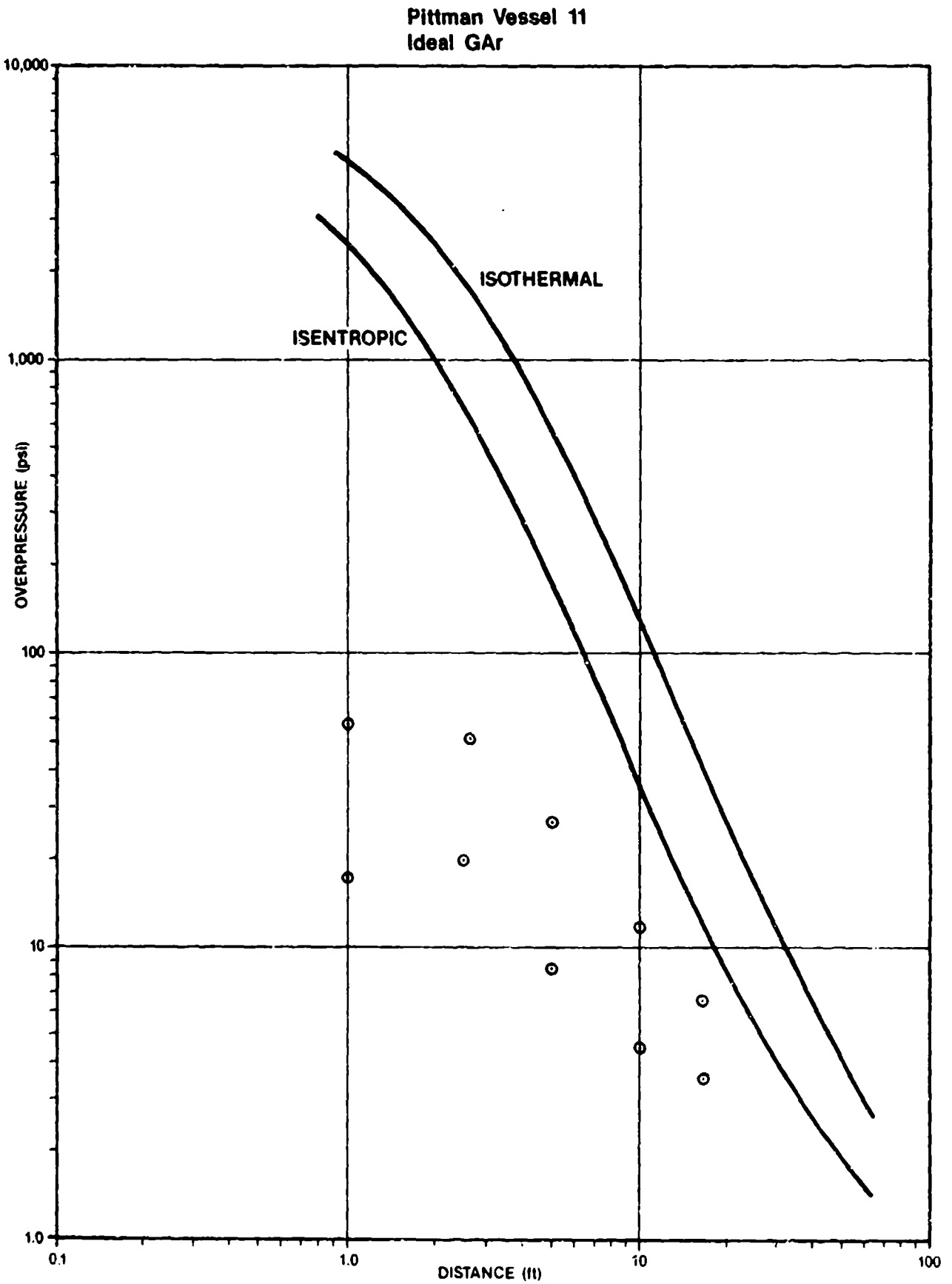
Pittman Vessel 11
Ideal GAr
10,000
1,000
100
10
1.0
OVERPRESSURE (psi)
ISOTHERMAL
ISENTROPIC
0.1
1.0
10
100
DISTANCE (ft)